ANALYSIS OF COBALT, TANTALUM, TITANIUM, VANADIUM AND CHROMIUM IN TUNGSTEN CARBIDE BY INDUCTIVELY COUPLED PLASMA-OPTICAL EMISSION SPECTROMETRY

Submitted in partial fulfilment of the requirements

for the degree of

MASTER OF SCIENCE, CHEMISTRY

in the faculty of Natural and Agricultural Sciences of the

UNIVERSITY OF PRETORIA

March 2004

ANALYSIS OF COBALT, TANTALUM, TITANIUM, VANADIUM AND CHROMIUM IN TUNGSTEN CARBIDE BY INDUCTIVELY COUPLED PLASMA-OPTICAL EMISSION SPECTROMETRY

by

Marcellé Archer

Promotor:
Prof. E.R. Rohwer
University of Pretoria

Co-Promotor:
Prof. R.I. McCrindle
Department Chemistry and Physics,
Tswane University of Science and Technology

SYNOPSIS

Inductively coupled plasma-optical emission spectroscopy was used to measure the concentrations of cobalt, tantalum, titanium, vanadium and chromium in solutions of tungsten carbide. The main advantage of the method described here lies in the speed, convenience and effectiveness of the dissolution procedure. Aliquots of powdered tungsten carbide are dissolved in 5% aqua regia in 30% hydrogen peroxide. Complete dissolution was usually achieved within 10 minutes. The accuracy and precision of this novel method was assessed by the analysis of certified reference materials, secondary reference materials and matrix spiking. The method was successfully applied to commercial type samples with differing compositions.

SAMEVATTING

Induktief gekoppelde plasma-optiese emissie spektrometrie is gebruik om die konsentrasie van kobalt, tantaal, titaan, vanadium en chroom in oplossings van wolframkarbied te bepaal. Die hoofvoordeel van die metode wat hier beskryf word, is die spoed, gemak en doeltreffendheid van die monster-voorbereiding. Verpoeierde wolframkarbied monsters het gewoonlik binne 10 minute opgelos na die byvoeging van 'n mengsel bestaande uit 5% aqua regia in 30% waterstofperoksied. Die akkuraatheid en presisie van hierdie nuwe metode is ondersoek deur gesertifiseerde verwysingsmateriale en sekondêre verwysingsmateriale te ontleed, asook deur matrysbyvoegings. Die metode is suksesvol toegepas op kommersieële monsters met verskillende samestellings.

ACKNOWLEDGEMENTS

This study was undertaken as part of a project by the former Analytical Services group of the Division of Material Science and Technology, CSIR.

The help and encouragement of Prof Silvana Luyckx of the University of the Witwatersrand and Virginia de Klerk, formerly of the CSIR, are gratefully acknowledged.

I also wish to thank the National Metrology Laboratory of the CSIR for their support during the later stages of the project.

I am especially grateful to my husband, Christo Kriek and my daughter, Laura, for their understanding and support throughout my studies.

CONTENTS

CONTENTS

LIST OF TABLES

LIST OF FIGURES

Page

Page

APPENDICES

LIST OF ABBREVIATIONS

AAS – Atomic absorption spectrometry

g/ 100 g – Grams per 100 grams

ICP – Inductively coupled plasma

ISO – International Organization for Standardization

LOD – Limit of detection

LOQ – Limit of quantification

mg/ ℓ – Milligrams per litre, sometimes expressed as parts per million (ppm)

nm – Nanometre (10^{-9} m)

OES – Optical emission spectrometry

r^2 – Coefficient of determination

RSD – Relative standard deviation

XRD – X-ray diffraction

XRF – X-ray fluorescence

CHAPTER 1

INTRODUCTION

1.1 BACKGROUND

In the early 1900's, it was found that the outstanding machining properties of high-speed steel were due to the presence of very hard carbide particles, notably tungsten carbide, in the steel matrix (Brookes, 1979). Because tungsten carbide-cobalt, next to diamond, is one of the hardest materials known, it is used in masonry drill bits, saw blades, cutting discs, sanding blocks, files, metal-cutting tools, mining tools and other hand tools. One of the main uses for tungsten carbide-cobalt is in rockdrilling bits for geological purposes. Tungsten carbide compounds are also known as hardmetals.

The properties of hardmetals are affected by the cobalt concentration and the impurities present in the material (Luyckx, 1997). Other metals, such as tantalum, titanium, vanadium and chromium are added to the tungsten carbide for various reasons, but mainly to inhibit grain growth (Brookes, 2001). Grain growth describes the merging of the tungsten carbide particles during sintering of the pressed product. Grain growth is undesirable because it may weaken the product, especially that of cutting tools (Luyckx, 1997). According to Piippanen (1997a), used materials are also recycled and the composition is of importance in deciding the most suitable use of the material. In a powder metallurgy research environment, the concentrations of these metals must be accurately known to predict the physical properties of the finished product.

Various analytical methods have been used for the measurement of metallic elements in tungsten carbide (Brookes, 1979; Chen, Shao, 1986; ISO 1983, 1985; Kinson, Knott, Belcher 1976;

Kubsch, Herman, Stahlberger, Goerner, 1975; Piippanen, Jaatinen, Piirjeta and Tummavuori, 1997a, 1997b; Thomsen, Baker, 1995; Vasilescou, Abraham and Maruntu, 1980). Most are time-consuming and some may be outside the scope of commercial laboratories. A faster method that still produces reliable, high-quality results was investigated.

1.2 FIELD OF RESEARCH

For the measurement of metallic elements in tungsten carbide, the most frequently used method is x-ray fluorescence spectrometry (XRF) as discussed by Brookes (1979), Kinson et al. (1976) and Townshend, Worsfeld, Haswell, Werner, Wilson (1995) but it may not be sensitive enough for some applications. In general, XRF analysis requires prior fusion of the sample, a task requiring considerable practice (Naish, Clennel, Kingwood, 1953). Atomic absorption methods have been published by ISO (1983, 1985) and Piippanen et al. (1997b). Emission measurement methods have been used by Thomson (1995) and Piippanen et al. (1997a) but these are the only published methods found.

Tungsten carbide powder is highly resistant to acid attack and the dissolution process is lengthy, even when hydrofluoric acid is added. The published dissolution methods by ISO (1983, 1985) and Piippanen et al. (1997b) all have the drawback of being fairly time-consuming (from 45 to 75 minutes per sample) and employ undesirable reagents such as hydrofluoric acid, boric acid and phosphoric acid. Hydrofluoric acid in an analytical solution may etch glassware and instrument components. It may be complexed with boric acid but then research into the possible interference of boric acid on the analysis must be done. It has been proved by Kawaguchi (1995) that the presence of 'heavy' acids, such as phosphoric and sulphuric acid, in a solution for ICP analysis tends to give rise to nebulization (physical) interferences unless strict matrix

matching techniques are applied. Another problem with the dissolution method is a tendency for tungsten oxides to precipitate out of the acid solution and co-precipitation of the elements under investigation (Piippanen et al, 1997a).

The official method of chemical analysis of metallic elements in hardmetal powders is by dissolution in nitric acid and hydrofluoric acid and measurement by flame atomic absorption spectrometry (FAAS), using the method of standard additions (ISO, 1983, 1985). This method is very time-consuming, involving instrument set-up for each element and measurement of five different solutions of each sample. If replicate dissolutions are done, five different solutions of each replicate must be measured.

1.3 HYPOTHESIS

The purpose of the study was to provide an alternative, faster and less expensive method of dissolving tungsten carbide-cobalt powder by the use of nitric acid, hydrochloric acid, hydrogen peroxide and tartaric acid. In this manner, no additional metallic elements would be introduced into the sample matrix and the use of hydrofluoric acid will be avoided.

An efficient way to prevent the precipitation of tungsten oxides will also be investigated. The effect of tartaric acid, instead of phosphoric acid, as a stabilising agent was studied. This research differs from previous published methods for the chemical analysis of tungsten carbide mainly in the dissolution procedure for the tungsten carbide-cobalt powder prior to analysis by ICP-OES.

The experimental work included the investigation of the most efficient measurement procedure

for cobalt, tantalum, titanium, vanadium and chromium by inductively coupled plasma-optical emission spectrometry (ICP-OES). Slightly more emphasis was placed on the measurement of vanadium, since no information on the measurement of this element in solutions of tungsten carbide by ICP-OES could be found. Investigation of the interference effects in the sample was essential for accurate results which are comparable to other published analytical methods.

1.4 OBJECTIVES

This study was undertaken to show whether:

a) an alternative, rapid dissolution method which avoids the use of reagents that have the potential to complicate the analysis could be found

b) the ICP-OES measurement technique is suitable for the measurement of cobalt, tantalum, titanium, vanadium and chromium in a tungsten carbide solution, and

c) accurate and precise results can be obtained with such a technique.

1.5 SPECIFIC AIMS

This treatise investigates the dissolution of tungsten carbide powder in a solution of 5% aqua regia (1 part nitric acid and 3 parts hydrochloric acid, v/v) in hydrogen peroxide. The efficiency of the dissolution procedure was evaluated by the use of certified or secondary reference materials and by matrix spiking. A visual examination of the solution to determine the effectiveness of the solvent is not always conclusive, since a slight precipitate which is invisible to the eye may result in significant error. Further, there are often particles of free carbon present which may lead to false conclusions. The only practical way to evaluate the effectiveness of the dissolution procedure was to compare the results of the ICP-OES measurement to the certified or theoretical concentrations of cobalt, tantalum, titanium, vanadium and chromium.

Further research on the most suitable ICP-OES analytical wavelengths and the effect of the complex sample matrix on the measurement of the elements of interest was undertaken. These effects are not very well described in the literature (Piippanen et al., 1997a; Thompson and Walsh, 1983; Townshend et al, 1995) and not at all for vanadium in tungsten carbide by ICP-OES. The only study of the measurement of some of the metallic elements in tungsten carbide by ICP-OES was published by Piippanen (1997a).

In order to investigate the effect of each of the elements that may be found in a solution of tungsten carbide on each other, acidic solutions containing each element, in the concentration range expected for actual samples, were prepared and the ICP emission measured at the chosen analytical wavelengths. These elements were tungsten, cobalt, tantalum, titanium, vanadium and chromium. Since tungsten was not assigned as an analyte, it was evaluated purely as a potential interferent. Each of the potentially interfering elements were added in turn to a solution of the element under investigation and the change in emission at the same wavelength recorded. In this manner, it could be determined which of the chosen analytical lines were suitable for quantitative analysis. If no interference-free wavelengths for some of the analyte elements could be found, the need for matrix-matching of the calibration reference solutions with the interfering element could also be evaluated.

In addition to being faster and less expensive, the results must be shown to be accurate. In order to properly evaluate the results, certified reference materials and/ or secondary reference materials were dissolved and the solutions analysed by ICP-OES. In certain cases, materials of the appropriate composition were not available. Spiking of a tungsten carbide solution in which

the specific element was not present was employed, and the recoveries calculated to ensure accuracy.

CHAPTER 2

ANALYTICAL METHODS FOR TUNGSTEN CARBIDE POWDERS

2.1 INTRODUCTION

A considerable amount of work has been done on the physical properties of hardmetals (Brookes,1979; Fry, 1982; internet: http://www.infim.ro/1/190/result.htm; Luckyx, 1997), such as density, hardness, transverse rupture stress, etc. Whole volumes have been issued on the microstructure of tungsten carbide (internet: http://www.infim.ro/1/190/result.htm) but very little has to date been published on the chemical analysis of the metallic elements in hardmetals.

2.2 SAMPLE PREPARATION

In most of the published work (ISO, 1983, 1985; Piippanen et al, 1997a, 1997b), hardmetal powders are dissolved in nitric and hydrofluoric acids. When hydrofluoric acid is used it is necessary to complex it with boric acid before analysis to avoid etching the glass parts of the analytical instrumentation. The addition of a metallic element like boron to the already complex matrix necessitates an investigation into its effect on the measurement of the elements of interest, in addition to the effects of the other elements already present in the matrix. Piippanen et al (1997a, 1997b) experimented with phosphoric acid as a complexing agent for tungsten. The main difficulty with both these dissolution methods is that tungsten trioxide ($WO_3.xH_2O$) is easily precipitated from the solution at pH < 1.5 (Townshend et al, 1995). It has been found by Piippanen et al (1997a) that some co-precipitation of the analyte elements can occur. The dissolution procedure is also lengthy (longer than 45 minutes per sample) and difficult.

Older methods of dissolution were based on the fusion of powdered samples with potassium nitrate, extraction of the melt with hot water and acid dissolution of the insoluble fraction (Naish et, al, 1953). WO_3 and SiO_2 were removed by filtration. This method takes several hours to perform, and co-precipitation is a serious problem.

2.3 ANALYTICAL TECHNIQUES

Techniques which have been used for the chemical measurement of metals in tungsten carbides include spark emission spectrometry (Thomson, 1995), x-ray diffraction spectrometry (Chen et al, 1986), titrimetry (Vasilescu et al, 1980), x-ray fluorescence (Kinson et al, 1976), neutron activation (Kubsch et al, 1975) and atomic absorption spectrometry (ISO, 1983, 1985; Piippanen et al, 1997b). Only one published account of analysis by ICP-OES could be found (Piippanen et al, 1997a).

2.4 COMPARISON OF TECHNIQUES

3.4.1 Spark Emission

Spark excitation sources use a current pulse (spark) between two electrodes to vaporise and excite analyte atoms (Tissue, 1995-2000). The electrodes are either metal or graphite. If the sample to be analysed is a metal, it can be used as one electrode. Non-conducting samples are ground together with a graphite powder and placed in a cup-shaped lower electrode. Spark sources can excite atoms for atomic emission spectrometry or ionise atoms for mass spectrometry. According to Townshend et al, (1995), spark sources have been largely phased out in favour of plasma and laser sources but are still widely used in the metals industry.

2.4.2 X-Ray Diffraction (XRD)

The wavelengths of x-rays are of the same order of magnitude as the distances between atoms or ions in a molecule or crystal, 10^{-10} m (Tissue, 1995-2000). A crystal diffracts an x-ray beam passing through it to produce specific angles depending on the x-ray wavelength, the crystal orientation and the structure of the crystal. X-rays are predominantly diffracted by electron density and analysis of the diffraction angles produces an electron density map of the crystal. Since hydrogen atoms have very little electron density, determining their positions requires extensive refinement of the diffraction pattern (Tissue, 1995-2000; Townshend et al, 1995). Electron diffraction and neutron diffraction are sensitive to nuclei and are often used to determine hydrogen positions. X-ray tubes generate x-rays by bombarding a metal target with high-energy (10 – 100 keV) electrons that knock out core electrons. An electron in an outer shell fills the hole in the inner shell and emits an x-ray photon. These sources produce a continuous spectrum of x-rays and require a crystal monochromator to select a single wavelength.

2.4.3 Titrimetry

Titrimetry is defined as the "process of determining the quantity of a substance, A, by adding measured increments of substance B, the titrant, with which it reacts until exact equivalence is achieved" (Townshend et al, 1995). The detection of the equivalence point can be achieved in two ways: visually, if an indicator is present, or by measuring a physical property of the solution being titrated (pH, conductivity, absorbance). Titrimetry is one of the oldest analytical techniques but continues to be used today because of its

high accuracy and precision, and relatively low costs. It has in fact been recognised as a primary method of analysis (Milton, Quinn, 2001). The equipment used ranges from a simple graduated burette, operated manually, to complex automated systems. Titrations are classified according to the nature of the end-point measurement. For the analysis of cobalt, for example, Vasilescu et al (1980) used a complexiometric titration, with EDTA as the complexing agent in the presence of murexide. The same authors measured iron, after extraction by hydrochloric acid, by photocalorimetric titration. Iron can also be measured by redox titration (Basset, Denney, Jeffery, Mendham, 1978).

2.4.4 X-Ray Fluorescence

X-ray fluorescence (XRF) is a spectroscopic method that is commonly used for solids in which secondary x-ray emission is generated by excitation of a sample with x-rays (Tissue, 1995-2000; Townshend et al, 1995). The x-rays eject inner-shell electrons. Outer-shell electrons take their place and emit photons in the process. The wavelength of the photons depends on the energy difference between the outer and inner shell electron orbitals. The amount of the x-ray fluorescence is very sample-dependent and quantitative analysis requires calibration with standards that are similar to the sample matrix.

Solid samples are usually powdered and pressed into a wafer or fused in a borate glass. The sample is then placed in the sample chamber of an XRF spectrometer and irradiated with a primary x-ray beam. The x-ray fluorescence is recorded with either an x-ray detector after wavelength dispersion or with an energy-dispersive detector. According to Tissue (1995-2000) and Townshend et al (1995) very high precision can be achieved with XRF, even in routine operation.

2.4.5 Neutron Activation

Neutron activation is a powerful nondestructive multielement technique (Townshend, 1995). It can be applied to over sixty elements in a broad range of matrices and no sample dissolution is required. The sample is activated in a source of neutrons, followed by ?-ray spectrometry to identify and quantify the induced activity. The basis of this method is the fact that most elements have one or more stable isotopes that can be made radioactive on interaction with neutrons. A neutron source is required, the most commonly used one is the nuclear reactor (a core of uranium enriched in ^{235}U). A 14 MeV neutron generator, or a ^{252}Cf or Am/Be source may also be used.

2.4.6 Atomic Absorption Spectrometry (AAS)

Matter can capture electromagnetic radiation and convert the energy of a photon to internal energy. This process is called absorption. Energy is transferred from the radiation field to the absorbing species. The energy change of the absorber is described as an excitation from a lower energy level to a higher energy level. Since the energy levels of matter are quantized, only light of energy that can cause transitions from one level to another will be absorbed. The type of excitation depends on the wavelength of the light. In atomic absorption, as used in analytical chemistry, the absorption spectrum is that of light and is a function of wavelength (Tissue, 1995-2000).

Several methods of atomisation are in use, the most common being a flame, using air/acetylene or nitrous oxide/acetylene. A light source of a specific wavelength is required and the most widely used source is the hollow-cathode lamp (HCL), in which the cathode

is lined with the element to be determined (Haswell, 1991). Electrons are released from the cathode when a striking potential is applied. The electrons cause impact ionisation of the background noble gas, and acceleration of the noble gas cations to the cathode causes vaporisation of the cathode lining. An atomic vapour is produced and excitation occurs. Emission from the lamp passes as a beam though the flame. The beam then passes through a monochromator to a photomultiplier tube, and the photons are converted to an electrical signal. A readout in absorbance units is obtained. Atoms in the flame absorb energy, provided it is of a suitable wavelength, from the beam, which registers as an increase in absorbance units (the logarithmic function of transmission). The technique is quantitative since the absorbance of an absorbing species is proportional to its concentration (Beer's law).

2.4.7 Inductively Coupled Plasma-Optical Emission Spectrometry (ICP-OES)

The electrons in atoms, ions or molecules that are excited to high energy levels can decay to lower energy levels by emitting radiation (emission or luminescence). For atoms excited by a high-temperature energy source this light emission is called atomic or optical emission. The emission intensity of an emitting substance is linearly proportional to analyte concentration, provided that all other parameters stay constant, and is used to quantify emitting species (Kawaguchi, 1995; Moore, 1989; Thompson & Walsh, 1983; Tissue, 1995-2000; Townshend et al, 1995).

A full description of inductively coupled plasma-optical emission spectroscopy is included

under Section 5.2.

2.5 CONCLUSIONS

Although a minimum of sample preparation is needed, the XRD technique cannot be considered a quantitative method. XRD spectrometry is primarily used to characterise a material and to study internal defects in the atomic arrangement in crystalline material (Townshend, 1995).

With spark emission, the amount of sample introduced into the spectrometer cannot be easily controlled, necessitating the use of an internal standard. The detection limit is generally poor and strong matrix effects require that a large library of solid reference materials is available (Tissue, 1995-2000; Townshend, 1995).

The use of titrimetry for the measurement of metals in tungsten carbide solutions is rather limited. Although titrimetry is a highly accurate and specific method and requires relatively inexpensive equipment, conditions such as pH may have a large influence. Essentially, only one element can be measured at a time, making this a time-consuming method if a number of elements are to be measured. Vasilescu et al (1980) applied titrimetric analysis only to cobalt and iron, which were present as impurities due to machining and sintering. The preparation method was an extraction procedure with hydrochloric acid, rather than a complete dissolution of the metal carbide matrix.

Neutron activation is a sensitive method which can produce very accurate results if properly applied. It is also rapid, since no sample preparation is required and it is very useful for the

analysis of substances that do not dissolve easily. However, this technique is not as well used as most of the others mentioned, possibly because the most common neutron source is a nuclear reactor (Tissue, 1995-2000). It is relatively expensive to buy and access to a reactor is needed. It also requires a high level of operator skill.

XRF spectrometry, AAS and ICP-OES can all be used as quantitative techniques. However, as already mentioned, quantitative XRF analysis requires a reference material of known composition that is close to that of the sample. These standards are not always available and may be relatively expensive if they can be obtained. Another disadvantage of the method when applied to hardmetal samples, is that the samples must be fused with Li-La tetraborate and then briquetted with graphite (Kinson et al, 1976).

Atomic absorption spectrometry (AAS) has been shown to be very accurate but in most cases, only one element (one wavelength) can be measured at a time, after which the hollow cathode lamp must be changed. On older instruments the operating parameters should be re-optimised. This makes the technique very time consuming. With AAS the ability to compensate for interferences is limited and in some cases the method of standard additions must be applied, which makes the method more time-consuming (ISO 1983, 1985). In general the calibration curves are linear at low absorbance values but exhibit an increased curvature at higher concentrations (Haswell, 1991). The sample concentrations must therefore fit a much narrower measurement range than for ICP-OES.

ICP-OES is a technique which can measure multiple elements in the same solution, either

sequentially or simultaneously. This is a great advantage over AAS. The same element can be measured at several different wavelengths, which is helpful in eliminating interferences. The linear range of ICP-OES is also over several orders of magnitude. This means that elements present in different concentrations in the solution can be measured without the need to make several dilutions (Moore, 1989).

CHAPTER 3

THE PRODUCTION OF TUNGSTEN CARBIDE

3.1 INTRODUCTION

To understand why the analysis of certain metals in tungsten carbide is important, it is necessary to briefly describe the process of tungsten carbide production.

Prior to 1945, tungsten carbide was prepared by melting tungsten, carbon black and metal oxides at a temperature of 2000 °C but the tools made from this metal were found to be far too brittle for industrial use. Today, tungsten carbide tools are made by pressing the tungsten carbide powder in a die to produce a green compact, which is then sintered in a vacuum oven. The process, known as powder metallurgy, was introduced by Karl Schröter in 1914 (Brookes, 1979; Luyckx, 1997) and is used because:

- Tungsten carbide decomposes before melting
- The component materials retain their original properties
- It can be used to produce a large number of small parts (for example bolts) which require close tolerances and minimum finishing, and is economical
- There are no stresses on the finished product (so that they are shock-resistant), in contrast to brazed tools which suffer from stresses left by the process and which can cause fractures

The technique has certain limitations:

- design
- requires a high press capacity
- the powders must have certain properties or the density will not be uniform

3.2 COMPOSITION OF HARDMETALS

Different combinations of tungsten carbide, cobalt and metal carbides produce products with different mechanical properties. As an example, the typical composition of some grades of tungsten carbide for use in tool tips are illustrated in Table 3.1. The full table with the historical development from 1923 to 1975 is given in Appendix 2. Today most of these combinations are still in use, together with more advanced materials (Brookes, 1979, 2001; Luyckx, 1997).

Table 3.1: Standards for hardmetal tools tips (Brookes, 1979)

Composition (%)				
WC	**TiC**	**TaC**	**VC**	**Co**
34.5	60	-	-	5.6
69	25	-	-	-
78	16	-	-	-
78	14	-	-	-
85	-	-	-	-
88	5	-	-	-
89	-	-	-	-
91.5	-	1	0.5	-
94	-	-	-	-
94	-	-	-	-

It can be seen in Table 3.1 that the composition of hardmetals may vary widely. The exact cobalt content, for example, affects factors such as density, hardness, transverse rupture strength, tensile strength and thermal expansion of the sintered product (Brookes, 1979, 2001). The properties of the product may be similarly affected by the concentration of titanium, tantalum and vanadium. These and other physical properties are usually measured to control the quality of the material (Luyckx, 1997). In order to link the measured physical properties with

composition, it is important to measure the concentrations of the elements that affect these properties.

Appendix 1 contains a table detailing the changes in the properties of sintered tungsten carbide with changing cobalt concentration (Brookes, 1979).

3.3 PRODUCTION OF TUNGSTEN METAL

Tungsten occurs in nature as wolframite, $FeMnWO_4$, and scheelite, $CaWO_4$ (Brookes, 1979; Luyckx, 1997; Townshend et al, 1995). The ore is digested in hydrochloric acid to remove the calcium and to precipitate tungstic acid, H_2WO_4, which is then dissolved in ammonia and crystallized as ammonium tungstate, $(NH_4)_2WO_4$. Ammonium tungstate is evaporated by boiling to give ammonium paratungstate, or APT, $5(NH_4)_2O.12WO_3.5H_2O$. At temperatures below 50°C, fine APT is obtained. By calcining APT or tungstic acid, tungsten oxide, WO_3, is obtained. The lower the temperature, finer the WO_3 produced (Luyckx, 1997).

When WO_3 is reduced in hydrogen, tungsten, W, is produced:

$WO_3 + 3H_2$? $W + 3H_2O$,

because oxygen forms a more stable bond with hydrogen than with tungsten (Brookes, 1979; Luyckx, 1997; Townshend et al, 1995). In this procedure, the tungsten oxide is spread in thin layers in nickel boats and passed through a small push- or rotary-type furnace at 800 to 1100°C in the opposite direction to the hydrogen flow. The water vapour is condensed in drying towers and the purified hydrogen re-circulated. To obtain a uniform product, the oxide particles must all be at the same temperature and in the same atmosphere. This is where the rotary

furnace has the advantage by exposing all the particles to the hydrogen atmosphere. If the tungsten oxide is too coarse, layers of tungsten will form around the particles and prevent reduction of the oxide in the centre.

Several changes may take place during the reduction process. These are summarized in Table 3.2. The changes are due to changes in the stability of the oxides, relative to the stability of the water with changing temperature (Luyckx, 1997).

Table 3.2: Changes occurring during the reduction of tungsten oxide (Luyckx, 1997)

Temperature (°C)	Appearance	Approximate composition
400	Green-blue	$WO_4 + W_4O_{11}$
500	Intense blue	$WO_4 + W_4O_{11}$
550	Violet	W_4O_{11}
575	Purple-brown	$W_4O_{11} + WO_2$
600	Chocolate brown	WO_2
650	Brown-black	$WO_2 + W$
700	Grey-black	W
800	Grey	W
900	Metallic grey	W
1000	Coarse metallic	W

3.4 CARBON POWDER

The carbon used in hardmetals is usually pressed lampblack, of which the ash content should not exceed 0.2%.

3.5 COBALT POWDER

Cobalt metal powder is obtained by the reduction of cobalt oxide in hydrogen, at temperatures of between 600 and 700°C, according to the following reaction:

$Co_3O_4 + 4H_2$? $3Co + 4H_2O$

Generally, the lower the reduction temperature, the finer the particle size of the powder produced (Luyckx, 1997). Powders with a particle size of less than 5 µm do not require milling (a source of contamination) before addition to the tungsten carbide powder but the coarser powders are milled for 24 hours. Cobalt liquidizes during the sintering process and acts as a glue to bond the WC particles. Some of the desirable properties of tungsten carbide tools are undermined with increasing cobalt concentration. According to Luyckx (1997), these include:

- high impact resistance,
- high modulus of elasticity,
- high compressive strength,
- low tensile strength,
- low impact strength,
- low coefficient of thermal expansion, and
- high thermal conductivity

Charts of the changes in the properties with changes in the cobalt concentration are included under Appendix 1. Carbide particles are 'cemented' by a binder metal, such as cobalt, which is liquid at sintering temperature (Brookes, 1979; Luyckx, 1997).

3.6 OTHER ADDITIVES

In more than 98% of all carbide production, cobalt is the binder. Nickel is sometimes used as a binder and the carbides of tantalum, titanium, molybdenum, vanadium, chromium and niobium may be alloyed with the tungsten carbide as grain growth inhibitors (Brookes, 2001; Luyckx, 1997).

Chromium, as Cr_3C_2, or vanadium, as VC, are added as grain growth inhibitors. TaC, NbC and TiC are also used as grain growth inhibitors but as the nominal grain size of the powder becomes smaller, only VC and Cr_3C_2 are effective (Brookes, 1979, 2001; Luyckx, 1997; Fry, 1982). These authors hold that VC also imparts high hardness resulting from a very fine microstructure.

TiC is used to resist diffusion attack during sintering that causes 'cratering', a structural defect in the product that reduces strength. TiC-based tools are considerably more brittle than tungsten carbide tools, so the TiC content is kept as low as possible (Brookes, 1979).

Tantalum also helps to resist 'cratering' but at a considerably higher cost. In addition, it improves the shock-resistant properties of the hardmetal. Niobium has a similar effect to tantalum but to a lesser degree. Although the complete separation of tantalum and niobium when used in hardmetal production is difficult (they have similar properties) and not really necessary, both the niobium and tantalum content of a powder are usually measured. If the raw materials already contain one of these elements, then the added concentration of the other must be adjusted to be able to predict the effect on the product properties. Similarly, if only one of the elements (niobium or tantalum) is measured during the quality control procedure, a false indication of the properties is obtained if the other element is also present undetected (Luyckx, 1997).

In research environments, a knowledge of the exact additive concentration in the tungsten carbide powder is required to determine how the physical properties of the product are affected. For example, Figure 3.1 shows the classification of crater resistance as a function of

tantalum or titanium concentration in carbide materials.

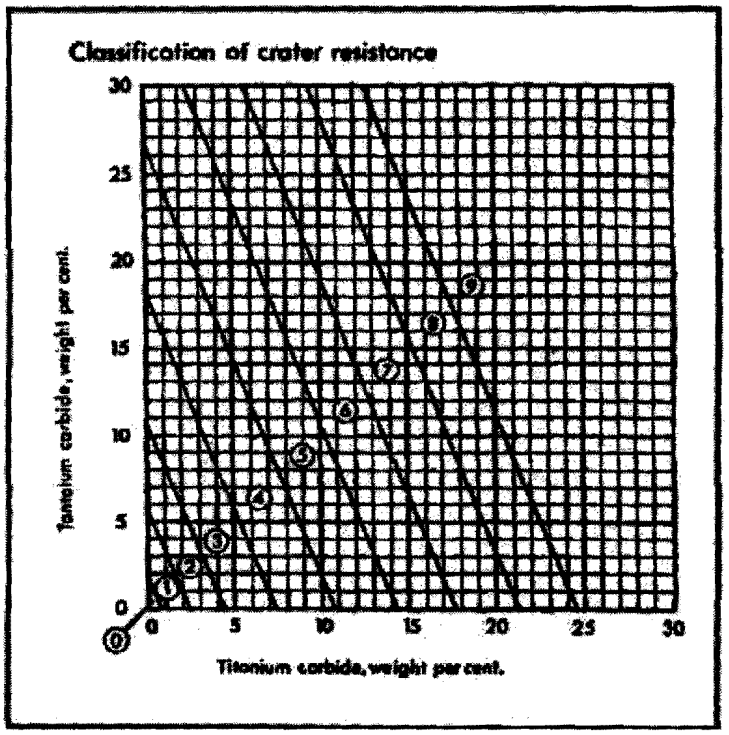

Figure 3.1: British Hard Metal Association (BHMA) numerical coding system for hardmetal properties. A three-digit code serves to classify the crater resistance property of the hardmetal (Brookes, 1979)

Although the coding system is hardly of interest here, Table 3.1 does show that the properties of the product change with change in the titanium or tantalum concentration.

3.7 TUNGSTEN CARBIDE POWDER (WC)

Tungsten carbide is produced by blending dry tungsten powder with carbon black and the required metal oxides, then firing this in a hydrogen atmosphere at temperatures of between 1400 and 2650°C (Luyckx, 1997). The chosen temperature depends on the particle size desired, again with smaller particle sizes being produced at the lower temperatures. The reaction, known as carburisation, proceeds as follows:

W + C ? WC

In the process, gaseous hydrocarbons are formed:

$CH_4 + W + C$? WC

and these combine with the tungsten to form W_2C, also known as "eta phase" tungsten carbide nuclei. As additional carbon is absorbed, polycrystalline WC particles are formed (Luyckx, 1997).

To obtain a 1:1 ratio of W:C, the amounts are calculated as follows:

$$\text{Mass of carbon in WC} = \frac{12 * 100}{184 + 12} = 6.12 \text{ g / 100 g},$$

but in practice a 3 to 10% excess of carbon is added, since a slight excess of carbon in the product has little effect on the properties. However, if the carbon content is too low, W_2C, is formed, which is undesirable. Figure 3.2 presents a flow chart for the production of tungsten carbide powder from the raw materials described above.

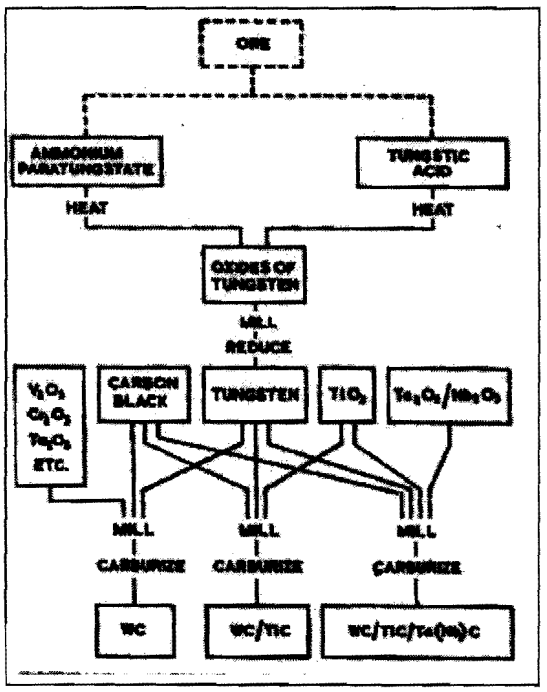

Figure 3.2: Simplified flow chart for the production of carbide powders (Brookes, 1979)

3.8 IMPURITIES AND QUALITY CONTROL

There are many sources of impurities and the quality of the raw materials is strictly controlled by testing before blending. According to Luyckx (1997), the presence of impurities and trace elements may lead to serious defects in the product, including pores, large crystals, weak interfaces, unwanted phases and inclusions. Tungsten carbide tools are used under extreme conditions (Brookes, 1979, 2001), for example in rock drilling and cutting of very hard materials, and the use of weakened products may have serious and expensive consequences. Table 3.3 (Luyckx, 1997) gives the desired characteristics of the starting materials and intermediate products.

In Table 3.4 (Luyckx, 1997) the maximum limits of impurities have been tabulated. The potassium and sodium content of coarse grain powders tend to be higher than in finer grades. The oxygen content of fine grain powders, however, tends to be higher (Luyckx, 1997).

Table 3.3: European data for the characteristics of starting materials and intermediate products (Luyckx, 1997)

Material	**Particle size range(μm)**	**Weight increase on annealing in air (%)**	**Approximate chemical analysis (%)**
Ammonium paratungstate	0.5-65	-	W: 70.2 Fe: 0.01 C: 0.01 S: 0.01 Si: 0.04 Alkalies: 0.03
Tungstic acid	0.5-11	-	W: 73.5 Fe: 0.05 C: 0.01 S: 0.01 Si: 0.04 Alkalies: 0.05
Tungsten trioxide	0.5-15	-	W: 78.6 Fe: 0.05 C: 0.01 S: 0.06 Si: 0.03 Alkalies: 0.1
Tungsten from tungstic acid	0.5-3	350°C for 5 min: 18-21	O_2: 0.2-0.4 Impurities: approx. as above
Tungsten from tungsten trioxide	0.5-5	350°C for 5 min: 18-21	O_2: 0.1-0.35 Impurities: approx. as above
Carbon, reduced	0.5-10	400°C for 30 min: 2.3	W: 99.2 Fe: 0.09 C: 0.06 S: 0.01 O_2: 0.4
Cobalt	1-3	400°C for 30 min: 28	Co: 98.6 Fe: 0.08 C: 0.1 Mn: 0.1 Si: 0.05 Ni: 0.1 Zn: 0.05 O_2: 0.6 Alkalies: 0.08
Graphite (milled)	-	-	C: 98.2 Ash: 0.6 Moisture 0.2 Volatiles: 0.9
Carbon black	-	-	C: 97.9 Ash: 0.05 Moisture: 0.1-2 S: 0.3-0.5 Volatiles: 1
Sugar charcoal	-	-	C: 94.7 Ash: 0.7 Moisture: 1.4 S: 0.3 Volatiles: 2.6

Table 3.4: Limits of impurities in raw materials (Luyckx, 1997)

Element	**Tungsten carbide (WC) powder (mg/kg)**	**Cobalt powders (mg/kg)**
Aluminium (Al)	<20	<50
Arsenic (As)	<5	-
Calcium (Ca)	<20	<100
Cobalt (Co)	<300	-
Chromium (Cr)	<30	-
Carbon (C)	-	<500
Copper (Cu)	<10	<20
Iron (Fe)	<200	<100
Lead (Pb)	<10	<10
Magnesium (Mg)	<10	<100
Manganese (Mn)	<10	<100
Molybdenum (Mo)	<90	-
Nickel (Ni)	<20	<500
Oxygen (O_2)	<500	-
Phosphorus (P)	<30	<10
Potassium (K)	<50	<50
Silicon (Si)	<40	<40
Sodium (Na)	<30	<50
Sulphur (S)	<30	<50
Tantalum (Ta)	<30	-
Tin (Sn)	<10	-
Vanadium (V)	<5	-
Zinc (Zn)	-	<50

CHAPTER 4

DISSOLUTION OF TUNGSTEN CARBIDE POWDERS

4.1 INTRODUCTION

In Chapter 2, the published dissolution methods of hardmetal powders were discussed. The methods used have mainly consisted of treating the sample with nitric, hydrofluoric and phosphoric acids. The drawbacks of using hydrofluoric and phosphoric acid have also been discussed and the problem of precipitation when using these methods pointed out.

4.2 THEORY

The complexity of the carbides make them very resistant to acid attack but they have been completely dissolved using hydrofluoric and nitric acid (ISO, 1983, 1985; Piippanen et al, 1997a, 1997b). Apart from the undesirability of hydrofluoric acid in an analytical solution, the precipitation of tungstic acid and tungsten fluoroborates is a problem (Piippanen, 1997a). Piippanen et al (1997a) attempted to stabilise the solution with phosphoric acid. The stabilising effect may be due to the solubility of tungstophosphoric acid in water, which is stated to be 1 part in about 0.5 parts water (Naish et al, 1953; The Merck index, 1989; Townshend et al, 1995). However, the presence of 'heavy' acids, such as phosphoric and sulphuric acid, in a solution for ICP analysis tends to give rise to nebulization interferences unless strict matrix matching techniques are used (Kawaguchi, 1995).

Piippanen et al (1997a) used a two-step dissolution method with phosphoric acid and hydrochloric acid, followed by the addition of hydrofluoric acid and nitric acid. Since the volume of hydrofluoric acid was low (0.2 to 0.5 ml), no boric acid was added to complex the

hydrofluoric acid after the dissolution.

A dissolution method using hydrogen peroxide was very briefly described in a CSIR in-house manual. Rogers, Matthews, van Maarseveen et al (1987:33) stated that a one gram piece of tungsten carbide "was dissolved in a solution containing 5% aqua regia and 95% H_2O_2" at a temperature of 85°C. No other details were available.

In an attempt to determine the mechanism, the dissolution of tungsten carbide in water over a period of 1400 hours was studied by Andersson and Bergström (2000). They found that the WC was continually oxidised to WO_3 when the pH was above 3. The overall dissolution reaction in an unbuffered solution was postulated to be:

$$15WO_3 + 21H_2O \; ? \quad H_3W_6O_{21}^{3-} + 9(WO_3 \,.\, 2H_2O) + 3H^+$$

Andersson et al (2000) also found that when cobalt is present, the solubility decreased, suggesting that cobalt was able to passivate the oxidised WC surface. The solubility was also found to decrease when the pH was below 3.

A brief reference to the use of tartaric acid as an alternative complexing agent for tungsten was found in a manual of in-house methods (Stoch, 1986). No details of the experiment were given.

4.3 SAMPLE DISSOLUTION

The problems with the dissolution methods for tungsten carbide described in the literature are covered in Chapter 1. These published dissolution methods were found to be time-consuming (45 to 75 minutes per sample) and consistent dissolution results could not be obtained. Some aliquots dissolved well, while other aliquots of the same sample produced a copious precipitate under the same conditions. The hydrogen peroxide dissolution method described by Rogers et al (1987:33) was therefore tested.

A 0.5000 g aliquot of finely powdered tungsten carbide-cobalt was treated with 30 ml of 5% (v/v) aqua regia (1 part nitric acid and 3 parts hydrochloric acid) in 30% hydrogen peroxide in a 150 ml glass beaker covered with a watch glass. The mixture was gently heated on a water bath at 80°C to start the reaction. The mixture was removed from the heat at this stage, since the hydrogen peroxide tended to bubble vigorously when heated. A 0.6 g portion of solid tartaric acid was added to help complex the tungsten and prevent it from precipitating.

The solutions were kept covered and occasionally manually swirled during the next 10 minutes until the sample was completely dissolved. If a tendency to precipitation was observed, a few drops of 30% hydrogen peroxide were added.

The solutions were then made up to 100 ml with deionised water; vanadium and chromium were analysed by ICP-OES. The solution was diluted further in order to measure the cobalt, tantalum and titanium concentrations.

Differing weights of tartaric acid, from 0.2 g to 1 g were added to the mixture in order to

determine the optimum effective amount. The method was also tested on larger pieces of tungsten carbide.

4.4 QUALITY CONTROL

A reference material of powdered cemented carbide (SRM 889) containing 9.50% cobalt, 4.60% tantalum and 4.03% titanium was purchased from the National Institute of Standards & Technology (NIST). This material was analysed with every batch of samples which contained cobalt, tantalum and titanium.

No certified reference material which contained vanadium could be obtained but a sample of tungsten carbide-cobalt powder, containing 0.63% vanadium, which had been analysed by the manufacturer, was procured. This material could be used as a secondary reference standard when samples were analysed. No reference material containing chromium could be located.

Where the composition of the sample did not match that of the available reference materials and in the analysis of chromium, sample solutions were spiked at appropriate concentration levels with the element of interest. For these spiked quality control solutions, certified reference solutions of the required element, obtained from Merck Chemicals, were used.

The calibration reference solutions were made up by serial dilution from Merck certified single element reference solutions, with matrix-matching as described in Chapter 5.

4.5 DISCUSSION/ CONCLUSIONS

Complete dissolution of powdered tungsten carbide-cobalt samples was generally achieved within 10 minutes. The role of oxidation in the dissolution of tungsten carbide (Andersson, 2000) may well explain why hydrogen peroxide has such a dramatic effect on the solubility of tungsten carbide. The fact that an oxidising acid (nitric acid) was used in published dissolution methods (ISO, 1983, 1985; Piippanen, 1997a) also points to the importance of oxidation processes in the dissolution mechanism.

The aqua regia was used mainly to improve the solubility of the metallic elements present in the sample. When 5% (v/v) nitric acid in 30% hydrogen peroxide was used instead of aqua regia, the sample was still completely dissolved but the dissolution time was increased, in some cases by 35 minutes.

It was observed that as the hydrogen peroxide in the solution dissociated, tungstic acid tended to precipitate from the solution. The addition of a few drops of hydrogen peroxide was found to re-dissolve the precipitate. The hydrogen peroxide could thus not be removed from the solutions prior to ICP-OES measurement without causing tungsten compounds to precipitate. To investigate the concentration of the analyte elements remaining in the solution after some precipitation had occurred, several solutions were filtered and analysed by ICP-OES. It was found that up to 75% of the cobalt, tantalum, and titanium had co-precipitated with the tungsten compounds. No vanadium or chromium were detectable in the filtered solutions, possibly because the concentration in the solid samples was generally less than 0.2%.

During ICP-OES measurement, the mandatory presence of hydrogen peroxide in the analytical

solutions was found to produce fine bubbles in the nebulizer tubing, with a resultant deterioration in precision. However, the precision was found to be acceptable; the %RSD of three measurements at a 0.5 ppm level were generally found to be less than 7%. The measurement values were verified by the re-measurement of the same solution during a run to ensure satisfactory results. As a further check, replicate aliquots of each sample were routinely analysed. The efficiency of the dissolution can only be demonstrated by accuracy of the measurement results for certified reference materials. In Table 4.1 some of the results for elements measured in reference materials are tabulated. Further details of the results for each individual element are available in Chapter 5.

Table 4.1: Measurement results after aqua regia/ hydrogen peroxide dissolution of tungsten carbide-cobalt

Element measured	**Certified/ expected concentration in reference material* (g/100 g)**	**Measured concentration after aqua regia/ hydrogen peroxide dissolution (g/ 100 g)#**
Cobalt	9.50 ± 0.15	9.56 ± 0.19
Tantalum	4.60 ± 0.15	4.48 ± 0.28
Titanium	4.03 ± 0.10	3.96 ± 0.16
Vanadium	0.63	0.59 ± 0.06

** According to the NIST Certificate of Analysis, the estimated uncertainty is based on judgement and represents an evaluation of the combined effects of method imprecision, possible systematic errors among methods and material variability.*
 # The uncertainty is based on equation 5.3 (Chapter 5) and involves replicate measurements taken over a period of several months. In all cases, n>10.

The confidence limits for the vanadium secondary reference material were not known and so it is difficult to properly evaluate the result. However, spiking experiments suggest that there may be a slight measurement problem (the details are given in Chapter 5). The results for the other elements lie within the stated uncertainty ranges. Since no reference material containing chromium was available, no results for chromium are included in Table 4.1. From the results in Table 4.1 there is no evidence that the dissolution procedure is not effective.

Approximately one hundred samples of tungsten carbide of differing compositions were

dissolved by the aqua regia/ hydrogen peroxide method over a period of three years. No dissolution problems were encountered and it was not found necessary to adapt the method when samples with different compositions were analysed.

It was observed that tartaric acid additions of less than 0.5 g were not effective in preventing precipitation, in spite of the high hydrogen peroxide concentration. This would indicate that hydrogen peroxide alone is not enough to keep the sample in solution. On the other hand, even when 1 g of tartaric acid was added to the solution, precipitation still occurred when the hydrogen peroxide was removed. It was found that for all the samples analysed, 0.6 g tartaric acid added to a solution of 0.5 g tungsten carbide sample prevented the precipitation of tungsten compounds while hydrogen peroxide was also present. No attempt was made to determine the optimum hydrogen peroxide concentration. It is thought that tartaric acid may react with tungstate in a similar manner as citrate with tungstate to form a more stable complex (Williams, 1979: 67).

It was found that single pieces of solid tungsten carbide (as opposed to powdered samples) larger than 0.5 g could not be completely dissolved by the nitric/ hydrofluoric acid method, even after 30 hours, but pieces of up to 1 g were found to dissolve overnight in the aqua regia/ hydrogen peroxide solution. Since the hydrogen peroxide dissociates over a period of time, more problems were experienced with tungstic acid precipitation when lengthy dissolution procedures were necessary.

In contrast, the acid dissolution methods (ISO, 1983, 1985; Piippanen et al, 1997a) were not found to give consistent results with some samples, notably the ones with added iron, which reacted violently with the acid. Sometimes the composition of the commercial samples was

unknown on receipt at the laboratory, with predictably messy results when the nitric/ hydrofluoric acid dissolution was attempted. The precipitation of tungstic acid and the co-precipitation of analyte elements could not be reliably controlled. The first step of the method described by Piippanen (1997a) requires 30 minutes. The rest of the dissolution method, including the cooling step, normally required about 1 hour.

In addition to the reduced time required for the dissolution step during the aqua regia/ hydrogen peroxide dissolution procedure, the reagents were found to be up to five times less expensive than those used by previous researchers. The aqua regia/ hydrogen peroxide method does not require the use of hydrofluoric acid, which requires stringent safety precautions and well as being corrosive to glassware and instrumentation parts. In general, Teflon beakers are required for use with hydrofluoric acid and they are at least six times more costly than glass beakers of the same volume.

The aqua regia / hydrogen peroxide dissolution method can thus be shown to be effective and reliable, as well as faster and less expensive than previous published dissolution methods. No additional metallic elements which could possibly interfere with the ICP-OES measurement of the analyte elements were introduced. In spite of the fact that hydrogen peroxide causes small bubbles in the nebulizer tube during ICP-OES measurement (this can be classified as a physical interference) the effect is not serious and accurate results are still obtained. No matrix matching of the calibration and quality control reference solutions is required with respect to hydrogen peroxide, as would have been required had phosphoric acid been used. As can be seen from Table 4.1, the precision is negatively affected when compared to the precision of certified reference materials but still within reasonable limits. The details for each element are recorded in Chapter 5.

CHAPTER 5

INSTRUMENTATION

5.1 INTRODUCTION

Detailed information on ICP-OES systems can be obtained from the works of Moore (1989), Boss & Fredeen (1999), Thompson et al (1983), Tissue (1996) and Townshend et al (1995). A brief description from these sources follows.

Inductively coupled plasma analysis usually involves the introduction, in liquid form, of the elements to be analysed in an argon plasma, induced by a high-frequency field and realizing temperatures in the region of 8 000 K. With the aid of a stream of argon gas, a nebulizer transforms the liquid into an aerosol. Separation of the large droplets is achieved in a spray chamber. The aerosol/ argon mixture passes through an injector tube into the plasma. There the aerosol is atomised and excited.

When the atoms of an element are excited, their electrons change energy levels by absorbing energy, and light with a characteristic wavelength is emitted when the electrons return to their ground state. The energy required to excite the atoms or ions is supplied by a radio frequency generator. High frequency radiation is used to ionise a stream of argon, which forms a plasma via an induction coil. The sample within the plasma is mostly reduced to an atomic or ionic state and the atoms are excited by the plasma.

Discrimination between these wavelengths is performed by a spectrometer which can take the form of a monochromator or polychromator. The beam of light is focussed onto the primary slit

of the spectrometer by a convergent lens and then reaches an interferometric (holographic) diffraction grating. When light strikes the grating, which has closely spaced grooves etched into its surface, the light is diffracted at an angle that is dependent on the wavelength of the light and the line density of the grating.

A photomultiplier tube or solid state detector behind the exit slit receives the radiation and transforms it into electrical signals which are captured by the data processing system. As each angular position of the grating corresponds to a well-defined wavelength, each beam of light passing though the exit slit of the monochromator is characteristic of the elements analysed (qualitative analysis). The intensity of the light beam falling onto the detector is measured and is proportional to the concentration of each element in the sample aerosol. A calibration curve for each element can be drawn up by the data processing system and the concentration of the elements may be determined (quantitative analysis).

Figure 5.1 (Tissue, 1996) shows a simplified representation of an atomic emission system. Detailed descriptions of each component part of the ICP-OES system follow in this chapter.

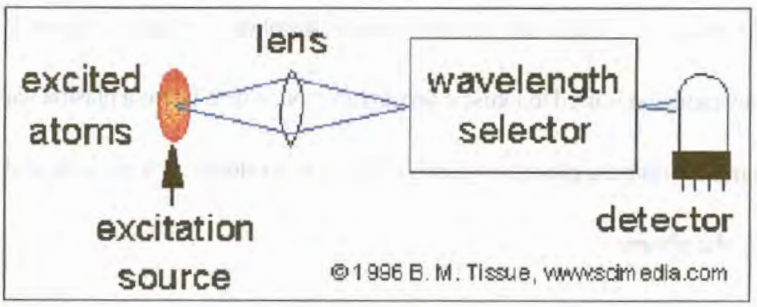

Figure 5.1: Schematic diagram of an atomic emission system (Tissue, 1996)

5.2 INSTRUMENTATION /THEORY

The experimental work was performed using a Jobin Yvon JY-24 sequential ICP-OES system, shown in Figure 5.2. The JY-24 is equipped with a 0.64 m Czerny-Turner monochromator, a direct drive 2400 lines per mm grating and a 40.68 MHz generator.

Figure 5.2: The Jobin Yvon inductively coupled plasma-optical emission spectrometer (Jobin Yvon Emission Instruments S.A.)

The sample introduction system is thermoregulated and includes an argon humidifier. A separate attachment for argon sheath gas is supplied. The use of the sheath gas attachment allows a tangential stream of argon to reduce contact of the sample aerosol with the injector tube. According to Jobin Yvon Emission Instruments S.A, sheath gas prevents crystallization at the top of the inner torch tube when samples with a high salt content are analysed, and it also helps to reduce memory effects. With the JY-24, the sheath gas flow rate is automatically adjusted when alkali elements are analysed, so that the plasma is optimised for the best limits of detection.

A Meinhard concentric nebulizer with a 3 ml/ minute flow rate and a Schott double pass glass spray chamber were used. All the work was carried out using a demountable torch.

5.2.1 The Monochromator

Accoding to Moore (1989), sequential instruments are designed to move sequentially from one wavelength to the next during the measuring sequence. It therefore measures the elements in the sample one after the other. Faster results are obtained with simultaneous (measuring all the elements at the same time) instruments. The main reason that sequential instruments are used is to save costs but there is also increased flexibility. An almost unlimited range of analytical lines can be used.

In sequential instruments, a monochromator enables a specific spectral band to be selected. The emission spectrum of an ICP plasma is composed primarily of spectral lines over a continuous background and is very complex. Each element emits radiation at characteristic wavelengths and so the precision of the analytical results depends on the separation of the spectral lines.

The JY-24 utilises a 0.64 m focal length monochromator with a plane interferometric (holographic) grating. A wavelength drive is used with a computer-controlled stepper motor. A schematic representation of the Czerny-Turner mounting is presented in Figure 5.3 (Thompson et al, 1983). The grating is rotated and the spectrum is moved across the exit slit.

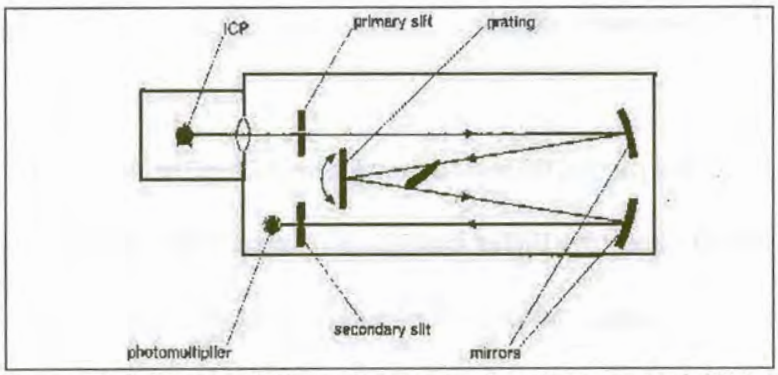

Figure 5.3: Schematic of a Czerny-Turner mounting (Thompson et al, 1983)

The JY-24 also includes a second, smaller monochromator, a reference monochromator. When using an internal standard in the sample solution, the emission for this element is measured by the reference monochromator at the same time as the primary monochromator measures the element of interest at the chosen wavelength. In this manner the operator can compensate for small fluctuations in the measurement system and produce more accurate results. If the primary monochromator were used to measure the emission of the internal standard as well as that of the sample, the monochromator would have to move from one wavelength to the other during the procedure. This means that the measurements would not be simultaneous, but sequential, and true internal standardization would not have taken place. Internal standards, such as yttrium, are normally used to correct for small system instabilities (e.g. power or nebulizer pressure fluctuations). They would not correct for systemic effects, such as spectral interferences.

Diffraction gratings are dispersive optical components with grooves or lines parallel to each other. The JY-24 includes an interferometric (holographic) grating, on which the lines are produced by the interaction of an interference pattern with a photosensitive layer (ruled gratings are mechanically produced by a ruling engine or laser). Interferometric gratings are considered superior to ruled gratings as they have a very high stray light rejection and the lines are better distributed across the surface of the substrate. Because interferometric gratings have negligible

groove errors, very high resolution is possible.

The higher the number of lines per mm, the better the resolution which can be obtained. The JY-24 has a grating with 2400 lines/ mm. Higher resolution is obtained with instruments using a 3600 lines/mm grating but sodium, lithium and potassium cannot be measured due to a decreased wavelength measurement range (Jobin Yvon Emission Instruments S.A.).

A schematic diagram of how the diffraction grating separates two wavelengths of light is shown in Figure 5.4 (Boss & Fredeen, 1999).

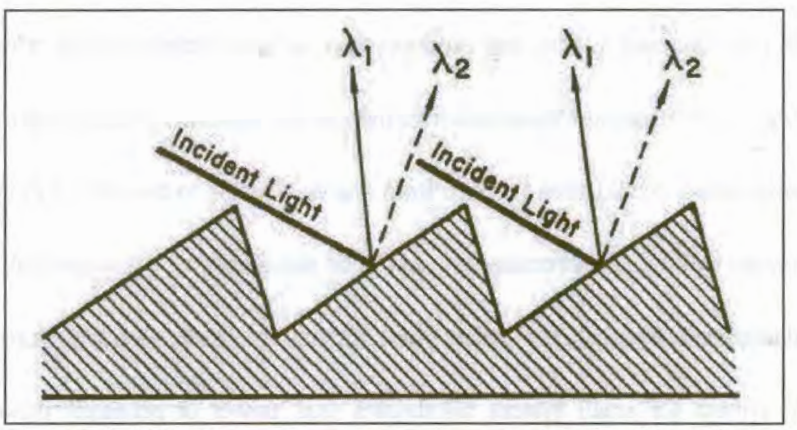

Figure 5.4: Diffraction grating separating two wavelengths of light (Boss & Fredeen, 1999)

5.2.2 The Generator

The 40.68 MHz radio frequency generator of the JY-24 ICP-OES has a system of anode lines tuned to a quarter wavelength controlling frequency. It is equipped with a voltage stabilizer and a reflected power controller. The power can be set at two pre-selected levels (1 kW or 1.1 kW) or may be varied continuously up to a maximum incident power of 2300 VA. The power is transmitted to the plasma torch via a water-cooled 3-turn induction coil. The power setting used

for the work described here was 1 kW. The generator also has an automatic plasma ignition system and protection against leaks and outside radio frequencies.

5.2.3 The Torch

The demountable ICP torch consists of two concentric quartz tubes (connected to the argon source) which surround the central injector tube. The injector tube is connected to the nebulizer via the sheath gas system and is constructed of alumina, quartz or sapphire. A 3 mm alumina tube was used in all the experimental work. When solutions of tungsten carbide are analysed by ICP-OES, a black deposit builds up on the quartz torch. The deposit cannot be removed and eventually makes the quartz brittle, causing it to flake off the edges. Alumina was found to remain smooth in spite of the deposit. A schematic representation of the demountable torch is shown in Figure 5.5.

One argon inlet on the torch supplies cooling gas and supplies the plasma itself, while another supplies auxiliary (argon) gas, required during the analysis of samples containing organic solvents. There is also an inlet from the nebulizer and a sheath gas supply. The latter two are used for the formation, transport and injection of the sample aerosol into the heart of the plasma. An argon flow rate of 14 ℓ/ min was used for the cooling/ plasma generation supply. Argon flow rates for the sheath gas and nebulizer were set at 0.2 ℓ/ min and 0.3 ℓ/ min, respectively. The auxiliary gas supply was not required.

As mentioned above, the analysis of tungsten carbide samples was found to cause a black deposit to build up on the quartz outer torch tube. This outer tube is shown in Figure 5.5. When other types of sample were analysed on the same instrument, the demountable system allowed

the replacement of only the outer torch tube. It also contributes to considerable cost savings when the tube is to be replaced.

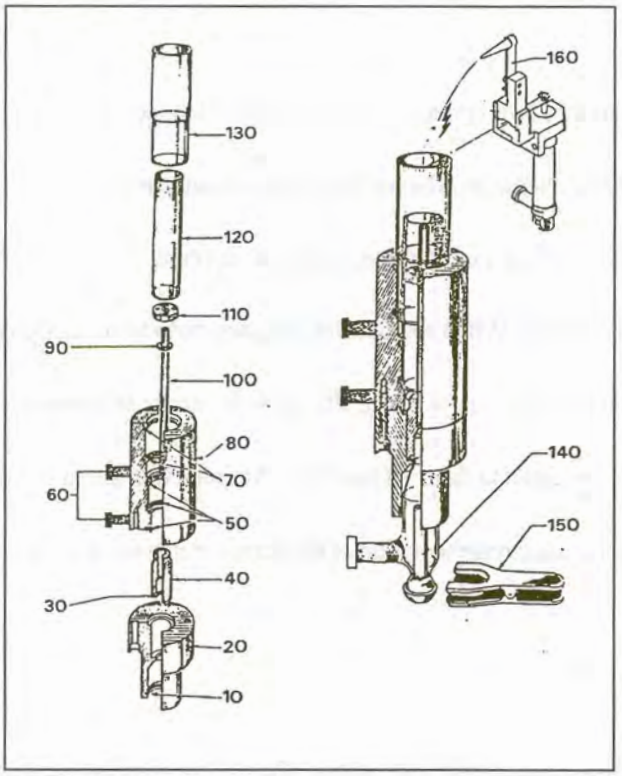

Figure 5.5: Schematic of the Jobin Yvon demountable torch and holder, (Jobin Yvon Emission Instruments, S.A.) where:
130 is the outer torch tube with a ground fitting
120 is the inner torch tube
100 is the alumina injector tube, which is centred in the torch by a spacer (110)
60 is the argon inlet, the upper coupling supplies the plasma while the lower coupling supplies the auxiliary gas
20, 40 and 80 are supports for the sheath gas device, the injector and the torch, respectively
10, 30, 50, 70 and 90 are o-rings which ensure a leak-free system
140 is the sheath gas device
160 is the plasma ignitor
150 is the clamp connecting the spray chamber to the sheath gas device

5.2.4 The Plasma

The following description of an ICP plasma was found in the works of Moore (1989) and Thompson et al (1983). A plasma consists of partially ionised atoms or molecules. Radio frequency currents in the induction coil create oscillating magnetic fields whose force lines are

orientated axially to the inside of the quartz tube. Induced currents (Foucault currents) are formed. This works on the same principle as the secondary winding of a transformer in short circuit. The electrons are accelerated at each half-period, since the induced magnetic fields vary in both intensity and direction. Heating occurs because of the acceleration and resistance of the argon electrons to the movement (changes in kinetic energy).

Initially, the electrons or ions must be seeded in order to create the plasma. After this, the plasma is self-perpetuating in the same way as a transformer (with the induction coil as the primary winding and the plasma as the secondary winding). The plasma may reach temperatures in the order of 6 000 to 10 000 K. To prevent the quartz tube from melting, a flow of cooling argon gas isolates the plasma from the quartz tube. The dissociation and ionization of the sample aerosol will be more efficient if the particles pass through the centre of the plasma (7 000 to 10 000 K). A representation of an inductively coupled plasma is presented in Figure 5.6. (Tissue, 1996).

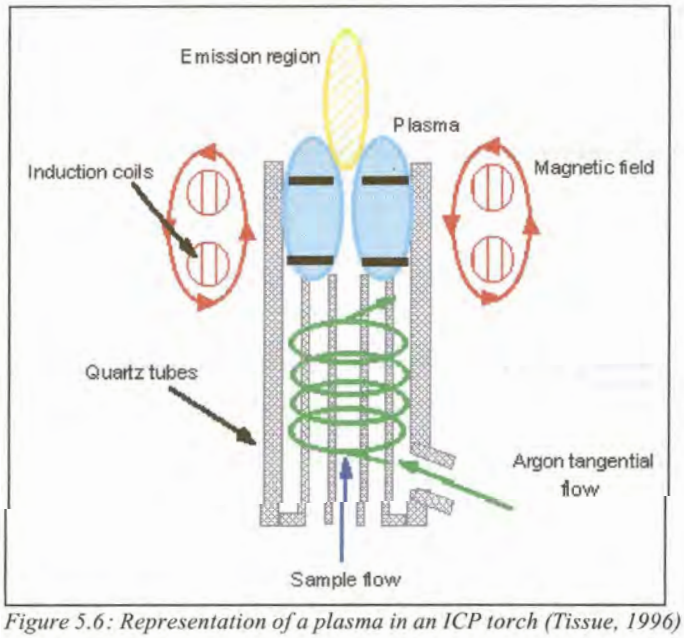

Figure 5.6: Representation of a plasma in an ICP torch (Tissue, 1996)

5.2.5 The sample introduction system

The sample, in liquid solution form, is pumped to the nebulizer via a peristaltic pump. Peristaltic pumps use a series of rollers that push the sample solution through the tubing (peristalsis). The pump itself does not come into contact with the solution and thus contamination from the pump is not a consideration. Pump tubing of inner diameter 0.030 cm was used. The pump speed was set at 30 ml/ min and this system was found to deliver the sample solution to the nebulizer at a rate of 2.5 ml/ min.

The nebulizer, in this case a glass Meinhard concentric nebulizer with a flow of 3 ml/ min, converts the liquid into an aerosol that can be transported to the plasma (Boss & Fredeen, 1999). The nebulization process is one of the critical processes in ICP analysis. Because only small droplets are useful in ICP analysis, the ability of the nebulizer to produce small droplets for a wide variety of samples largely determines the effectiveness of the nebulizer. Pneumatic nebulizers use high-speed gas flows to create the aerosol. The solution is forced through a capillary tube to a low pressure region created by a gas flowing rapidly past the end of the capillary. The low pressure and the high-speed gas combine to break up the solution into an aerosol. The construction of a Meinhard concentric nebulizer is shown in Figure 5.7. (Boss & Fredeen, 1999).

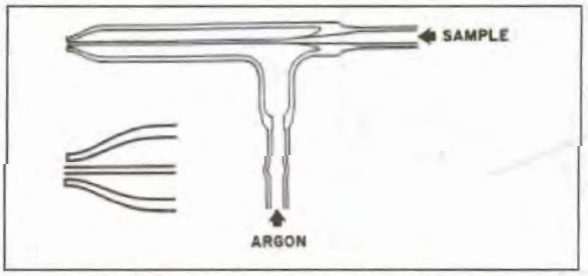

Figure 5.7: A Meinhard nebulizer used for ICP, constructed of borosilicate glass (Boss & Fredeen, 1999)

Because ICP nebulizers require lower sample carrier flow than atomic absorption nebulizers, the liquid and gas orifices are smaller. The concentric pneumatic nebulizers give excellent sensitivity and stability but are more subject to clogging, especially with solutions containing high concentrations of dissolved solids. The JY-24 is equipped with an argon humidifier, which produces moist argon and decreases the possibility of crystallization in the nebulizer. It also helps to keep the torch clean. The humidifier is, basically, a vessel filled with water though which the argon flows prior to reaching the nebulizer.

The aerosol passes into the spray chamber, which is designed to separate large drops from the aerosol and direct them to the drain. According to Moore (1989), spray chambers also smooth out pulses that occur during nebulization due to pumping of the solution. ICP spray chambers generally separate out droplets larger than 10 µm. This amounts to 95 to 99% of the sample being discarded. A Scott double pass spray chamber, similar to that shown in Figure 5.8 (Boss & Fredeen, 1999), was used in the experimental work.

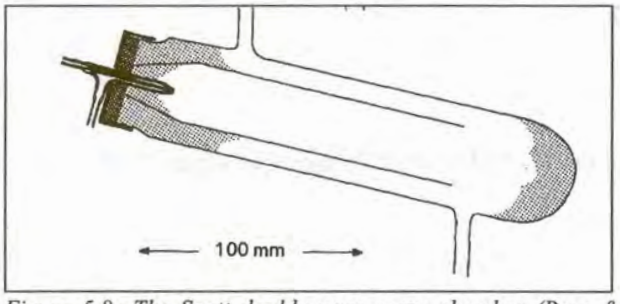

Figure 5.8: The Scott double pass spray chamber (Boss & Fredeen, 1999). The nebulizer is shown entering the spray chamber at the left.

From the spray chamber, the aerosol passes though the sheath gas device and is injected into the plasma through an injector tube. The injector tube is shown in Figure 5.5 and is held centrally in the inner torch tube by a specially designed spacer. A 3 mm alumina injector tube is used, since

alumina was found to withstand continuous use better than quartz, remaining smooth even when a deposit forms on the tip. The alumina injector tube could be used over a period of several months before it had to be replaced. However, dissolved solids may cause clogging in the injector tube. To overcome this problem, the JY-24 has a sheath gas system. The sheath gas device produces a stream of argon which perfectly 'sheaths' the sample and prevents the aerosol from coming into contact with the sides of the tube. This reduces memory effects from the tube and prevents clogging.

For sodium only two lines are generally recommended, 588.995 nm and 589.59 nm, and for potassium only the 766.49 nm line is used. Since these elements also behave differently from other elements, it is important that conditions for these elements are optimised. Sodium and potassium are measured using atom lines and they have lower ionisation potentials than other elements. The best emission intensities are obtained higher in the ICP plasma, where the degree of ionisation is lower (Thompson and Walsh, 1983). Therefore, when alkali elements are analysed, the sheath gas is automatically adjusted to give optimum sensitivity for these elements (Jobin Yvon Emission Instruments S.A.).

The sample introduction system of the JY-24 ICP-OES is shown in Figure 5.9.

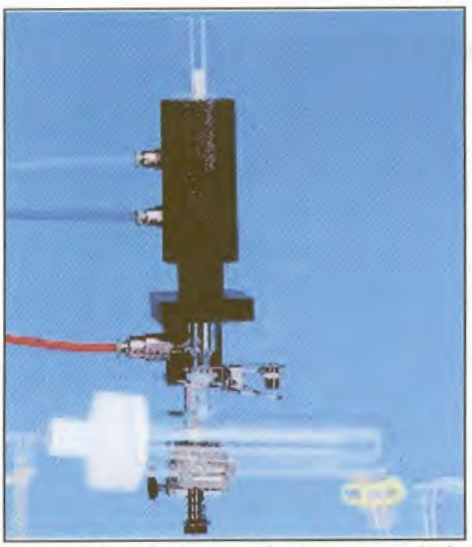

Figure 5.9: Sample introduction system (Jobin Yvon Emission Instruments S.A).
The spray chamber with a sheath gas device and the torch in its support are shown.
The nebulizer can be seen in the spray chamber to the left.

5.2.6 The Detector

Once the proper emission line has been isolated by the spectrometer, the detector is used to measure the intensity of the emission line. According to Boss & Fredeen (1999), the most common is still the photomultiplier tube (PMT), which is also used in the JY-24. The PMT is a vacuum tube that contains a photosensitive material, the photocathode. The photocathode ejects electrons when it is struck by photons of light. These ejected electrons are accelerated towards a dynode which ejects two to five secondary electrons for every electron that strikes its surface. The secondary electrons strike another dynode and a multiplicative effect is caused. Typical PMTs contain 9 to 16 dynode stages. The final step is the collection of the secondary electrons at the last dynode by the anode. A typical PMT is shown in Figure 5.10 (Boss & Fredeen, 1999). The electrical current measured at the anode is used as a relative measure of the intensity of the radiation at the PMT. The PMT can be used to amplify very weak signals and its range of

response can be extended over nine orders of magnitude in light intensity.

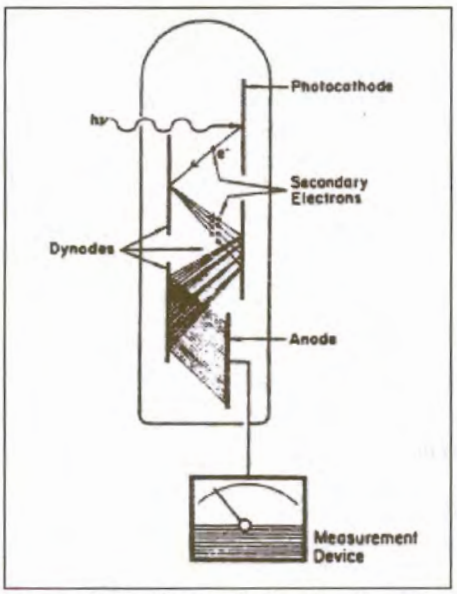

Figure 5.10: Photocathode, dynode and anode layout of a photomultiplier tube (Boss & Fredeen, 1999)

5.3 INSTRUMENT CONDITIONS

The radio frequency on the JY-24 ICP-OES is 40.68 MHz. The monochromator has a focal length of 0.64 m and the grating is grooved at 2400 lines/ mm. The following conditions were maintained for all the sample measurements:

RF power:	1000W
Reflected power:	<1W
Plasma argon flow:	14 ℓ/ min
Nebulizer argon flow:	0.3 ℓ/ min
Sheathing argon flow:	0.2 ℓ/ min

The JY-24 is capable of measuring a chosen reference line before every analysis. This is to check that the monochromator is still properly aligned to measure the correct wavelength. The

carbon line at 193.026 nm was chosen because it is possible for the instrument to measure atmospheric carbon dioxide (and so no special sample needs to be introduced though the nebulizer).

The entrance slit of the monochromator was set at 20 motor steps and the exit slit at 25 steps. As each motor step corresponds to 0.001 nm, the slits are effectively 0.020 nm and 0.025 nm wide. This is the recommended setting for measurements in the concentration range 0.5 to 50 mg/ ℓ for the JY-24 instrument. The resolution of the monochromator is defined by the width of the slit used. The narrower the slit, the better the sensitivity and resolution but a higher integration time when measuring is also required (Jobin Yvon Emission Instruments, S.A.).

For the data acquisition (measurement) phase of the analysis, the 'Gaussian' mode was selected. The software scans around the theoretical position of the peak and determines a gaussian curve corresponding to these points. This mode can compensate for small variations in the peak position. The integration time for each point is short (0.5 s) because a relatively large number of data points were chosen. For the measurement, 9 data points were selected while the calculation of the gaussian curve was based on 5 points. This setting gives the best compromise between measurement speed and precision. When 11 measurement points and 7 calculation points are selected, for example, the measurement would be slower but precise. A choice of 7 measurement points and 5 calculation points would result in a faster but less precise measurement.

5.4 REAGENTS AND REFERENCE MATERIALS

Certified stock reference solutions of tungsten, cobalt, tantalum, titanium, vanadium and chromium were obtained as 1000 mg/ ℓ solutions from Merck Chemicals. The cobalt solution used to matrix match the calibration solutions was prepared from the dissolution of pure cobalt sponge (BDH) in dilute hydrochloric acid.

The stock solutions were diluted with 8.2 MΩ.cm deionised water and analytical reagent (AR) grade hydrochloric acid.

The hydrogen peroxide used for the dissolution step was BDH analytical grade and the tartaric acid Merck AR grade.

5.5 STATISTICAL TREATMENT

Several statistical methods were used during the evaluation of the results and were applied mainly to assess the precision, accuracy and confidence limits. The work of Miller & Miller (1993) was used as a guide. These methods were also used to compare the results of two different sets of measurements. Only statistical methods which were used in the evaluation of experimental results are discussed, and this section is not intended as an exhaustive guide to statistics.

The mean was calculated according to the formula:

$$\bar{x} = \frac{\sum_i x_i}{n} \qquad (5.1)$$

in order to report a single representative value from a series of measurements.

The standard deviation, s,

$$s = \left\{ \frac{\sum_i \left(x_i - \bar{x}\right)^2}{n-1} \right\}^{\frac{1}{2}} \qquad (5.2)$$

gives a measure of the spread of the results around the mean value. The standard deviation is used in many calculations (e.g. confidence and tolerance intervals, significance tests, evaluation of proficiency studies). If the data tends towards a normal distribution, the standard deviation may be used to estimate the confidence limits of the mean. The rule of such distribution predicts that 95% of the measurements will fall within 2s of the mean, while 99% of the results will be within 3s of the mean.

The standard deviation is sometimes expressed as a percentage, i.e. $100s/\bar{x}$, and is called the relative standard deviation (RSD) or the coefficient of variation (CV). The RSD has the advantage of enabling the comparison of the spread of different sets of results with differing means.

The confidence limits of the mean are generally calculated from the formula

$$\mu = \bar{x} \pm \frac{ts}{\sqrt{n}} \qquad (5.3)$$

which is especially appropriate for small sample sizes. In practice the t-values provided by statistical tables or by computer software are related to the number of degrees of freedom (usually given the symbols d.f. or the Greek letter ν) involved in the calculation. Confidence levels of 95% were employed throughout.

Rearrangement of equation 5.3 gives

$$t = | \bar{x} - \mu | \frac{\sqrt{n}}{s} \quad \text{or} \quad t = \frac{|\bar{x} - \mu|}{s/\sqrt{n}} \qquad (5.4)$$

and allows the comparison of the mean of an experiment with a reference value. The calculation is normally done in a 2-tailed form, since it is not known beforehand whether the mean will be higher or lower than the expected ('true') value. The t-tests were performed with the aid of Microsoft Excel spreadsheets.

The estimated standard deviation, s_{x0}, on the concentration values, x_0, can also be calculated to obtain a measure of the uncertainties involved. According to Miller and Miller (1993: 113) it can be shown that the optimum number of standards in a calibration curve is seven. In this study, four-point calibration curves were used, since the samples were analysed in a routine laboratory where the best quality results are balanced with turn-around time and cost reduction. The calculation of s_{x0} gives an estimate of the error in the measurement, but other effects, such as sampling, sample dissolution and dilution errors also affect the uncertainty. At least two aliquots of each sample were dissolved and analysed, mostly at two analytical lines, and equation 5.3 was used as an approximation of the combined measurement uncertainty. The recent international trend towards comprehensive uncertainty calculations would certainly require that a more complete estimate be produced.

The F-test, conveniently performed with the help of a Microsoft Excel spreadsheet, is used to compare the standard deviations of two samples, i.e. relating to the precision of the results. F is given by

$$F = \frac{S_1^2 / \sigma_1^2}{S_2^2 / \sigma_2^2} \qquad (5.5)$$

The null hypothesis is that H_0: $\sigma_1^2 = \sigma_2^2$ thus the equation 5.5 becomes:

$F = s_1^2/s_2^2$, or s_2^2/s_1^2 (5.6)

with F always larger than 1. Values of F greater than the critical values (Microsoft Excel provides probability values directly) indicate that the ratio of the variances calculated is larger than would be expected at the confidence level in use (normally 95%), and hence that the null hypothesis of equal variances can be rejected.

The least squares principle was used for the regression statistics, where the least squares straight line is given by

$$y = bx + a \qquad (5.7)$$

and

$$b = \frac{\sum_i (x_i - \bar{x})(y_i - \bar{y})}{\sum_i (x_i - \bar{x})^2} = \frac{n\sum_i x_i y_i - \sum x_i \sum y_i}{n\sum_i x_i^2 - \left(\sum x_i\right)^2} \qquad (5.8)$$

The correlation coefficient was calculated from the formula

$$r = \frac{\sum xy}{\sqrt{\sum x^2 . \sum y^2}} \qquad (5.9)$$

but the coefficient of determination (r^2) was used throughout this text to estimate the linear fit to the data. The data was plotted and linearity confirmed by visual inspection.

The random error in x and y of the regression line: y = bx + a was found from

$$s_{y/x} = \left\{ \frac{\sum_i (y_i - \hat{y}_i)^2}{n-2} \right\}^{1/2} \tag{5.10}$$

The error of the slope was calculated from

$$s_b = \frac{s_{y/x}}{\left\{ \sum_i (x_i - \bar{x})^2 \right\}^{1/2}} \tag{5.11}$$

while the error in the intercept is given by

$$s_a = s_{y/x} \left\{ \frac{\sum_i x_i^2}{n \sum_i (x_i - \bar{x})^2} \right\}^{1/2} \tag{5.12}$$

The limit of detection (LOD) was calculated as the analyte concentration giving a signal equal to the blank signal, y_B, plus three standard deviations of the blank, s_B:

$$\text{LOD} = y_B + 3s_B \tag{5.13}$$

CHAPTER 6

MEASUREMENT OF COBALT

6.1 WAVELENGTHS SELECTED

According to the Thompson and Walsh (1983), the most common line used for cobalt analysis is the Co II line at 228.616 nm. This is the line used by Piippanen et al (1997a) for the measurement of cobalt in a tungsten carbide matrix. Thompson and Walsh also cited the cobalt line at 238.346 nm as relatively sensitive and interference-free. However, vanadium emits weakly at 238.892 nm and tantalum has a strong line at 238.346 nm (Boumans, 1984).

The lines 228.616 nm and 238.346 nm were evaluated for suitability for the measurement of cobalt in a tungsten carbide matrix.

6.2 INVESTIGATION OF MATRIX EFFECTS AND INTERFERENCES

Before quantitative measurements could be made, it was necessary to determine the effect of the matrix elements present in the solution on the measurement of cobalt at the chosen analytical wavelengths. These elements were tungsten, tantalum, titanium, vanadium and chromium. In order to study these effects, 10 mg/ ℓ cobalt was prepared by serial dilution of the 1000 mg/ ℓ Merck stock solution in each of the following matrices:

i) 0.5 M hydrochloric acid (a 5% dilution from concentrated 32% hydrochloric acid)

ii) 1000 mg/ ℓ tungsten

iii) 10 mg/ ℓ of tantalum, titanium, vanadium and chromium in 0.5 M hydrochloric acid

iv) 10 mg/ ℓ of tantalum, titanium, vanadium and chromium in 1000 mg/ ℓ tungsten.

Because the tungsten concentration in a commercial tungsten carbide sample was expected to be approximately 1000 mg/ ℓ in the prepared solution when the cobalt concentration in the solution was about 10 mg/ ℓ, the effects at these concentrations were studied. The emission intensities of 10 mg/ ℓ cobalt in the two different matrices (0.5 M hydrochloric acid and 1000 mg/ ℓ tungsten) were measured at 228.616 nm and 238.346 nm and compared. It was found that the tungsten matrix of the solution did not have a large influence on the emission intensity of cobalt at either of the two analytical lines. It was therefore not deemed necessary to matrix match the cobalt calibration solutions with tungsten. Accurate results were obtained when a certified reference material of cemented tungsten carbide was analysed without matrix-matching (see Table 6.3). The profiles are shown in Figure 6.1 and Figure 6.2. In these profiles and those in the sections which follow, relative emission measurements are shown, that is, they are dependant on the adjustments made to optimise the element signal at that wavelength. The comparisons in a given figure were made with the same adjustment settings.

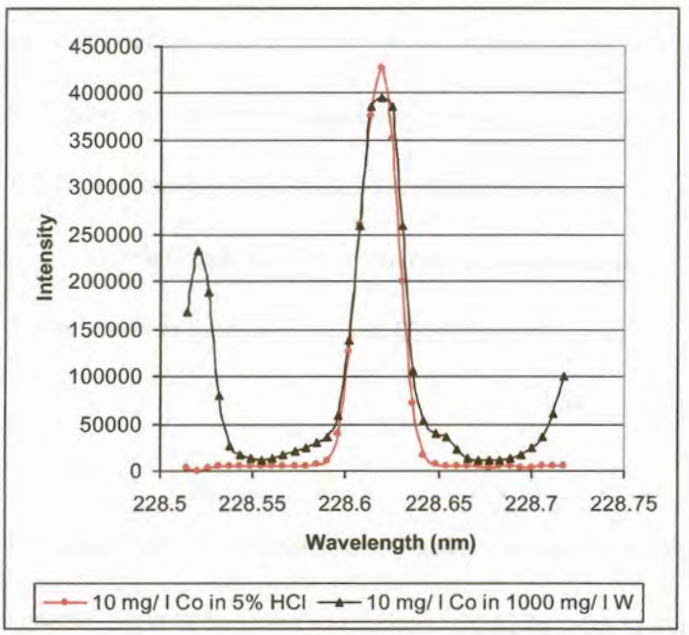

Figure 6.1: The effect of W on Co at 228.616 nm (JY-24 ICP-OES),

where 5% HCl refers to a 0.5 M solution (5% v/v dilution from concentrated HCl)

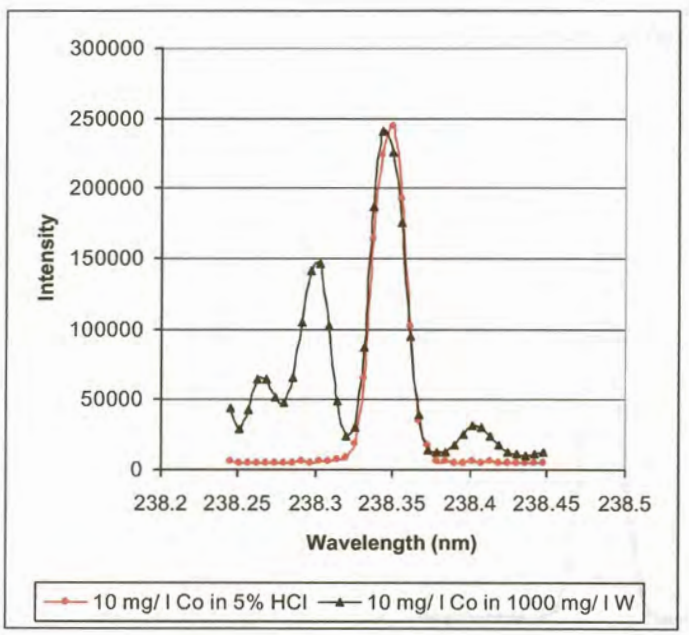

Figure 6.2: The effect of W on Co at 238.346 nm (JY-24 ICP-OES),

where 5% HCl refers to a 0.5 M solution (5% v/v dilution from concentrated HCl)

When 10 mg/ ℓ cobalt was mixed with respectively 10 mg/ ℓ of chromium, vanadium, tantalum and titanium, the comparison of their emission profiles showed that tantalum and titanium at these levels have no significant effect on the emission intensity of cobalt at 228.616 nm and 238.346 nm. However, chromium and vanadium showed a tendency to enhance the cobalt signal. This may be because of a chromium emission line at 238.333 nm, and vanadium emission lines at 228.659 nm 238.344 nm (Harrison, 1969).

The emission profiles and intensities of 10 mg/ ℓ cobalt in 0.5 M hydrochloric were compared at 228.616 nm and 238.346 nm to those of 10 mg/ ℓ cobalt in a matrix of 10 mg/ℓ tantalum, titanium, vanadium and chromium in 0.5 M hydrochloric acid. Figure 6.3 and Figure 6.4 show that the emission is apparently slightly enhanced at both wavelengths when tantalum, titanium, vanadium and chromium are added to the cobalt solution.

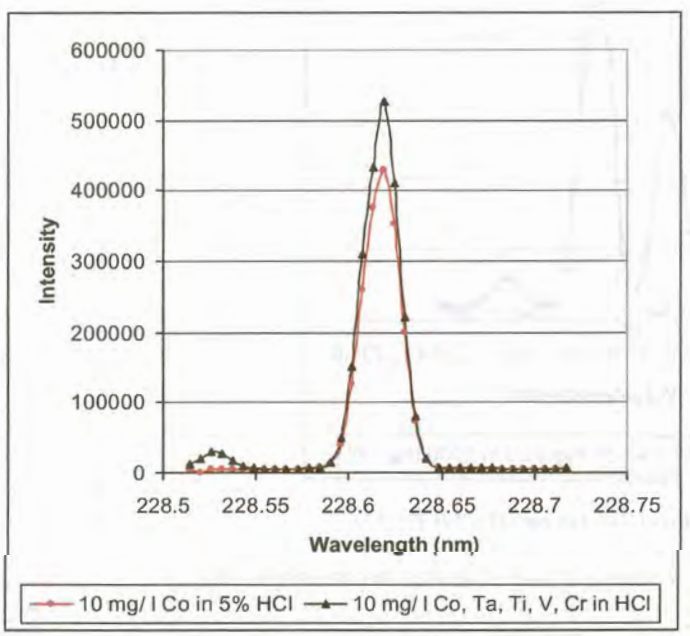

Figure 6.3: Effect of Ta, Ti, V, Cr on Co at 228.616 nm (JY-24 ICP-OES), where 5% HCl refers to a 0.5 M solution (5% v/v dilution from concentrated HCl)

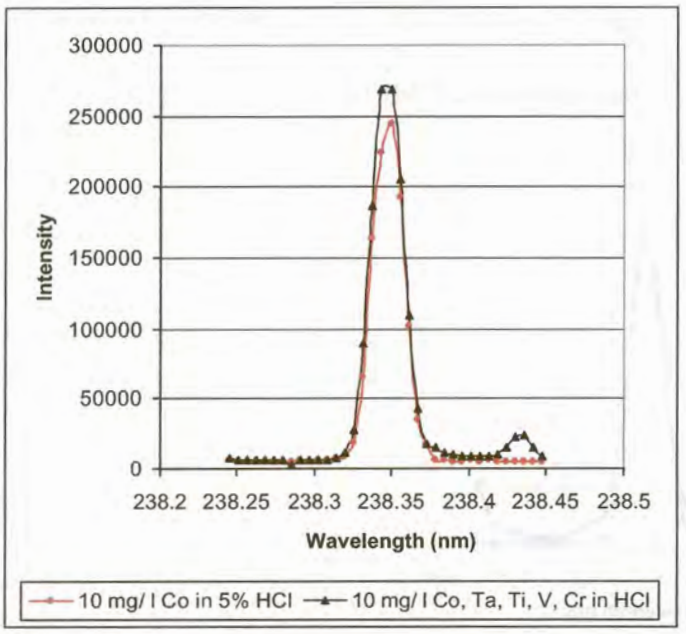

Figure 6.4: Effect of Ta, Ti, V, Cr on Co at 238.346 nm (JY-24 ICP-OES),
where 5% HCl refers to a 0.5 M solution (5% v/v dilution from concentrated HCl)

Since chromium and vanadium were previously found to influence the emission, it was necessary to matrix-match the calibration solutions with vanadium and chromium when these elements were also present in sample solutions at 10 mg/ ℓ levels. In practise, none of the tungsten carbide samples analysed contained chromium or vanadium in concentrations above 1 g/ 100 g in the powder. This would typically result in a maximum solution concentration of 1 mg/ ℓ of chromium or vanadium when the cobalt concentration in solution is 10 mg/ ℓ. With solutions of the above composition, it was found that the effect of chromium and vanadium on the measurement of cobalt was negligible and matrix-matching of the calibration solutions was not required.

The matrix of the above solution (10 mg/ ℓ cobalt, tantalum, titanium, vanadium and chromium) was modified to 1000 mg/ ℓ tungsten instead of 0.5 M hydrochloric acid. To test the effect on

tungsten on the emission at both analytical wavelengths, the profiles of the two solutions were compared. From Figure 6.5, it can be seen that tungsten at the 1000 mg/ ℓ level had no significant effect on the measurement of cobalt at 228.616 nm.

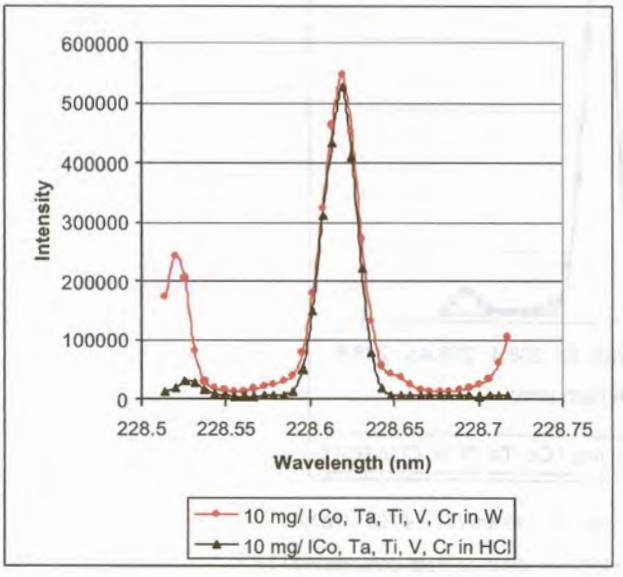

Figure 6.5: Effect of W on Co, Ta, Ti, Cr at the Co emission wavelength 228.616 nm (JY-24 ICP-OES)

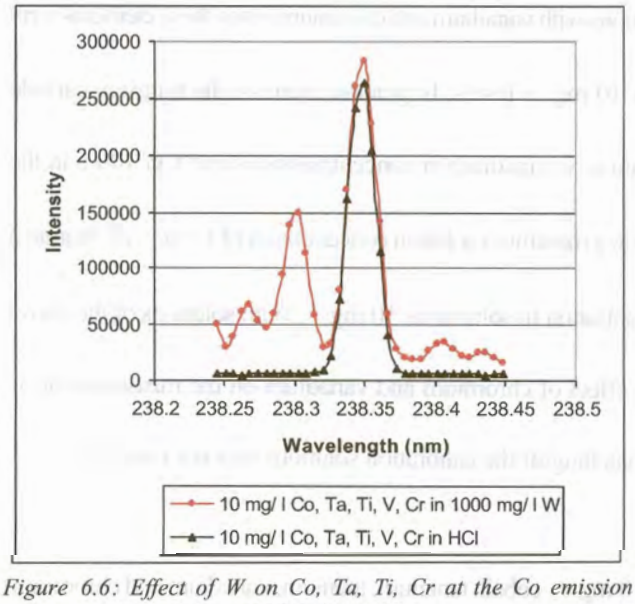

Figure 6.6: Effect of W on Co, Ta, Ti, Cr at the Co emission wavelength 238.346 nm (JY-24 ICP-OES)

There are tungsten emission lines at 238.320 nm and 238.354 nm (Harrison, 1969) and these can be observed in the profiles in Figure 6.6. It will be demonstrated in Section 6.4 that accurate measurements of cobalt were still obtained without matrix matching.

The above result (Figure 6.6) shows that even with tantalum, titanium, vanadium and chromium present in the solution at the maximum expected levels, tungsten has no effect on the measurement of cobalt. This experiment also confirms the results obtained when mixtures containing only cobalt and tungsten were measured. It was therefore not necessary to add tungsten to the calibration solutions during the measurement of cobalt in tungsten carbide solutions. Evidence of a baseline shift may be seen in Figure 6.6, which may result in false positive results for cobalt. However, the analysis is performed at two analytical lines and there would be a significant difference in the concentrations between the two wavelengths if no cobalt was, in fact, present in the sample. According to the quality control procedures the results would not be reported until the cause of the discrepancy had been investigated.

6.3 CALIBRATION SOLUTIONS

In the sample dissolution step, described in Section 4.3, the powdered tungsten carbide was initially diluted by a factor of 200 (0.5 g/ 100 ml). The concentration of cobalt in these solutions was consequently in the range 200 mg/ ℓ to 750 mg/ ℓ. This is much higher than the concentrations of the other elements of interest and therefore the solution was diluted further, and cobalt was analysed separately from the other elements.

According to Jobin Yvon Emission Instruments S.A., the JY-24 ICP-OES has a linear measurement range from 0 to 1000 mg/ ℓ for most elements. However, Miller & Miller (1993:

113) have shown that the most accurate results (i.e. those with the least error associated with them) are made in the middle portion (centroid) of the calibration curve. If all the elements were to be measured in the same solution, cobalt would be present at very high concentrations (say, 750 mg/ ℓ) while elements like vanadium, for example, would be present at relatively low concentrations (about 1 mg/ ℓ). This would clearly result in almost no measurements in the middle of the calibration curve, which would not be analytically desirable. The sample solutions for cobalt analysis were therefore further diluted by a factor of 10 with 0.5 M hydrochloric acid, bringing the cobalt concentration into the 20 to 75 mg/ ℓ range.

A summary of the composition of the analytical solution with respect to cobalt and tungsten is given in Table 6.1.

Table 6.1: Analytical solution for the analysis of cobalt in tungsten carbide

Analyte	Cobalt
Sample mass dissolved	0.5 g
Final sample volume	1000 ml
Dilution factor	2000
Concentration cobalt in sample solution	25 – 75 mg/ ℓ
Concentration tungsten in sample solution	~ 450 mg/ ℓ
Matrix matching for calibration solutions?	None required

A series of four calibration solutions were prepared from a 1000 mg/ ℓ Merck certified cobalt reference solution. The exact concentrations are indicated in Table 6.2 and cover the whole range of possible cobalt concentrations in the sample solutions.

Table 6.2: Preparation of Co calibration reference solutions

Cobalt concentration required (mg/ ℓ)	Concentration of Co stock solution (mg/ ℓ)	Volume of Co stock solution (ml)	Volume of 32% HCl (ml)	Final volume (ml)
0	-	-	5	100.00
10	100	10.00	5	100.00
50	1000	5.00	5	100.00
100	1000	10.00	5	100.00

The JY-24 ICP-OES was calibrated with the calibration solutions in Table 6.2 at 228.616nm and 238.346 nm. A typical calibration curve, with a squared product-moment correlation coefficient (r^2) of 0.9998, was obtained for the 228.616 nm line. A plot of the data, given in Appendix 4, Figure A1, shows a linear curve. The limit of detection was calculated from this data, using the statistical principles of Miller and Miller (1993). A limit of detection (LOD) for the 228.616 nm line was found to be 2 mg/ ℓ while the quantification limit was found to be 7 mg/ ℓ. Since the measured cobalt concentrations in the analytical solutions were in the range 25 to 75 mg/ ℓ , the calibration range was considered to be correct.

For the 238.346 nm line, a typical calibration curve with a squared product-moment correlation coefficient (r^2) of 0.9999 was obtained. The curve, which was demonstrably linear, is shown in Appendix 4, Figure A2. The limit of detection (LOD) for the 238.346 nm line was found to be 1 mg/ ℓ, while the quantification limit was found to be 4 mg/ ℓ.

6.4 REFERENCE MATERIALS AND QUALITY CONTROL

A standard reference material of powdered cemented carbide (NBS 889) with a certified cobalt concentration of 9.50 ± 0.15 g/ 100 g, was obtained from NIST, USA. The certificate of

analysis for this material is included under Appendix 3. It was analysed with several commercial samples over a period of two years. The results are summarized in Table 6.3.

Table 6.3: Analytical results for cobalt in cemented carbide NBS 889

Co concentration (g/100 g)	Number of aliquots analysed
9.48 ± 0.58	2
9.29 ± 0.25	2
9.17 ± 0.50	1
9.56 ± 0.34	2
9.86 ± 0.19	2
9.62 ± 0.25	2
9.66 ± 0.17	1
9.30 ± 0.48	3
Mean	**9.51**
Std dev (s)	**0.2858**
RSD (%)	**3.01**
Confidence limits	**± 0.58**

Where the number after the ± symbol was calculated according to the formula $\mu = \bar{x} \pm \frac{ts}{\sqrt{n}}$ (Miller & Miller, 1993). For each aliquot analysed, the solution was measured at two different wavelengths; n in the formula is thus equal to 2 times the number of aliquots analysed.

The final mean, standard deviation, RSD and confidence limits in Table 6.3 were calculated according to the principles of Miller and Miller (1993) from 30 cobalt measurement values. The confidence limits were also calculated according to the formula

$$\mu = \bar{x} \pm \frac{ts}{\sqrt{n}}$$

where s = 0.286, n = 30 and $t_{(0.05, 29)} = 2.045$.

All the values in Table 6.3, except 9.86 ± 0.19 g/ 100 g, fall within the certified range of the NBS 889 reference material. The average cobalt concentration of the 15 analyses, at 9.51 ± 0.58 g/ 100 g, also falls in the certified range. The confidence limits for the ICP-OES

measurements are much larger than those of the certified range (± 0.58 vs ± 0.15 g/ 100 g). In a commercial laboratory, it is often difficult to include sufficient replicate analyses of a sample for complete statistical analysis of the results. This is due to financial and time constraints and was also the case with these analyses. Dixon's Q ratio, to determine if the value 9.86 is an outlier, was found according to the formula:

Q = |suspect value – nearest value| / (largest value – smallest value)

which gives Q = (9.86 – 9.66)/ (9.86 – 9.17) = 0.29

From tables (Miller & Miller, 1993) the critical value of Q is given as 0.524 for n = 8 (P=0.05). The calculated value does not exceed this, so statistically 9.86 is not an outlier.

To test if there is a significant difference in the measurement results obtained at the two different wavelengths, a single factor ANOVA analysis was performed, using a Microsoft Excel spreadsheet. This spreadsheet is shown in Table 6.4. The calculated F value for the between group variation is 1.481, while the critical F value for a 95% level of confidence is 4.600. Since F_{crit} is larger than $F_{1,14}$ this is an indication that there is no significant difference between the results obtained for the different wavelengths.

Table 6.4: Single factor ANOVA analysis on cobalt results for two wavelengths

	Cobalt (g/100 g)	
Analysis no.	**228.616nm**	**238.346nm**
1	9.715	9.235
2	9.384	9.197
3	9.286	9.053
4	9.614	9.507
5	9.569	9.662
6	9.841	9.879
7	9.701	9.622
8	9.409	9.158

Anova: Single Factor

SUMMARY

Groups	*Count*	*Sum*	*Average*	*Variance*
Column 1	8	76.519	9.564875	0.036361
Column 2	8	75.313	9.414125	0.086376

ANOVA

Source of Variation	*SS*	*df*	*MS*	*F*	*P-value*	*F crit*
Between Groups	0.09090225	1	0.090902	1.481258	0.243697	4.600111
Within Groups	0.85915575	14	0.061368			
Total	0.950058	15				

To check the instrument stability, a quality control (QC) solution of a known concentration of cobalt was analysed after every third sample solution during a run. If only one or two samples were analysed during the run, a QC solution was measured after every second sample. On Jobin Yvon and Varian measurement validation software for ICP-OES, a quality control limit of ±5% for measurement of a sample of known concentration is usually set. Measurements within 5% of the prepared value are deemed acceptable. Therefore, if the measured concentration, after instrument calibration, differed more than 5% from the prepared concentration (Table 6.2), the instrument was recalibrated with the calibration solutions and the run repeated. In Table 6.5, a typical spread of between-sample measurement results for a 10 mg/ ℓ cobalt QC solution is analysed by a two-factor ANOVA, using a Microsoft Excel spreadsheet.

Table 6.5: ANOVA analysis of typical results for a between-sample QC solution of 10 mg/ ℓ cobalt over a period of approximately 90 minutes.

	Measured Co concentration (mg/l)	
	228.62nm	**238.35nm**
1	9.651	9.927
2	9.874	10.04
3	9.806	9.95
4	9.793	9.591
5	9.612	9.651
6	10.15	9.999
7	9.873	10.145
8	9.78	9.668
9	9.753	9.608
10	10.27	9.943
11	10.14	9.892

Anova: Two-Factor Without Replication

SUMMARY	*Count*	*Sum*	*Average*	*Variance*
Row 1	2	19.578	9.789	0.038088
Row 2	2	19.914	9.957	0.013778
Row 3	2	19.756	9.878	0.010368
Row 4	2	19.384	9.692	0.020402
Row 5	2	19.263	9.6315	0.000761
Row 6	2	20.149	10.0745	0.011401
Row 7	2	20.018	10.009	0.036992
Row 8	2	19.448	9.724	0.006272
Row 9	2	19.361	9.6805	0.010513
Row 10	2	20.213	10.1065	0.053464
Row 11	2	20.032	10.016	0.030752
Column 1	11	108.702	9.882	0.045608
Column 2	11	108.414	9.855818	0.036967

ANOVA

Source of Variation	*SS*	*df*	*MS*	*F*	*P-value*	*F crit*
Rows	0.596726	10	0.059673	2.605564	0.073431	2.97824
Columns	0.00377	1	0.00377	0.164623	0.693481	4.964591
Error	0.22902	10	0.022902			
Total	0.829516	21				

In the case of between-wavelength variations (columns, Table 6.5) as well as between-measurement variations (rows, Table 6.5), the calculated F value is smaller than F_{crit} for a 95% level of confidence, indicating that there were no significant differences in the measurement results. A run time for a typical ICP-OES analysis of cobalt in tungsten carbide is usually more than an hour when 5 to 10 samples are analysed in duplicate and the sample matrix, because of its complexity, may cause changes in the sample introduction system of the instrument (nebulizer clogging, memory effects, torch deposits). The results in Table 5.5 show that the instrument was stable during the entire measurement run. This is an indication that the sample measurement solutions (commercial tungsten carbide solutions, produced by the hydrogen peroxide dissolution method) are not contributing to clogging by precipitation of tungsten complexes.

All the samples were dissolved at least in duplicate. If the final cobalt concentrations of the two aliquots were not within 5% of each other, additional aliquots were dissolved and analysed.

Some of the sample solutions were also reanalysed at the end of the measurement run to check the within-run repeatability. The initial measurements for two samples during different measurements runs are listed in Table 6.6, together with measurements of the same samples approximately one hour later without re-calibration of the instrument. The results for the initial and subsequent measurements of each sample are within 5% of each other. Similar results to those in Table 6.6 were obtained for all the samples analysed for cobalt by this method.

Table 6.6: Within-run repeatability of sample measurements for cobalt in tungsten carbide

Measurement of:	**Measured Co concentration from raw data (mg/ ℓ)**	
	at 228.616 nm	**at 238.346 nm**
Sample 1, initial	23.81	23.12
Sample 1, 60 min later	24.27	23.76
Sample 2, initial	30.48	30.23
Sample 2, 60 min later	31.36	30.51

The elemental composition of tungsten carbide tends to vary. Some batches may contain iron, other experimental elements or the concentrations of the known elements may vary. The cobalt measurement may therefore be influenced by these matrix variations. Since the effect may not be noticeable when only one analytical wavelength is used, it was found prudent to select at least two analytical lines per element. If the results were found to differ by more than 5% using the two specified lines, an unforeseen interference may have been the cause and an investigation could have been done. No such effect was, in fact, observed.

6.5 DISCUSSION AND CONCLUSIONS

All except two of the results (9.17 g/ 100 g and 9.86 g/ 100 g) in Table 6.3 for the analysis of cobalt in the NBS 889 tungsten carbide reference material lie within 2.5% of the certified value. This shows that an accuracy of at least ±2.5% can be achieved relatively easily in a commercial laboratory. The narrower range of ±1.6% indicated by the certified uncertainty of the NBS 889 reference material could be achieved but at the expense of speed and sample throughput. More aliquots of each sample would have had to be dissolved and better instrumental precision would have had to be attained. This was not considered practical in laboratories where time and money were at a premium, and the clients indicated that they were satisfied with the accuracy

and precision obtained. Therefore, the analyses were repeated only when the measured cobalt concentration for the NBS 889 reference material fell outside the range 9.26 g/ 100 g to 9.74 g/ 100 g.

The cobalt content of the tungsten carbide samples analysed ranged from about 4 g/ 100 g to about 15 g/ 100 g. If the sample were diluted by a factor of 2000 times during the preparation step, solution concentration ranges of between 20 and 75 mg/ ℓ would be obtained. The measurement range would lie towards the centroid of the calibration curve if the instrument were calibrated from 0 to 100 mg/ ℓ.

Under the analytical conditions employed for cobalt (dilution factor = 2000), a 0.5 mg/ ℓ measurement inaccuracy would lead to a deviation of 0.1 g/ 100 g in the final results. In practice, using the quality control measures described in Section 6.4, a measurement inaccuracy of not more than ±0.5 mg/ ℓ was achieved (see Table 6.5) even though the presence of hydrogen peroxide in the solution tended to produce fine bubbles during nebulization (leading to a decrease in precision). At the cobalt levels measured, this resulted in a relative deviation from the true value of ±2%. Other factors also combine to increase the final uncertainty level.

To maintain analytical credibility, it is recommended that a certified reference material be analysed with every batch of commercial samples. This may become costly when a large number of samples are analysed. The problem can be overcome by using a secondary reference material which has been analysed repeatedly against a certified reference material.

The results obtained using this method are satisfactory for a laboratory making routine measurements of cobalt in tungsten carbide. There is no evidence that the hydrogen peroxide/ aqua regia acid dissolution is not effective for cobalt in tungsten carbide.

CHAPTER 7

MEASUREMENT OF TANTALUM

7.1 WAVELENGTHS SELECTED

Lines recommended in the literature for the ICP-OES analysis of tantalum are 226.230 nm, 233.198 nm, 240.063 nm, 263.558 nm and 268.517 nm (Thompson & Walsh, 1983). Piippanen et al (1997a) used the 296.513 nm line for the analysis of tantalum in tungsten carbide.

On testing the 226.230 nm, 233.198 nm, 240.063 nm, 263.558 nm and 268.517 nm lines for suitability of use with the tungsten carbide matrix, the 240.063 nm and 268.517 nm lines were finally selected for quantitative work. None of the lines were found to be free of interference from high concentrations of tungsten; only the degree of interference differed. Positive results were initially obtained for samples which contained no tantalum because of the effect of tungsten, which is present in relatively high concentrations in all the samples. These results were rejected upon further investigation.

7.2 INVESTIGATION OF MATRIX EFFECTS AND INTERFERENCES

To study the interference effects of cobalt and tungsten on the measurement of tantalum, mixtures of 10 mg/ ℓ tantalum in the following matrices were prepared:

i) deionised water

ii) 500 mg/ ℓ cobalt

iii) 1000 mg/ ℓ tungsten.

According to Boumans (1984) and Harrison (1969), a tungsten emission line occurs at 226.232 nm, which is very close to the tantalum emission line at 226.230 nm. A profile of 10 mg/ ℓ tantalum in 0.5 M hydrochloric acid was compared with that of the same concentration of tantalum in 1000 mg/ ℓ tungsten. In Figure 7.1 it can be seen that 1000 mg/ ℓ tungsten has the effect of apparently enhancing the tantalum signal at 226.230 nm. This is more probably interfering emission from tungsten.

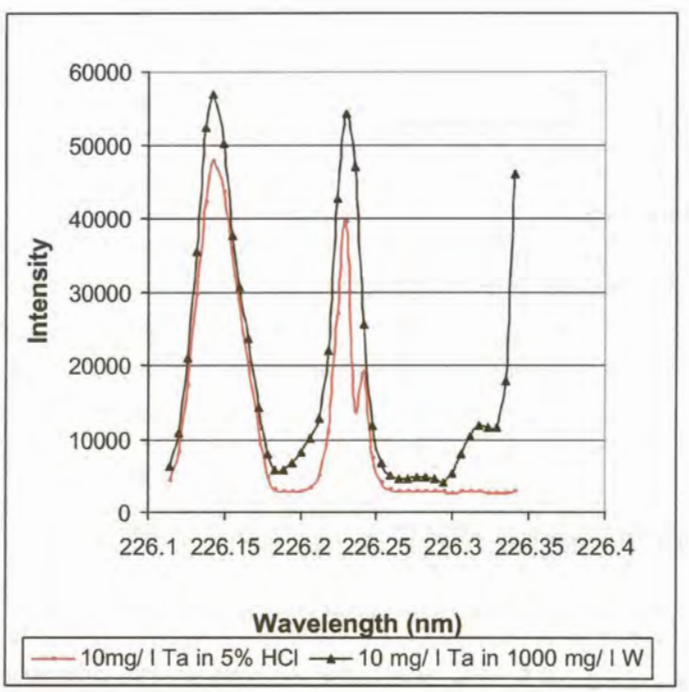

Figure 7.1: Effect of W on Ta at 226.230 nm (JY-24 ICP-OES), where 5% HCl refers to a 0.5 M solution (5% v/v dilution from concentrated HCl)

At a sample dilution factor of 200, the cobalt concentration in the solution was expected to be in the range 200 to 750 mg/ ℓ, while the tantalum concentration in the same solution was not expected to exceed 10 mg/ ℓ. It can be seen in Figure 7.2 that 500 mg/ ℓ cobalt has very little effect on the measurement of 10 mg/ ℓ tantalum at 226.230 nm but the slight emission from

cobalt at 226.260 nm (Harrison, 1969) may cause quantification errors.

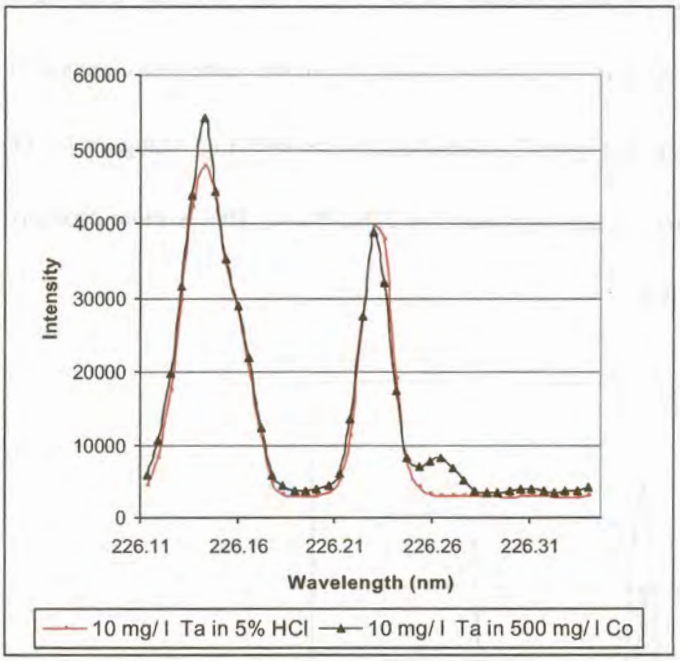

Figure 7.2: Effect of Co on Ta at 226.230 nm (JY-24 ICP-OES ,
where 5% HCl refers to a 0.5 M solution (5% v/v dilution from concentrated HCl)

The effect of 500 mg/ ℓ cobalt on the measurement of 10 mg/ ℓ tantalum at 233.198 nm can be seen as a baseline shift in Figure 7.3. This is due to a cobalt emission line at 233.210 nm (Harrison, 1969) and may also cause quantification errors unless the matrices of the calibration solutions are carefully matched to the sample solution matrix.

At the 233.198 nm tantalum emission line, a tungsten emission line occurs at 233.191 nm (Boumans, 1984; Harrison, 1969). The interference can be clearly seen by comparing the emission profiles of 10 mg/ ℓ tantalum in 0.5 M hydrochloric acid and tantalum in 1000 mg/ ℓ tungsten (Figure 7.4). By measuring tantalum at this wavelength in a matrix of tungsten carbide, it would appear as if the tantalum emission peak had shifted to a slightly lower wavelength, while in

reality the tungsten emission was being measured. In this way, an erroneous positive result could be obtained for a sample which contained no tantalum.

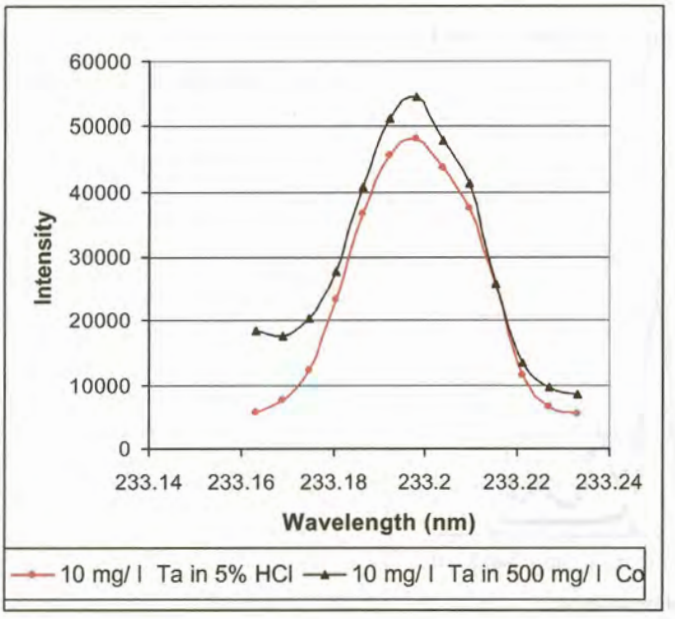

Figure 7.3: Effect of Co on Ta at 233.198 nm (JY-24 ICP-OES),
where 5% HCl refers to a 0.5 M solution (5% v/v dilution from concentrated HCl)

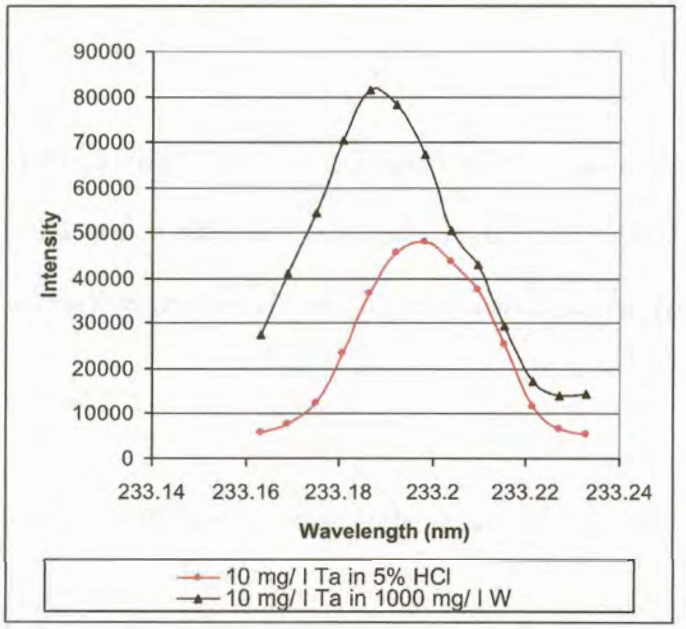

Figure 7.4: Effect of W on Ta at 233.198 nm (JY-24 ICP-OES),
where 5% HCl refers to a 0.5 M solution (5% v/v dilution from concentrated HCl)

According to Boumans (1984) and Harrison (1969) there is a fairly strong cobalt emission line at 240.084 nm, near the 240.063 nm tantalum emission line. The effect of 500 mg/ ℓ cobalt on 10 mg/ ℓ tantalum at 240.063 nm is documented in Figure 7.5.

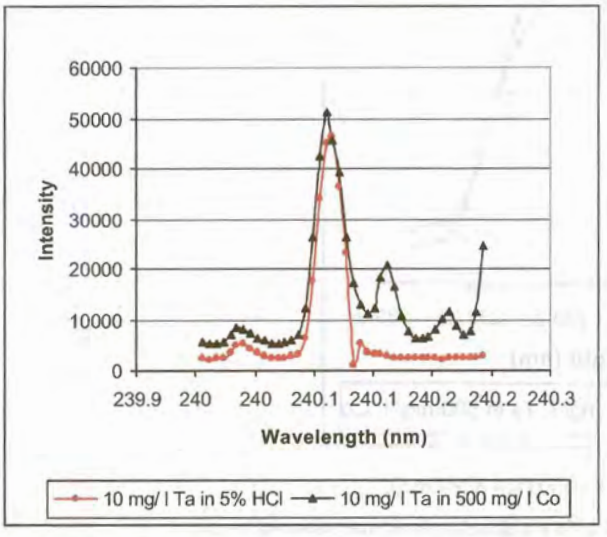

Figure 7.5: Effect of Co on Ta at 240.063 nm (JY-24 ICP-OES), where 5% HCl refers to a 0.5 M solution (5% v/v dilution from concentrated HCl)

There is also a tungsten emission line at 240.130 nm (Boumans, 1984; Harrison, 1969). Emission from this line can clearly be observed in Figure 7.6, as a 'shoulder' at about 240.13 nm. It was found that both cobalt and tungsten interfere slightly with the measurement of tantalum at 240.063 nm.

At 263.654 nm, cobalt at the 500 mg/ ℓ level was found to have only a slight effect on 10 mg/ ℓ tantalum , shown in Figure 7.7.

A weak tungsten emission line at 263.654 nm (Boumans, 1984) has a slight influence on the tantalum emission line at 263.558 nm. The emission profiles of 10 mg/ ℓ tantalum in 0.5 M hydrochloric acid and tantalum in 1000 mg/ ℓ tungsten are compared in Figure 7.8.

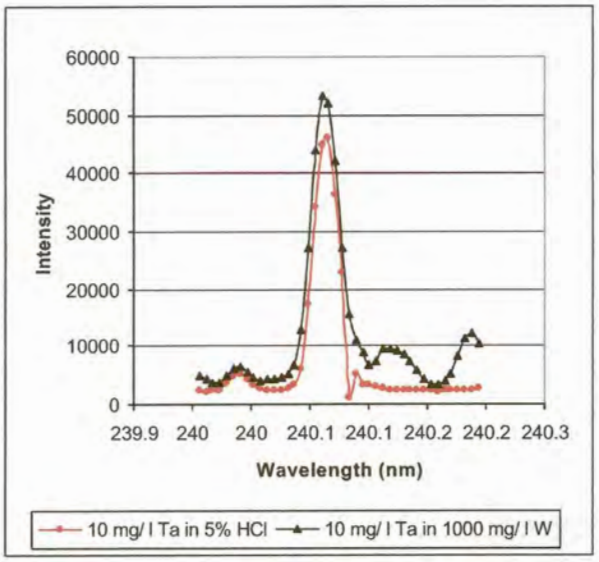

Figure 7.6: Effect of W on Ta at 240.063 nm (JY-24 ICP-OES), where 5% HCl refers to a 0.5 M solution (5% v/v dilution from concentrated HCl)

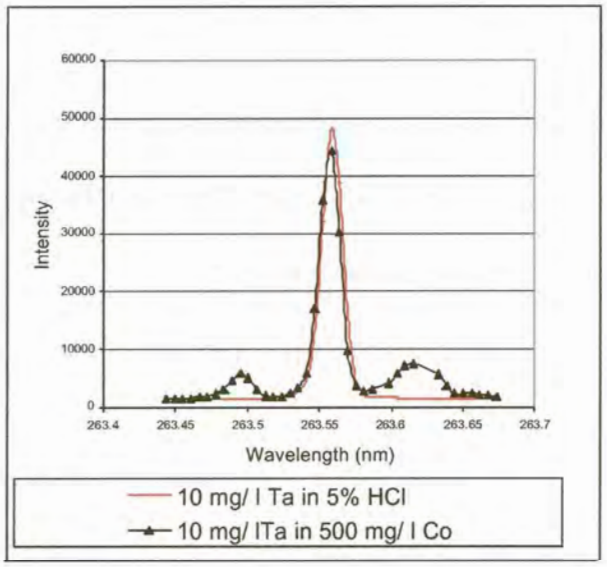

Figure 7.7: Effect of Co on Ta at 263.558 nm (JY-24 ICP-OES), where 5% HCl refers to a 0.5 M solution (5% v/v dilution from concentrated HCl)

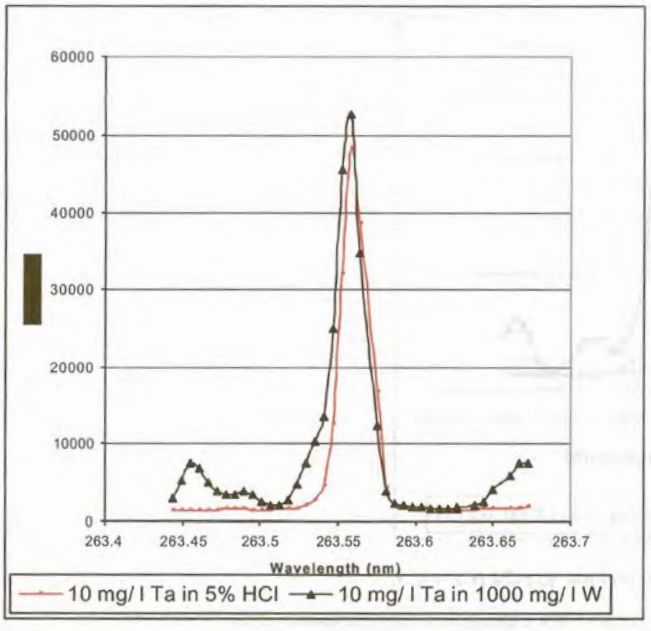

Figure 7.8: Effect of W on Ta at 263.558 nm (JY-24 ICP-OES), where 5% HCl refers to a 0.5 M solution (5% v/v dilution from concentrated HCl)

Cobalt also has an emission line at 268.534 nm (Boumans, 1984; Harrison, 1969), which is near the 268.517 nm tantalum analytical line. A slight interference was confirmed by profiling tantalum solutions in acid against tantalum solutions in 500 mg/ ℓ cobalt (Figure 7.9).

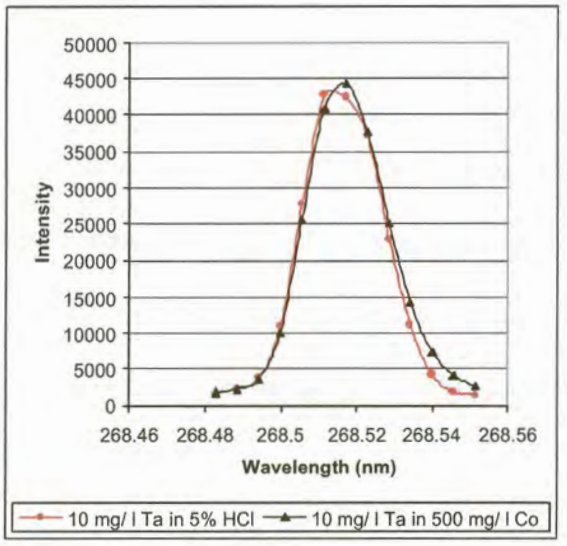

Figure 7.9: Effect of Co on Ta at 268.517 nm (JY-24 ICP-OES),
where 5% HCl refers to a 0.5 M solution (5% v/v dilution from concentrated HCl)

However, tungsten at levels of approximately 1000 mg/ ℓ were also found to give rise to emission intensities corresponding to 1 - 3 mg/ ℓ tantalum at 268.517 nm. Boumans (1984) gives no information on emission lines for tungsten in this region but Harrison (1969) documents a tungsten emission line at 268.534 nm The effect can be seen in Figure 7.10.

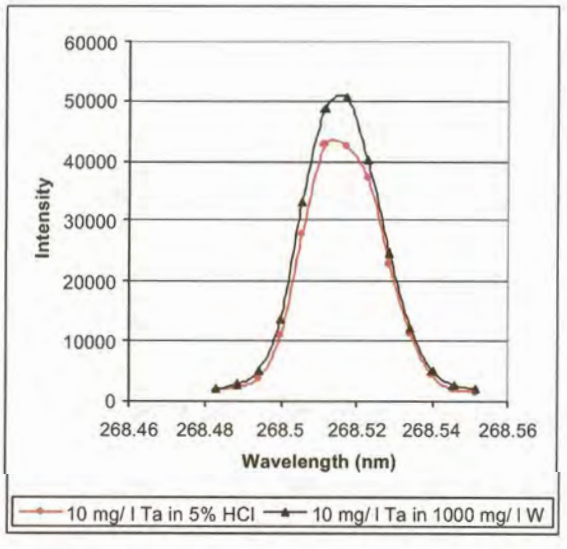

Figure 7.10: Effect of W on Ta at 268.517 nm (JY-24 ICP-OES),
where 5% HCl refers to a 0.5 M solution (5% v/v dilution from concentrated HCl)

7.3 CALIBRATION SOLUTIONS

The tantalum concentrations in commercial samples submitted for analysis were found to be below 1 g/ 100 g. This would result in up to 50 mg/ℓ tantalum in solution, given a dilution factor of 200 when the sample is dissolved as described in Section 4.3. To make matrix matching easier, this solution was diluted by a further factor of 5, giving a sample concentration of 0.5 g/ 500 ml.

As discussed in Section 7.2, the calibration solutions needed to be matrix matched with respect to both cobalt and tungsten. Unfortunately, the tungsten and cobalt stock reference solutions available for analytical use are not compatible. Tungsten is supplied in alkaline solution, while cobalt is supplied in acidic solution. Depending on the pH, either tungsten or cobalt precipitated if the two solutions were mixed. Cobalt forms insoluble cobaltous hydroxide in the alkaline tungsten solution, while tungsten forms insoluble tungstic acid in acid solution. This made proper matrix-matching of the reference solutions very difficult.

It was found, however, that when about 0.6% solid tartaric acid was dissolved in a 1000 mg/ℓ tungsten solution, which was then acidified with hydrochloric acid, the tungsten remained in solution. The cobalt and tantalum could then be added to the acidified tungsten solution.

The tungsten content in commercial tungsten carbide samples is about 80 g/ 100 g. Normally, a solution of a 0.5 g aliquot of a sample, diluted to 500 ml, was expected to contain about 800 mg/ℓ tungsten. The approximate tungsten concentration of every sample solution was confirmed by profiling against tungsten at 207.911 nm (a tungsten emission line). Accurate results for

tantalum could not be obtained if the tungsten concentration in the analytical solutions exceeded 900 mg/ℓ, since no suitable tungsten solution with a concentration of more than 1000 mg/ℓ was available for matrix-matching.

Three possible solutions to the matrix matching problem were investigated:

i) Tartaric acid was added to a concentrated tungsten solution in ammonia, and the solution acidified with hydrochloric acid. A range of calibration solutions were prepared, each containing 800 mg/ ℓ tungsten, with a cobalt concentration which matched the sample solutions and the appropriate concentration of tantalum for the calibration range. The calibration solutions were also used as quality control samples (QC) between sample solution measurements.

ii) A range of tantalum calibration solutions, matrix matched with cobalt, were prepared. One solution containing tantalum in the same concentration range as the sample solutions, and matrix matched with both cobalt and tungsten was prepared as in method i). The ICP-OES was calibrated with the tantalum solutions containing cobalt, and the solution containing both cobalt and tungsten was used during the run as a quality control (QC) sample. Because tungsten (present in the QC solutions, but not in the calibration solutions) also contributed to the signal at the analytical wavelengths used, the measured concentration of the QC solution was higher than the true concentration. A correction factor was applied to the measured sample concentrations to give the actual concentrations.

iii) The third solution to the problem was to match the tantalum calibration solutions with respect to cobalt and to calibrate the instrument with this range of solutions. The tungsten concentration in sample dilutions of 0.5 g/ 1000 ml was expected to be about 800 mg/ℓ. The emission of a 800 mg/ℓ tungsten solution was measured as a sample at the tantalum wavelengths, and the tungsten measurement value subtracted from the sample measurement values. The calibration solutions could be used as quality control checks for instrument stability between samples during the measurement run but since they did not contain tungsten, no correction was made to the measurements.

Table 7.1 gives a summary of a typical composition of the analytical solution with respect to tantalum, cobalt and tungsten.

Table 7.1:Analytical solution for the analysis of tantalum in tungsten carbide

Analyte	Tantalum
Mass dissolved	0.5 g
Final volume	500 ml
Dilution factor	1000
Concentration tantalum in solution	0 – 8.5 mg/ ℓ
Concentration cobalt in solution	10 – 150 mg/ ℓ
Concentration tungsten in solution	~ 800 mg/ ℓ
Matrix matching of calibration solutions?	Yes, with Co and W (see Section 7.2)

Table 7.2 shows a typical example of a scheme for the preparation of a series of tantalum calibration solutions. In this example, the tantalum solutions are matrix matched with cobalt. A separate quality control solution containing tantalum, cobalt and tungsten at the expected samples concentrations, or a separate solution containing only tungsten could be prepared for quality control use after calibration. A certified 1000 mg/ ℓ tantalum solution, obtained from Merck Chemicals was used. The tungsten and cobalt solutions were also obtained from Merck Chemicals as 1000 mg/ ℓ solutions.

The cobalt concentration in the sample was obtained from the analysis of cobalt, which is normally measured first. If the cobalt concentration in the samples to be measured for tantalum differed by more that 1%, separate quality control standard solutions were prepared. The instrument was calibrated with a series of tantalum solutions, all containing the same concentration of cobalt. Before and after the samples with a different cobalt concentration, a tantalum standard with the appropriate cobalt concentration was analysed and the sample tantalum concentration calculated from these, using a correction factor.

Table 7.2 Preparation of tantalum calibration reference solutions, matrix matched w.r.t. Co: sample tantalum concentration 1 – 5 g/ 100 g and cobalt concentration 9.6 g/ 100 g

Ta concentration required (mg/ ℓ)	Concentration of Ta stock solution (mg/ ℓ)	Volume of Ta stock solution (ml)	*Volume of 1000 mg/ ℓ Co (ml)	Volume of 32% HCl (ml)	Final volume (ml)
0	-	-	5.00	5	100.00
1	20	5.00	5.00	5	100.00
10	1000	1.00	5.00	5	100.00
20	1000	2.00	5.00	5	100.00

* the cobalt concentration in the calibration solutions must be matched to that of the sample solutions, in this case 50 mg/ ℓ

A four point calibration of the JY-24 ICP-OES was performed with the solutions in Table 7.2 at 240.063 nm and 268.517 nm. A typical calibration curve for tantalum at 240.063 nm, with a coefficient of determination (r^2) of 0.9993, was obtained as is shown in Appendix 4, Figure A3. The calibration data was used to calculate the detection limit (LOD) and the quantification limit (LOQ) according to the principles of Miller & Miller (1993). The LOD was calculated to be 1 mg/ ℓ and the LOQ 3 mg/ ℓ.

For the determination of tantalum at 268.517 nm, a calibration curve with a coefficient of determination (r^2) of 0.9999 was obtained, as is shown in Appendix 4, Figure A4. The LOD for this wavelength under the conditions used was found to be 0.4 mg/ ℓ, while the LOQ was 1 mg/ ℓ.

7.4 REFERENCE MATERIALS AND QUALITY CONTROL

A certified cemented carbide reference material, NBS 889, was obtained from NIST (Gaithersburg, USA). The concentration of tantalum in this material was certified as 4.60 ± 0.15 g/ 100 g tantalum.

Two samples of tungsten carbide with only cobalt added (1 to 10 g/ 100 g) and containing no tantalum, were obtained from the Boart Longyear Research Centre (Krugersdorp). These samples were used for spiking experiments.

Since the elemental composition of tungsten carbide tends to vary and the matrix elements may therefore differ from sample to sample, the tantalum measurement may be influenced by these matrix variations. The exact sample composition may not be known beforehand and the matrix effect may not be noticeable when only one analytical wavelength is used. In view of the problems encountered in the analysis of tantalum in tungsten carbide, it was considered advisable to select at least two analytical lines. If the results for the two different lines did not agree to within 5%, an investigation into the effect could have been done and the possibility of reporting an erroneous result avoided.

The method in which the calibration solutions were matched with cobalt only, but where the QC solution contained tantalum, cobalt and tungsten, was shown to be accurate (see Table 7.4). This method was considered less than ideal, especially as the QC solution sometimes blocked the nebulizer, necessitating dismantling of the sample introduction system for cleaning. The whole calibration procedure had to be repeated after reassembling and some time was consequently wasted.

The measurement method that was finally adopted was the one where the matrix of the calibration solutions was matched with cobalt to the same level as that of the sample solutions. A separate solution of tungsten (at the level present in the sample) was measured after calibration

of the instrument at 240.063 nm and 268.517 nm. A solution containing 1000 mg/ ℓ tungsten gave a reading of approximately 3 mg/ ℓ at 240.063 nm and approximately 1 mg/ ℓ at 268.517 nm. These values were then subtracted from the sample solution measurements before the final tantalum concentrations in the samples were calculated.

No correction for tungsten was made for the calibration solutions which were used as between-sample QC checks during the measurement run because they did not contain tungsten. The QC solutions were measured to check the instrument stability during the run. Within-run repeatability was considered excellent as a 10 mg/ ℓ tantalum solution gave a reading of 10.31 mg/ ℓ at the beginning of the run at 240.063 nm, and a reading of 10.42 mg/ ℓ at the end of the run, 30 minutes later. At 268.571 nm, the reading was 10.21 mg/ ℓ at the beginning of the run and 10.45 mg/ ℓ at the end of the run.

The effect of the matrix on the measurement of tantalum could be demonstrated by measuring solutions of tungsten carbide which contained no tantalum at different wavelengths. The instrument was calibrated with a series of tantalum solutions in 0.5 M hydrochloric acid and no matrix matching was done. The results of such an experiment are given in Table 7.3.

Table 7.3: Measurement of tantalum without matrix matching at different wavelengths

Sample	Measured concentration in mg/ ℓ at	
	226.230 nm	268.517 nm
1	36.7	3.5
2	39.4	3.4
3	85.2	3.7

Table 7.3 illustrates the enormous error that can occur if measurements are made without a thorough investigation of matrix effects. None of the samples listed in Table 7.3 did, in fact,

contain tantalum. The difference in the two sets of results also demonstrates that measurement errors and interferences can easily be detected when at least two analytical lines are used for quantitation.

The method in which all the calibration solutions are matched with both cobalt and tungsten was rejected. This method resulted in the use of large volumes of concentrated tungsten solution. Some of these mixtures also caused nebulizer blockages, although no precipitate could be observed. In addition, the preparation of the solutions was more complicated and took longer to prepare than the two other methods.

Tantalum was added to a dissolved tungsten carbide sample which contained no tantalum at a concentration of 4 mg/ ℓ. The ICP-OES was calibrated at 240.063 nm and at 268.517 nm with a series of tantalum solutions, matrix matched with cobalt. The approximate concentration of tungsten in the solution was previously determined by profiling a solution of known tungsten concentration against the sample at 207.911 nm (a tungsten emission wavelength). The tungsten concentration was found to be between 750 and 850 mg/ ℓ in the sample solution (this was consistent with the known composition of the sample). The tungsten solution was then measured at the two tantalum emission wavelengths and the result subtracted from each of the sample measurements before further calculation. An average result for the measurement of tantalum in the spiked sample was 4.2 mg/ ℓ, which is within 5% of the prepared concentration. The tantalum concentration ranges in the sample solutions were found to be between 0 and about 8 mg/ ℓ. The spiking experiment shows that accurate results can be obtained for tantalum at these levels, using the above method.

The highest tantalum concentration measured in tungsten carbide was 0.83 g/ 100 g. This sample was analysed repeatedly, using two of the calibration methods described in Section 7.3. The tantalum concentration in this sample was initially determined to be 0.83 ± 0.06 g/ 100 g, by the analysis of 5 separate aliquots at two wavelengths. The sample was later found to have been analysed by another laboratory; they found the tantalum concentration to be 0.8 g/ 100 g. This sample was then used as a secondary reference material when tantalum was analysed in commercial samples. Table 7.4 shows the two factor ANOVA treatment (Microsoft Excel) of the analytical results obtained for two measurement methods, three sets obtained by the use of a tantalum/ cobalt/ tungsten solution, and three sets obtained by the tungsten emission subtraction method. The analyses were done over an eight month period.

Table 7.4: Two factor ANOVA analysis of tantalum results obtained by two different measurement methods

	Ta (g/ 100 g)	
Method	240.063nm	268.517nm
A	0.776	0.853
A	0.850	0.917
A	0.741	0.895
B	0.802	0.932
B	0.783	0.728
B	0.844	0.728

Method A Calibration solutions matrix matched with Co. Tungsten measured separately and signal subtracted from results.

Method B Calibration solutions matrix matched with Co. QC solution matrix matched with Co and W.

Anova: Two-Factor Without Replication

SUMMARY	*Count*	*Sum*	*Average*	*Variance*
Row 1	2	1.629	0.8145	0.002965
Row 2	2	1.767	0.8835	0.002244
Row 3	2	1.636	0.818	0.011858
Row 4	2	1.734	0.867	0.00845
Row 5	2	1.511	0.7555	0.001512
Row 6	2	1.572	0.786	0.006728
Column 1	6	4.796	0.799333	0.001757
Column 2	6	5.053	0.842167	0.008529

ANOVA

Source of Variation	*SS*	*df*	*MS*	*F*	*P-value*	*F crit*
Rows	0.0231767	5	0.004635	0.820317	0.58338	5.050339
Columns	0.0055041	1	0.005504	0.974056	0.368992	6.607877
Error	0.0282534	5	0.005651			
Total	0.0569342	11				

No significant difference in the results of the two methods, or the results at the two wavelengths, were observed. The within-wavelength results as well as the between-wavelength results in Table 7.4, show no significant differences. The calculated F values are smaller than F_{crit} in both cases. The average of these results was 0.82 g/ 100 g. The confidence limits were calculated according to the formula (Miller & Miller, 1993):

$\mu = \bar{x} \pm \frac{ts}{\sqrt{n}}$, where $t_{(0.05, 11)} = 2.201$, s = 0.0719 and n = 12.

The final concentration of 0.82 ± 0.05 g/ 100 g was thus obtained. This is comparable to the initial concentration obtained (0.83 ± 0.06 g/ 100 g) and the value obtained by the external laboratory (0.8 g/ 100 g by XRF).

The certified cemented carbide, NBS 889, was analysed as well, even though its concentration, at 4.60 ± 0.15 g/ 100 g, fell outside the range encountered in commercial samples. Solutions of this material were further diluted to bring the concentration of tantalum in the solution within the calibration range. The matrix of the calibration solutions and quality control solutions had to be adjusted to the lower cobalt and tungsten concentrations in the sample solutions. A measurement result of 4.48 ± 0.32 g/ 100 g was obtained, which is within the uncertainty quoted for the sample.

7.5 DISCUSSION AND CONCLUSIONS

The analysis of the certified reference material, with a relatively high tantalum concentration presented only minor problems. The matrix-matching techniques are capable of minimising the interferences from cobalt and tungsten to a degree where results within 2.5% of the certified value can be obtained. The analysis of the cemented carbide reference sample, NBS 889, also showed that the dissolution procedure, using hydrogen peroxide and aqua regia, is effective in dissolving tantalum in the tungsten carbide.

It was shown that accurate results can be obtained by using the matrix matching technique and

there is enough evidence to show that the method produces accurate results even when the samples contain tantalum in concentrations as low as 0.8 g/ 100 g.

It is significant that Piippanen et al (1997a) added tungsten to all the calibration solutions (matrix matching) indicating that they also had problems with tungsten interference. They used the 296.513 nm line for the analysis of tantalum, which was not tested here but it can be assumed that tungsten interferences also occurred at this line.

The sample solutions had to be diluted by a factor of 1000 to bring the tungsten concentration to a level where the matrix of the calibration solutions could be matched (the highest concentration of tungsten solution available was 1000 mg/ ℓ). The quantification limit for tantalum in a solution was found to be between 1 and 3 mg/ ℓ. This meant that tantalum could not be accurately measured in samples which had a tantalum concentration lower than 0.1 g/ 100 g. None of the samples analysed had tantalum concentrations at this level. They either contained no tantalum or tantalum at concentrations above 0.25 g/ 100 g.

In the calibration and correction method finally adopted, there was no wastage of tungsten solution, no nebulizer blockages occurred and the messy, time-consuming complexing/ acidifying step was avoided.

In conclusion it can be said that the dissolution procedure has been proved efficient for the dissolution of tungsten carbide samples when the tantalum concentration is to be analysed. The IC P-OES measurement method, applied as described in this chapter, has also been shown to produce accurate results.

CHAPTER 8

MEASUREMENT OF TITANIUM

8.1 WAVELENGTHS SELECTED

Thompson & Walsh (1983) recommend the Ti II lines at 337.280 nm and 368.520 nm for titanium analysis. Both these lines were investigated and subsequently used for analysis of titanium in a matrix of tungsten carbide.

Pippannen et al (1997a) used the Ti II line 332.676 nm for titanium analysis. Harrison (1969) reported tungsten emission lines at 332.642 nm and 332.762 nm., and strong cobalt emission lines at 332.656 nm and 332.700 nm.

8.2 MATRIX EFFECTS AND INTERFERENCES

On profiling a 10 mg/ ℓ titanium solution in 0.5 M hydrochloric acid against a solution of 10 mg/ ℓ titanium in 500 mg/ ℓ cobalt a serious interference was observed using the 332.676 nm titanium emission line, as can be seen in Figure 8.1. The likely cause was thought to be the cobalt emission line at 332.700 nm, reported by Harrison (1969).

In addition, the effect of the tungsten emission lines at 332.642 nm and 332.762 nm on titanium measurements, also reported by Harrison (1969), can be clearly observed in Figure 8.2. Measurements for titanium made at 332.676 nm without careful matrix matching may result in erroneously positive titanium results or incorrect quantitation results.

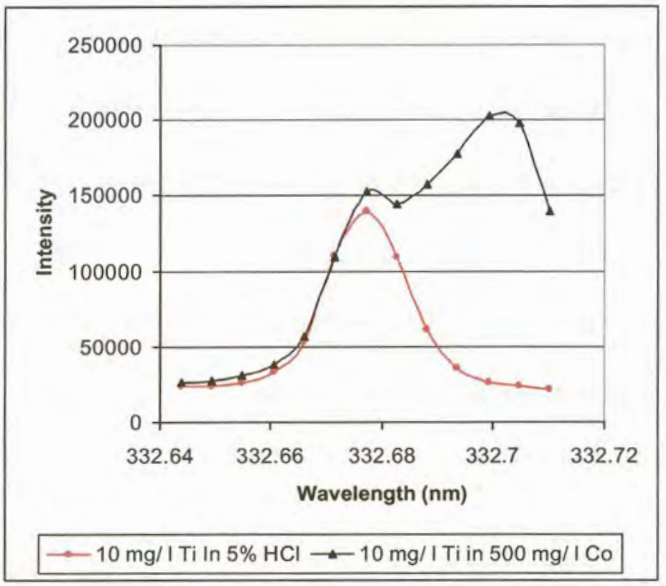

Figure 8.1: Effect of Co on Ti at 332.676 nm (JY-24 ICP-OES),
where 5% HCl refers to a 0.5 M solution (5% v/v dilution from concentrated HCl)

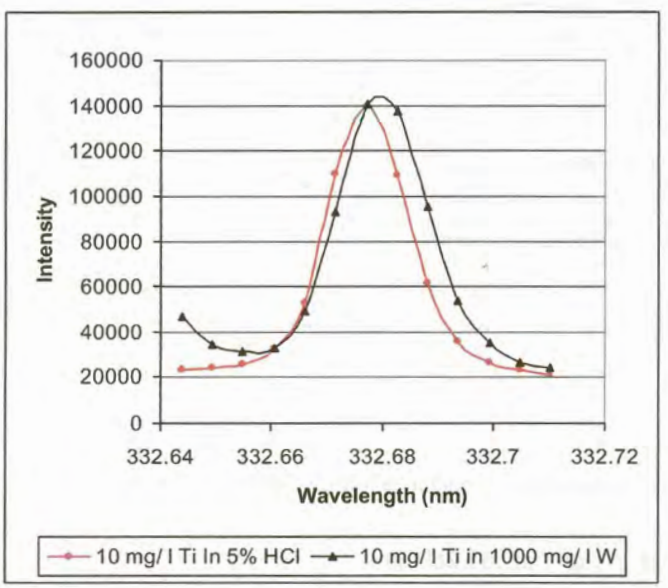

Figure 8.2: Effect of W on Ti at 332.676 nm (JY-24 ICP-OES),
where 5% HCl refers to a 0.5 M solution (5% v/v dilution from concentrated HCl)

No interferences from cobalt or tungsten are reported for the 337.280 nm titanium emission line (Boumans, 1984; Harrison, 1969). On profiling solutions of titanium in various matrices, it was experimentally confirmed that tungsten, titanium, tantalum, chromium and vanadium have negligible influence on titanium measurements. However, cobalt was found to slightly affect the measurement of titanium at 337.280 nm (Figure 8.3) and to obtain quantitative results matrix matching of the calibration solutions with respect to cobalt was performed.

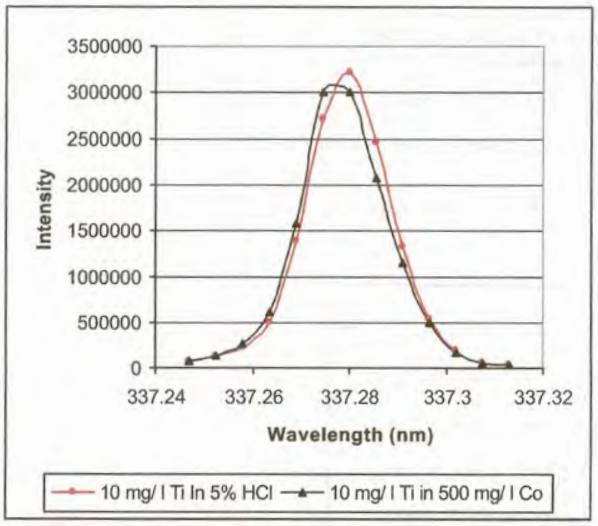

Figure 8.3: Effect of Co on Ti at 337.280 nm (JY-24 ICP-OES), where 5% HCl refers to a 0.5 M solution (5% v/v dilution from concentrated HCl)

As can be seen from Figure 8.4, tungsten at a concentration of 1000 mg/ ℓ has only a slight effect on a solution of titanium of 10 mg/ ℓ at 337.280 nm.

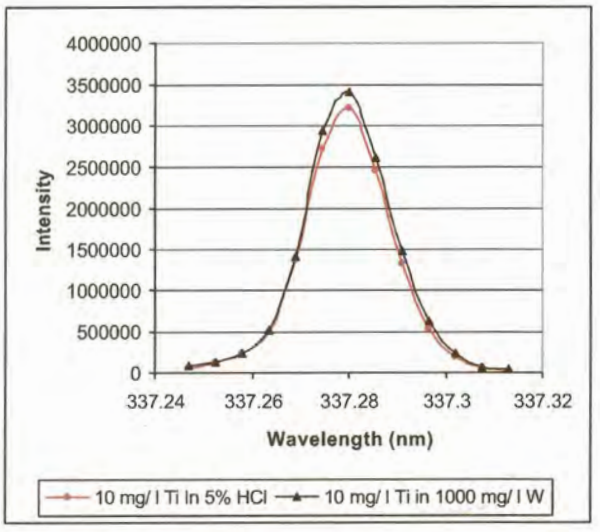

Figure 8.4: Effect of W on Ti at 337.280 nm (JY-24 ICP-OES), where 5% HCl refers to a 0.5 M solution (5% v/v dilution from concentrated HCl)

Although Boumans (1984) gives no information of a cobalt emission line near 368.520 nm and Harrison (1969) mentions only a cobalt emission line at 368.496 nm, cobalt at the 500mg/ ℓ level was found to have an effect on the titanium measurement at this wavelength, as is illustrated in Figure 8.5.

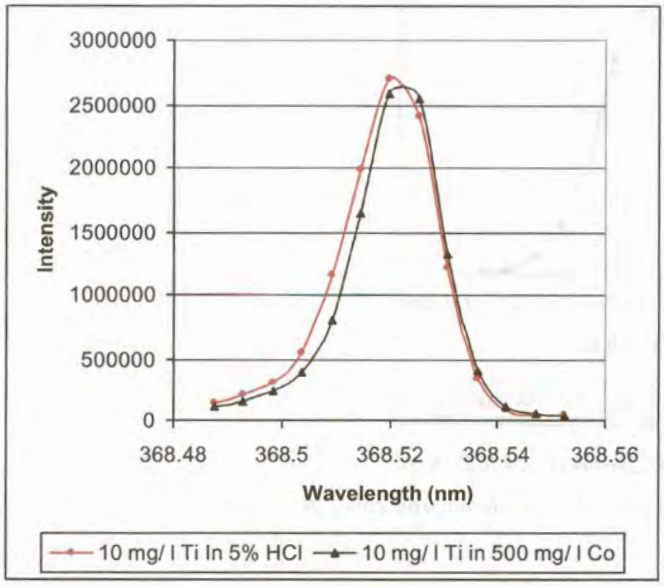

Figure 8.5: Effect of Co on Ti at 368.520 nm (JY-24 ICP-OES), where 5% HCl refers to a 0.5 M solution (5% v/v dilution from concentrated HCl)

A tungsten emission line is reported by Harrison (1969) at 368.502 nm and this was observed to have a slight effect on the titanium measurement at 368.520 nm (Figure 8.6).

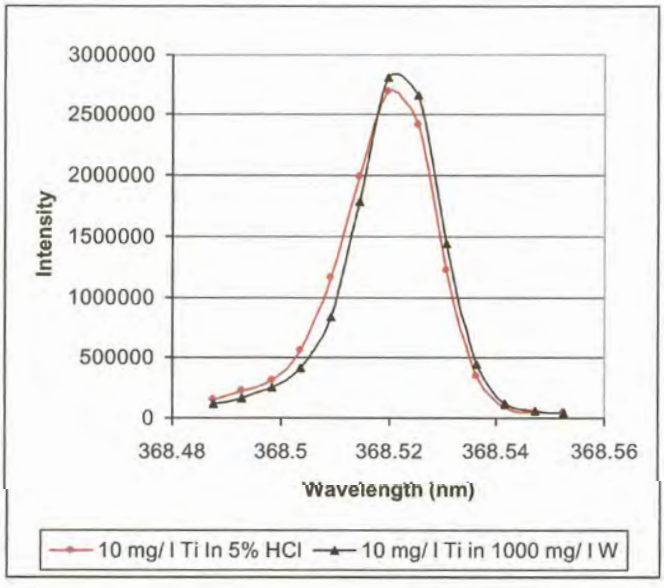

Figure 8.6: Effect of W on Ti at 368.520 nm (JY-24 ICP-OES), where 5% HCl refers to a 0.5 M solution (5% v/v dilution from concentrated HCl)

8.3 CALIBRATION SOLUTIONS

The titanium content of the commercial samples analysed during this study was found to be below 0.02 mg/ 100 g. To test the efficiency of the dissolution method for titanium, a certified reference material of cemented carbide, NBS 889 obtained from NIST (USA) was analysed. The certified titanium concentration was 4.03 ± 0.10 g/ 100 g. The measurement method for tungsten carbide samples containing titanium in the range 0 to 1 g/ 100 g was tested by titanium spiking of solutions of tungsten carbide which contained no titanium.

Initially, calibration solutions were prepared which matched the matrix of a solution of the NBS 889 cemented carbide with respect to cobalt. The sample dilution factor was 2000, with the solution cobalt concentration roughly 50 mg/ ℓ.

Table 8.1 gives a summary of a typical composition of the analytical solution with respect to titanium, cobalt and tungsten.

Table 8.1: Solution for the analysis of titanium in tungsten carbide

Analyte	Titanium
Mass dissolved	0.5 g
Final volume	1000 ml
Dilution factor	2000
Concentration titanium in solution	~ 20 mg/ ℓ
Concentration cobalt in solution	5 – 75 mg/ ℓ
Concentration tungsten in solution	~ 450 mg/ ℓ
Matrix matching of calibration solutions?	Yes (see above)

Table 8.2 gives a summary of a typical scheme for the preparation of a typical range of

calibration solutions for titanium analysis. The titanium and cobalt solutions were obtained as a certified 1000 mg/ ℓ solutions from Merck Chemicals.

Table 8.2: Preparation of titanium calibration reference solutions: sample titanium concentration 2-4 g/ 100 g and cobalt concentration 9.6 g/ 100 g.

Ti concentration required (mg/ ℓ)	Concentration of Ti stock solution (mg/ ℓ)	Volume of Ti stock solution (ml)	Volume of 1000 mg/ ℓ *Co (ml)	Volume 32% HCl (ml)	Final volume (ml)
0	-	-	5.00	5	100.00
1	20	5.00	5.00	5	100.00
10	1000	1.00	5.00	5	100.00
50	1000	5.00	5.00	5	100.00

* *The cobalt concentration must match those of the sample solutions*

A four point calibration of the ICP-OES was performed with the solutions in Table 8.2 at 337.280 nm and 368.520 nm.

At 337.280 nm, a calibration curve with a coefficient of determination (r^2) of 0.9999, was obtained. This curve can be viewed in Appendix 4, Figure A5. The limit of detection (LOD), calculated from this data according to the principles of Miller & Miller (1993), was 0.3 mg/ ℓ and the limit of quantification (LOQ) 1 mg/ ℓ.

The calibration curve at 368.520 nm, with a coefficient of determination (r^2) of 0.9999, can be viewed in Appendix 4, Figure A6. The LOD, calculated from this data, was 0.2 mg/ ℓ and the limit of quantification 0.7 mg/ ℓ.

When other titanium calibration series, with the highest titanium concentrations respectively 10

and 20 mg/ ℓ, were used for calibration, the r^2 value was never below 0.9999 and the LOQ never above 1 mg/ ℓ.

8.4 REFERENCE MATERIALS AND QUALITY CONTROL

The effect of cobalt and tungsten in the matrix on the measurement of titanium was checked by preparing solutions of titanium (10 mg/ ℓ) in respectively 0.5 M hydrochloric acid, 9000 mg/ ℓ tungsten, 50 mg/ ℓ cobalt, and a 10 mg/ ℓ mixture of chromium, tantalum and vanadium. These solutions were measured at 337.280 nm and 368.520 nm after calibration of the ICP-OES with titanium solutions in 5 % hydrochloric acid. The results are tabulated in Table 8.3.

Table 8.3: Measured effect of W, Co, Cr, Ta and V on titanium measurements

Matrix of the 10 mg/ ℓ titanium solution	Measured concentration of Ti (mg/ ℓ) at 337.280 nm	368.520 nm
0.5 M HCl	10.0	10.0
1000 mg/ ℓ W	9.9	10.3
50 mg/ ℓ Co	10.8	10.7
10 mg/ ℓ Cr, Ta, V	9.5	9.6

The data in Table 8.3 confirms the observations made regarding the effect of cobalt in Section 8.2. At both wavelengths, the measured titanium concentration was higher than expected when measured in a cobalt matrix. In both cases, the difference is more than 5% of the prepared concentration and the calibration solutions for the measurement of titanium were matrix matched with respect to cobalt. A slight interference by tungsten on titanium measurements was observed at 337.280 nm and 368.520 nm in Section 8.2. From the data in Table 8.3, it can be seen that the effect is negligible, since the measurements for titanium made in a tungsten matrix, were within 5% of the prepared concentration. The calibration solutions were therefore not matrix

matched with respect to tungsten.

The concentration of titanium in the cemented carbide reference material, NBS 889, is certified as 4.03 g ± 0.10 g/ 100 g. On measurement of the titanium in triplicate aliquots of this reference material, dissolved by the hydrogen peroxide/ aqua regia method described in Section 4.3, a titanium concentration of 3.96 ± 0.17 g/ 100 g was obtained. The dilution factor for the analysis was 2000, when 0.5 g sample was diluted to 1000 ml, giving a titanium concentration in the solutions of about 20 mg/ ℓ. The titanium concentrations obtained are tabulated in Table 8.4.

Table 8.4: Ti measurement results for cemented carbide NBS 889

	Concentration Ti (g/ 100 g) measured at 337.280 nm	368.520 nm	Average
Aliquot 1	3.85	3.95	3.90
Aliquot 2	3.96	3.94	3.95
Aliquot 3	4.03	4.03	4.03
Average			**3.96**
s (n = 6)			0.0669

The confidence limits for the results in Table 8.4 were calculated according to the formula (Miller & Miller, 1993):

$\mu = \bar{x} \pm \frac{ts}{\sqrt{n}}$, where x = 3.96, $t_{(0.05, 5)} = 2.5706$, s = 0.0669 and n = 6

giving a titanium concentration of 3.96 ± 0.17 g/ 100 g. Since the certified concentration was given as 4.03 ± 0.10 g/ 100 g, the results prove that the method is effective for the dissolution of titanium in tungsten carbide.

When solutions of tungsten carbide, prepared from titanium-free material, were spiked with 0.2 mg/ ℓ titanium, measured concentrations (after calibration with cobalt matched titanium solutions)

of 0.166 and 0.171 mg/ ℓ were obtained, at 337.280 nm and 368.520 nm respectively. The dilution factor for the solutions was 200, giving a cobalt concentration of about 250 mg/ ℓ in the solutions. Since the solutions were measured below the theoretical detection limit (Section 8.3), the results could be considered excellent. Other aliquots of the same solutions were spiked with 5 mg/ ℓ titanium and measurement results of 4.475 and 4.537 mg/ ℓ at the two wavelengths, respectively, were obtained. These concentrations are within 5% of the prepared concentration and accurate quantitation of titanium levels in samples with titanium concentrations between 0.01 and 1 g/ 100 g can realistically be expected to be achieved.

The measurement runs for titanium were always shorter than 30 minutes. A reference solution of titanium (QC) was always analysed at the beginning of an analytical run and at the end. The results for these measurements were always found to be within 5% of each other.

8.5 DISCUSSION AND CONCLUSIONS

Although none of the commercial samples contained titanium in measurable concentrations, there was enough data to calculate that titanium concentrations as low as 0.01 g/ 100 g in the sample could be analysed without major problems. No false positive results were obtained using the measurement methods described in this chapter.

The certified titanium concentration of the NBS 889 material was 4.03 ± 0.10 g/ 100 g. An analytical concentration of 3.96 ± 0.17 g/ 100 g was obtained, using the above method. This falls within the certified uncertainty range. The results also show that titanium in tungsten carbide is effectively dissolved by the hydrogen peroxide/ aqua regia method.

As shown during the analysis of cobalt and tantalum, it is good analytical practice to use at least two different analytical wavelengths for ICP-OES analyses if time permits. If samples of exactly the same elemental composition are routinely analysed, either wavelength may be used after validation. Although no evidence was found during the measurement of titanium that other elements influence the measurements, the range of different experimental tungsten carbide samples received by the laboratory justified the use of both analytical wavelengths for all the analyses.

CHAPTER 9

MEASUREMENT OF VANADIUM

9.1 WAVELENGTHS SELECTED

No references to the measurement of vanadium in tungsten carbide by ICP-OES could be found in the literature, although a standard method for the analysis of vanadium in tungsten carbide, using atomic absorption spectrometry by the method of standard additions (ISO, 1983), exists.

There are several lines which are recommended for vanadium analysis, the most commonly used being 268.796 nm, 270.094 nm (Jobin Yvon, version 5 software), 292.402 nm, 309.311 nm, 310.230 nm and 311.071 nm (Thompson & Walsh, 1983). All these lines were investigated by comparing the emission profiles of solutions of vanadium in acid with those of vanadium in tungsten and vanadium in cobalt. The vanadium emission lines at 292.402 nm and 311.071 nm were found suitable for analytical purposes.

Another vanadium emission line at 290.88 nm was recommended by Thompson & Walsh (1983) for the measurement of vanadium in soils. Since there are three tungsten emission lines at 290.840 nm, 290.849 nm and 290.912 nm (Harrison, 1969) which may interfere when vanadium in tungsten carbide is measured, this line was not evaluated.

9.2 MATRIX EFFECTS AND INTERFERENCES

Cobalt was found to cause no interferences at the 268.796 nm vanadium emission line. The emission profiles of vanadium in 0.5 M hydrochloric acid and vanadium in a cobalt solution are compared in Figure 9.1.

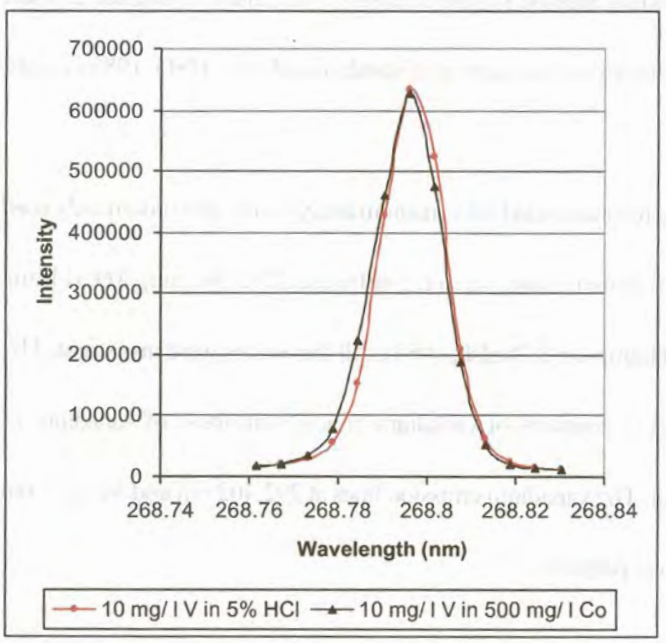

Figure 9.1: Effect of Co on V at 268.796 nm (JY-24 ICP-OES), where 5% HCl refers to a 0.5 M solution (5% v/v dilution from concentrated HCl)

However, the tungsten emission lines at 268.800 nm and 268.822 nm (Harrison, 1969) were found to interfere slightly with quantitative vanadium analysis at 268.796 nm, as can be observed in Figure 9.2.

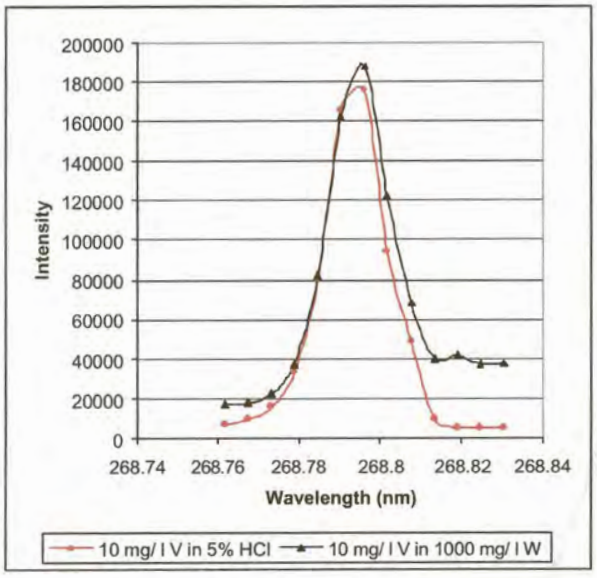

Figure 9.2: Effect of W on V at 268.796 nm (JY-24 ICP-OES), where 5% HCl refers to a 0.5 M solution (5% v/v dilution from concentrated HCl)

The 270.094 nm vanadium emission line was tested with vanadium in cobalt and tungsten matrices. Although the results in Figure 9.3 seem to show an interference by cobalt, it was found through measurements of solutions of the certified reference material (NBS 889) that no significant interferences from cobalt at the 500 mg/ ℓ level occurred.

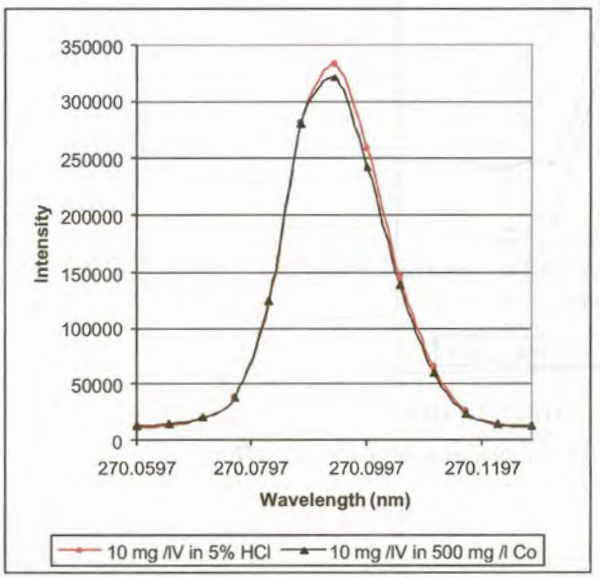

Figure 9.3: Effect of Co on V at 270.094 nm (JY-24 ICP-OES), where 5% HCl refers to a 0.5 M solution (5% v/v dilution from concentrated HCl)

A tungsten emission line is cited in the literature at 270.106 nm (Harrison, 1969). From Figure 9.4, it can be seen that this does indeed interfere with the measurement of vanadium at 270.094 nm.

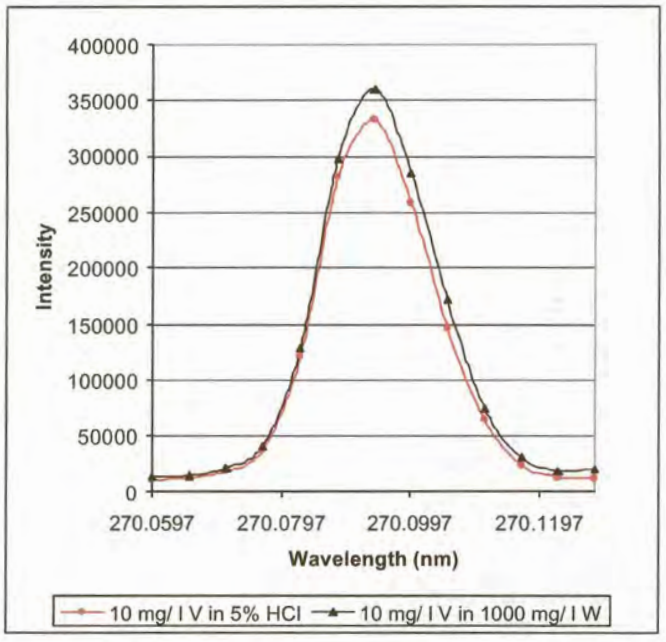

Figure 9.4: Effect of W on V at 270.106 nm (JY-24 ICP-OES), where 5% HCl refers to a 0.5 M solution (5% v/v dilution from concentrated HCl)

There is a tungsten emission line at 292.354 nm (Boumans, 1984; Harrison, 1969) but this is not close enough to the vanadium emission line at 292.402 nm to influence the measurements. Tungsten at the 1000 mg/ ℓ level was confirmed to have very little effect on vanadium analyses at 292.402 nm (Figure 9.5).

The presence of cobalt in the solutions was not found to affect the quantitative results at 292.402 nm, as can be seen in Figure 9.6. No cobalt emission lines are reported by either Boumans (1984) or Harrison (1969) near this wavelength.

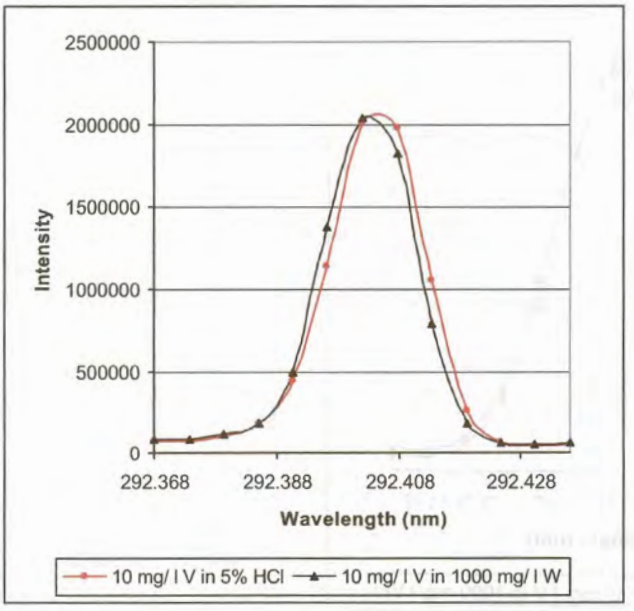

Figure 9.5: Effect of W on V at 292.402 nm (JY-24 ICP-OES),
where 5% HCl refers to a 0.5 M solution (5% v/v dilution from concentrated HCl)

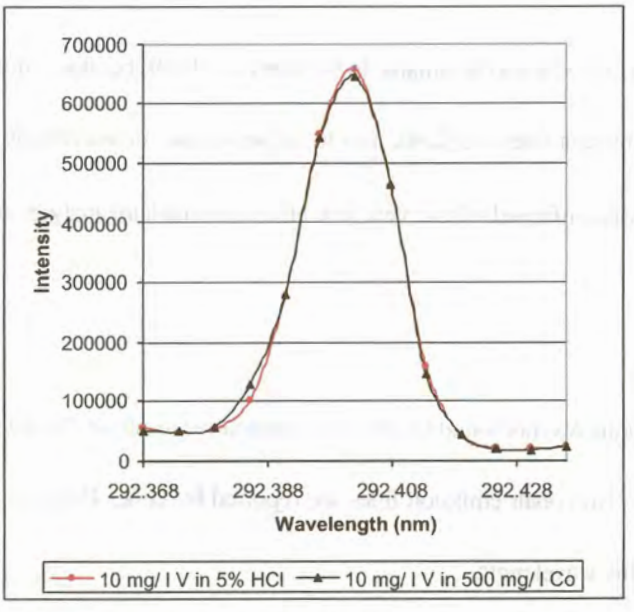

Figure 9.6: Effect of Co on V at 292.402 nm (JY-24 ICP-OES),
where 5% HCl refers to a 0.5 M solution (5% v/v dilution from concentrated HCl)

The 309.350 nm tungsten emission line (Boumans, 1984; Harrison, 1969) was found to interfere with quantitative vanadium analysis at 309.311 nm but this line could be used to confirm the approximate vanadium concentration in the sample solution.

A baseline shift was observed at the line 310.230 nm when vanadium solutions with an acid matrix were compared to solutions with a tungsten carbide-cobalt matrix. This was thought to be due to a tungsten emission line at 310.222 nm (Harrison, 1969).

The 311.071 nm vanadium emission line was found not to be subject to tungsten interference (Figure 9.7). Boumans (1984) and Harrison (1969) report a tungsten emission line at 311.112 nm but this was found not to have an influence on the vanadium measurements.

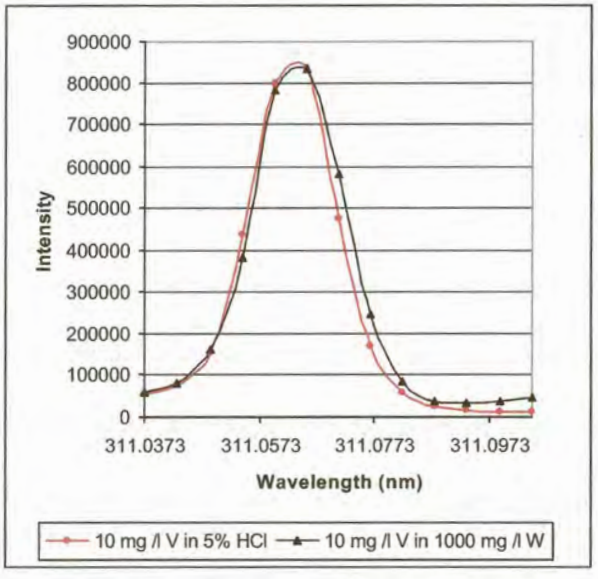

Figure 9.7: Effect of W on V at 311.071 nm (JY-24 ICP-OES), where 5% HCl refers to a 0.5 M solution (5% v/v dilution from concentrated HCl)

A cobalt emission line is reported by Harrison (1969) at 311.083 nm but it is not mentioned by

Boumans (1984). On comparing the emission profiles of solutions of vanadium in 0.5 M hydrochloric acid and in 500 mg/ ℓ cobalt solution (Figure 9.8) no significant effect could be observed.

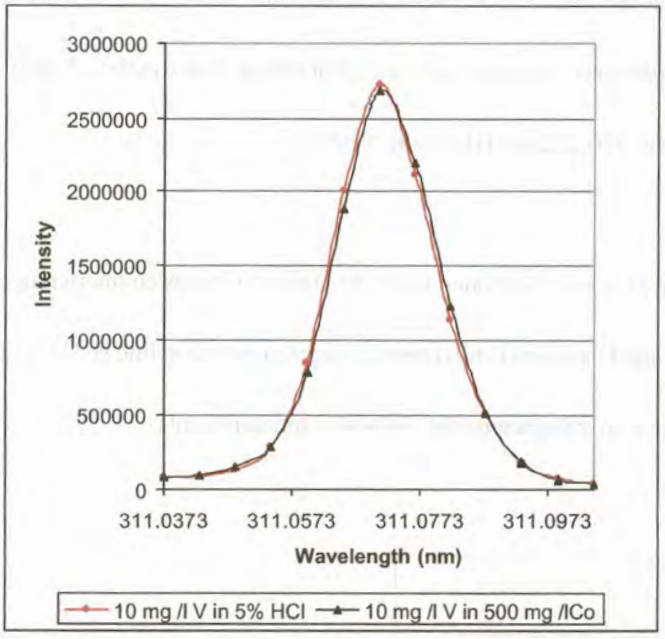

Figure 9.8: Effect of Co on V at 311.071 nm (JY-24 ICP-OES), where 5% HCl refers to a 0.5 M solution (5% v/v dilution from concentrated HCl)

To be certain that the effect of cobalt and tungsten on the measurement of vanadium at 311.071 nm had been correctly assessed, an aliquot of a cemented carbide reference material, NBS 889, which contained no vanadium, was dissolved in hydrogen peroxide/ aqua regia. Vanadium was added (spiked) to a portion of this solution at the 10 mg/ ℓ level. The emission profile of the spiked solution was compared to that of 10 mg/ ℓ vanadium in 0.5 M hydrochloric acid. From Figure 9.9, it is clear that there is no significant interference from tungsten or cobalt on vanadium measurements at 311.071 nm. At a dilution factor of 1000, the solution of NBS 889 contained about 95 mg/ ℓ cobalt and about 700 mg/ ℓ tungsten, as well as approximately 46 mg/ ℓ tantalum

and approximately 40 mg/ ℓ titanium. The experiment thus confirms that tantalum and titanium at these levels do not interfere with the vanadium measurement either.

A similar result was obtained when the experiment was repeated at 292.402 nm.

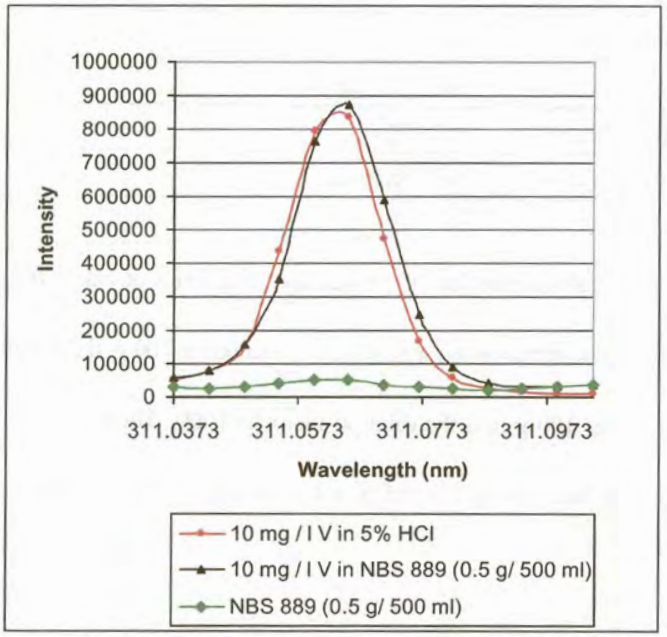

Figure 9.9: The effect of the matrix of an actual tungsten carbide sample on the measurement of V at 311.071 nm (JY-24 ICP-OES), where 5% HCl refers to a 0.5 M solution (5% v/v dilution from concentrated HCl)

9.3 CALIBRATION SOLUTIONS

The samples analysed contained vanadium in concentrations ranging from 0 to 8 g/ 100 g. In most of the samples, the vanadium concentration was in the region of 0.6 g/ 100 g. It was found convenient to dilute 0.5 g sample to 500 ml to give a vanadium concentration of in the measurement solution of about 6 mg/ ℓ.

Table 9.1 gives a summary of a typical composition of the analytical solution with respect to

vanadium, cobalt and tungsten.

Table 9.1: Summary of analytical solution composition during the analysis of vanadium in tungsten carbide

Analyte	Vanadium
Mass dissolved	0.5 g
Final volume	500 ml
Dilution factor	1000
Concentration vanadium in solution	0 – 80 mg/ ℓ
Concentration cobalt in solution	10 – 150 mg/ ℓ
Concentration tungsten in solution	~ 850 mg/ ℓ
Matrix matching of calibration solutions?	Not required

Table 9.2 gives a summary of a typical scheme for the preparation of a series of calibration solutions if the expected vanadium concentration in the sample is about 0.6 g/ 100 g, the cobalt content in the sample is about 9.6 g/ 100 g and the dilution factor is 1000. The vanadium solution was obtained from Merck Chemicals as a certified solution with a concentration of 1000 mg/ ℓ.

Table 9.2: Preparation of vanadium calibration reference solutions: sample vanadium concentration 0.6 g/ 100 g and cobalt concentration 9.6 g/ 100 g

V concentration required (mg/ ℓ)	Concentration of V stock solution (mg/ ℓ)	Volume of V stock solution (ml)	Volume of 32% HCl (ml)	Final volume (ml)
0	-	-	5	100.00
1	25	4.00	5	100.00
5	1000	0.50	5	100.00
10	1000	1.00	5	100.00

A four point calibration of the JY-24 ICP-OES was performed at 292.402 nm and at 311.071 nm. The calibration curve at 292.402 nm can be viewed in Appendix 4, Figure A7. A coefficient of correlation (r^2) of 1.0000 was obtained. The limit of detection (LOD), calculated from this

data according to the principles of Miller & Miller (1993), was 0.03 mg/ ℓ and the limit of quantification (LOQ) 0.1 mg/ ℓ.

At 311.071 nm, the coefficient of correlation (r^2) was found to be 0.9999, the LOD 0.1 mg/ ℓ and the LOQ 0.5 mg/ ℓ (Appendix 4, Figure A8).

When tungsten carbide samples with concentrations of vanadium above 0.7 g/ 100 g were analysed, the sample solutions were diluted so that the vanadium concentration in the solutions fell approximately in the middle of the calibration range. Sometimes the vanadium calibration range was extended to 50 mg/ ℓ. The usual linearity checks were performed and limit of quantitation calculated before sample measurements were made.

9.4 REFERENCE MATERIALS AND QUALITY CONTROL

Several checks were done to ensure valid results:

i) The certified reference material of cemented carbide, NBS 889 (obtained from NIST, USA), which was used for quality control with cobalt, tantalum and titanium contained no vanadium. A solution of this cemented carbide was spiked with vanadium to check the measurement procedure. Solutions of vanadium in different matrices (0.5 M hydrochloric acid, 60 mg/ ℓ cobalt, and 1000 mg/ ℓ tungsten) were also measured.

ii) A certified tungsten carbide reference material which contains vanadium was not available. However, a sample of tungsten carbide which had been analysed by the Boart Longyear Research Centre by XRF was obtained.

iii) The vanadium concentration in a commercial sample was measured using the external calibration procedure described in Section 9.3. It was then also analysed by the method of standard additions and the results compared.

An aliquot of vanadium-free cemented carbide, NBS 889, was dissolved by the hydrogen peroxide/ aqua regia method described in Section 4.3. Aliquots of this solution were spiked with vanadium to give final vanadium concentrations of 5 mg/ ℓ and 10 mg/ ℓ, respectively. The final solution had a dilution factor of 1000 and thus a cobalt concentration of about 96 mg/ ℓ. A series of vanadium calibration solutions, similar to those in Table 9.2, were prepared and the JY-24 ICP-OES calibrated with these solutions at 292.402 nm and 309.311 nm. The spiked solutions of the cemented carbide were then measured. Solutions of 5 mg/ ℓ vanadium in respectively, 0.5 M hydrochloric acid, 60 mg/ ℓ cobalt and 1000 mg/ ℓ tungsten, were also measured.

The measurements were repeated after the instrument had been calibrated with vanadium solutions in 60 mg/ ℓ cobalt. The results for the measurements after calibration with vanadium in hydrochloric acid are tabulated in Table 9.3.

Table 9.3: Analysis of solutions of cemented carbide, NBS 889, spiked with vanadium

Spiked concentration (mg/ ℓ)	Measured concentration (mg/ ℓ) at 292.402 nm	309.311 nm
5	4.950 4.881	4.849 4.827
10	9.901 9.872	9.698 9.654

The results in Table 9.3 show that measurement results within 5% of the expected concentrations can be obtained at 292.402 nm and 309.311 nm without matrix matching of the reference solutions. The results of the measurement of the vanadium solutions in the different matrices were all within 5% of the prepared concentrations. For a 5 mg/ ℓ solution of vanadium this would be a range of 4.75 to 5.25 mg/ ℓ, and for the 10 mg/ ℓ solution, a range of 9.5 to 10.5 mg/ ℓ. The results obtained after the instrument was calibrated with vanadium solutions in 60 mg/ ℓ cobalt also fell within this range. It was concluded that the accuracy of the vanadium measurements at 292.402 nm or 311.071 nm were not affected by cobalt, tungsten, tantalum or titanium.

The vanadium concentration in the sample which had been analysed by Boart Longyear Research Centre by XRF, was given as 0.63 g/ 100 g. This sample was dissolved a number of times by the hydrogen peroxide/ aqua regia method and the vanadium concentration measured by ICP-OES at 292.402 nm and 311.071 nm. The results are tabulated in Table 9.4.

Table 9.4: ICP-OES vanadium measurement results for a tungsten carbide sample previously measured by XRF

Aliquot number	**Vanadium measurement results (g/ 100 g) at**	
	292.402 nm	**311.071 nm**
1	0.578	0.576
2	0.586	0.571
3	0.595	0.572
4	0.574	0.573
5	0.590	0.576
6	0.578	0.573

When the results in Table 9.4 were analysed by a two factor ANOVA test using Microsoft Excel, there was no significant difference in the precision between the results obtained at the two wavelengths. There was a slight statistical difference in the accuracy of the results for the two

different wavelengths, the mean concentration being 0.58 g/ 100 g at 292.402 nm and 0.57 g/ 100 g at 311.071 nm. In Table 9.3 all the results of the spiked solutions fall within 5% of the prepared value, although the results at 311.071 nm are slightly lower than those at 292.402 nm. Whether the results at the two wavelengths differ significantly is not conclusive, and thus the average of the results for both wavelengths were used when commercial samples were analysed. The procedure of Miller & Miller (1993), using the formula:

$$\mu = \bar{x} \pm \frac{ts}{\sqrt{n}}, \quad \text{where } t_{(0.05;13)} = 2.160,\ s = 0.0071 \text{ and } n = 14$$

produces a concentration of 0.58 ± 0.01 g/ 100 g. All the values obtained in Table 9.4, except 0.595, fall within this range. The sample was used as a secondary reference material with commercial samples.

The vanadium concentration in a commercial sample was measured using the external calibration procedure described in Section 9.3 at the 292.402 nm vanadium emission line. An average vanadium concentration of 0.602 g/ 100 g was obtained. The sample solution was then divided into 6 portions and increasing concentrations of vanadium added to each portion. The added vanadium concentrations ranged from 0 to 10 mg/ ℓ. These solutions were then analysed at 292.402 nm by the method of standard additions. The results are tabulated in Table 9.5. By the method of standard additions, a result of 0.599 g/ 100 g was achieved. This is very close to the result for the external calibration method, which was 0.602 g/ 100 g.

Table 9.5: Results of ICP-OES analysis by the method of standard additions

Vanadium added (mg/ ℓ)	Signal (292.402 nm)
0	2380
1	2762
2.5	3422
5	4447
7.5	5418
10	6416

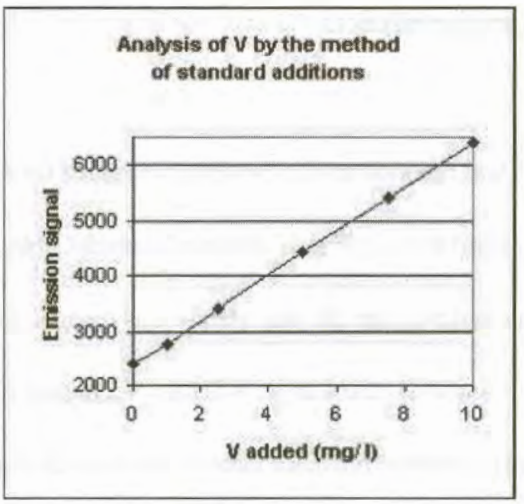

SUMMARY OUTPUT

Regression Statistics	
Multiple R	0.999873355
R Square	0.999746725
Adjusted R Square	0.999683406
Standard Error	28.04282929
Observations	6

ANOVA

	df	*SS*	*MS*	*F*	*Significance F*
Regression	1	12416567	12416567	15789.12	2.41E-08
Residual	4	3145.601	786.4003		
Total	5	12419713			

	Coefficients	*Standard Error*	*t Stat*	*P-value*	*Lower 95%*	*Upper 95%*
Intercept	2387.385714	18.04978	132.2668	1.96E-08	2337.271	2437.5
X Variable 1	404.6417582	3.220266	125.6548	2.41E-08	395.7008	413.5827

Concentration V in soln =	a/b =	5.900mg/ ℓ
Sample mass		0.4928 g
Sample volume		500 ml
Dilution factor		1014.61
Sample V concentration =		**0.599g/ 100 g**

9.5 DISCUSSION AND CONCLUSIONS

From the results of the spiking experiments, it can be concluded that accurate vanadium measurements can be made at 292.402 nm and 311.071 nm without matrix matching of the reference solutions. One of the samples was analysed by both the external calibration method and the method of standard additions at 292.402 nm. The results were very similar (0.602 and

0.599 g/ 100 g, respectively), confirming that the matrix did not contribute significantly to measurement errors.

As was reported earlier, the results obtained for the multiple ICP-OES analysis of the sample obtained from the Boart Longyear Research Centre, were significantly lower than the XRF result reported by them. No uncertainty was reported for the result of 0.63 g/ 100 g. On enquiry, it was found that the sample was part of a routine XRF analytical run. It was only analysed once and no certified reference material was used during the analysis. The results found by the Boart Longyear Research Centre were suitable for their particular research application and fell within their expected range. The average result for the ICP-OES analysis was 0.58 ± 0.01 g/ 100 g. There is no evidence that the ICP-OES measurement procedure did not give accurate results. Townshend et al (1995, p5098, p5364) suggest that nitric and hydrofluoric acid can be used to dissolve both tantalum and vanadium. Since tantalum in tungsten carbide was successfully analysed by the same dissolution procedure and measurement technique, there is no evidence that vanadium cannot be completely dissolved by the hydrogen peroxide/ aqua regia method.

In some cases, no vanadium could be detected in the samples at a dilution factor of 1000. The 0.5g/ 100 ml solutions were then measured by ICP-OES at the vanadium emission lines. From the calibration data at 292.402 nm, a vanadium detection limit (LOD) of 0.001 g/ 100 g and a limit of quantification (LOQ) of 0.002 g/ 100 g in the sample was therefore possible. The calculations were performed according to the guidelines of Miller & Miller (1993).

No significant effect from tungsten, cobalt, titanium and tantalum on the measurement of vanadium was observed at the levels found in commercial samples, but it has been found that additional elements may be introduced into tungsten carbide in a research environment. The effects of these elements had not been tested and it was therefore considered prudent to measure the vanadium concentration at two different analytical wavelengths. The effect of a certain element on the measurement of an analyte element is not likely to be exactly the same at two different emission wavelengths. A discrepancy between the results at two wavelengths would be cause for an investigation and the reporting of erroneous results could be prevented.

Although no certified reference material was available for analysis, it can be concluded from the validation methods investigated that vanadium in tungsten carbide can be accurately determined using the hydrogen peroxide/ aqua regia dissolution procedure together with the ICP-OES measurement technique.

CHAPTER 10

MEASUREMENT OF CHROMIUM

10.1 WAVELENGTHS SELECTED

Several chromium emission lines are recommended in the Jobin Yvon software (version 5): the Cr emission lines at 205.559 nm, 266.602 nm, 283.563 nm and 357.869 nm. Thompson & Walsh (1983) recommend the line at 267.654 nm for the analysis of chromium in soil. Each of these lines was investigated and only the 357.869 nm emission line, also recommended by Piippanen et al (1996a), gave consistently good results, as will be shown later. However, this line has cobalt emission lines at 357.890 nm and 357.903 nm (Harrison, 1969) but matrix matching could be applied to correct the problem. No interference from tungsten could be observed. All the other lines were found to have interferences from tungsten emission lines. Since the tungsten concentration in the sample solutions was very high compared to the chromium concentration (see Table 10.2), matrix matching with tungsten was not an option.

10.2 MATRIX EFFECTS AND INTERFERENCES

The potential interferences at each line were researched in the literature (Boumans, 1984; Harrison, 1969). Table 10.1 gives a summary of the information obtained.

Table 10.1: Summary of potential interferences in chromium analysis by ICP-OES

Cr emission line	Interferent	
	Element	Emission line
205.559 nm	W	205.602 nm
266.602 nm	W	266.564 nm, 266.577 nm, 266.608 nm
267.654 nm	W	267.631 nm, 267.641 nm
283.563 nm	W	283.564 nm
357.869 nm	Co	357.890 nm, 357.903 nm

The emission profiles of a solution of 10 mg/ ℓ chromium in 0.5 M hydrochloric acid and that of a 10 mg/ ℓ chromium solution in 1000 mg/ ℓ tungsten were compared at each wavelength. The effect of cobalt at 357.869 nm was also investigated. Some of the effects are documented in Figure 10.1.

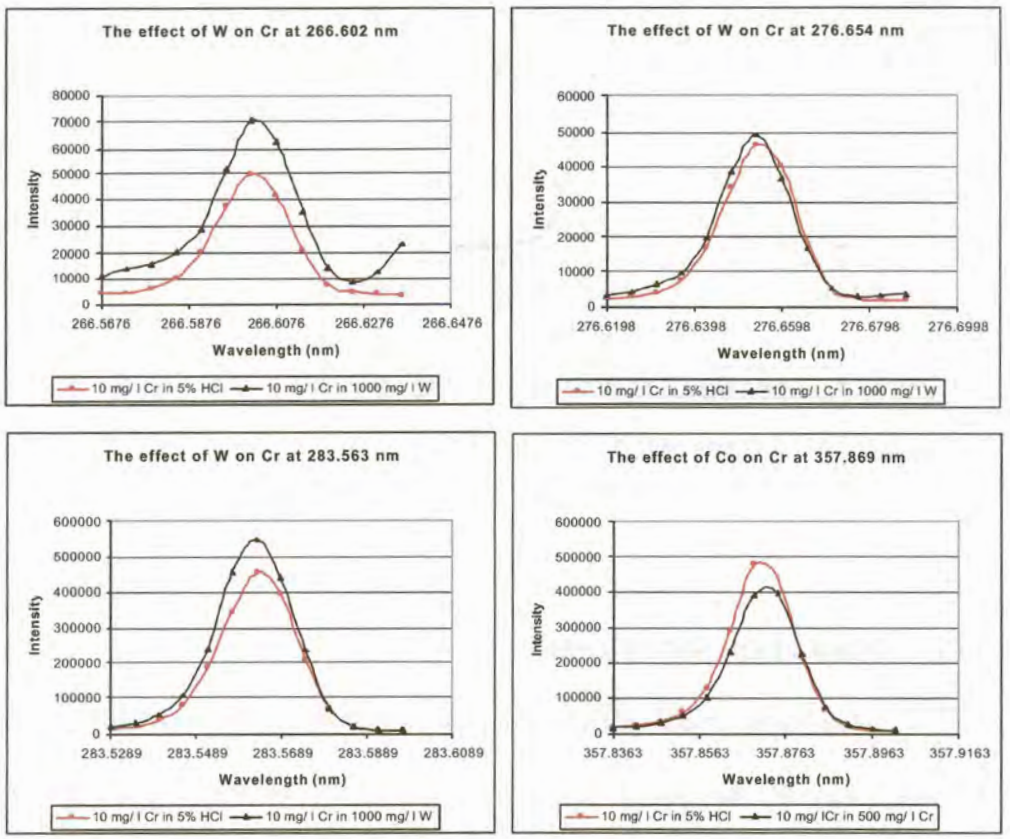

Figure 10.1: Effect of W and Co at various Cr emission lines (JY-24 ICP-OES), where 5% HCl refers to a 0.5 M solution (5% v/v dilution from concentrated HCl)

From Figure 10.1 it can be seen that the tungsten interference at all the Cr II lines precludes their use for the quantitative measurement of chromium.

Although no cobalt emission lines could be found in the literature near 276.654 nm, a cobalt interference was observed near this chromium emission line, as is shown in Figure 10.2.

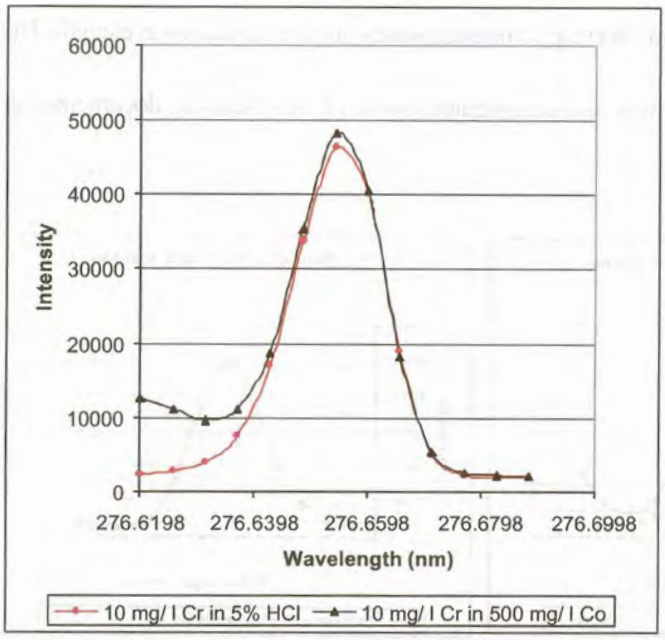

Figure 10.2: Effect of Co on Cr at 276.654 nm (JY-24 ICP-OES), where 5% HCl refers to a 0.5 M solution (5% v/v dilution from concentrated HCl)

10.3 CALIBRATION SOLUTIONS

The 357.869 nm chromium emission line was selected as the analytical line. As can be seen from Sections 10.1 and 10.2 the calibration and quality control solutions needed to be matrix matched with respect to cobalt. Since the chromium levels in the commercial samples rarely exceeded 0.07 g/ 100 g, a sample dilution factor of 200 was found to be appropriate. This dilution would result in cobalt concentrations in the solution of 250 to 750 mg/ ℓ.

Table 10.2 gives a summary of a typical composition of the analytical solution with respect to cobalt, tungsten and chromium.

Table 10.2: Summary of solution for the analysis of chromium in tungsten carbide

Analyte	Chromium
Mass dissolved	0.5 g
Final volume	100 ml
Dilution factor	200
Concentration chromium in solution	0 – 15 mg/ ℓ
Concentration cobalt in solution	50 – 750 mg/ ℓ
Concentration tungsten in solution	~ 4250 mg/ ℓ
Matrix matching of calibration solutions?	Yes , wrt to cobalt

Table 10.3 gives an example of a typical scheme for the preparation of a series of chromium calibration solutions, matrix matched with cobalt, for samples which contain 0.01 to 0.07 g/ 100 g chromium and about 10 g/ 100 g cobalt at a dilution factor of 200. The chromium was obtained from Merck Chemicals, as a 1000 mg/ ℓ certified solution. The cobalt solution was also obtained from Merck Chemicals.

Table 10.3: Summary of the preparation of a series of chromium calibration solutions: sample chromium content 0.01- 0.07 g/ 100 g, cobalt content 10 g/ 100 g. Sample dilution 0.5g /100 ml

Cr concentration required (mg/ ℓ)	Concentration of Cr stock solution (mg/ ℓ)	Volume of Cr stock solution (ml)	*Volume of 1000 mg/ ℓ Co (ml)	Volume of 32% HCl (ml)	Final volume (ml)
0	-	-	50.00	5	100.00
1	25	4.00	50.00	5	100.00
5	1000	0.50	50.00	5	100.00
25	1000	2.50	50.00	5	100.00

* Matrix matched to the cobalt concentration in the sample solutions, in this case 500 mg/ ℓ

A four point calibration of the ICP-OES was performed. A typical calibration curve at 357.869 nm, with a coefficient of correlation (r^2) of 0.99998, can be seen in Appendix 4, Figure A9. The limit of detection, calculated from this data according to the principles of Miller & Miller (1993),

was 0.2 mg/ ℓ and the limit of quantification 0.6 mg/ ℓ.

The above method uses relatively large volumes of high purity cobalt solutions. To avoid this problem, the instrument was calibrated with chromium solutions in 0.5 M hydrochloric acid. One solution, with a chromium concentration which matched the sample concentration, was made up and used as a QC reference solution during the measurement run.

Table 10.4 gives a summary of a typical scheme for the preparation of calibration solutions in hydrochloric acid and a quality control reference solution, matrix matched with cobalt.

Table 10.4: Summary of the alternative preparation of a series of chromium calibration solutions: sample chromium content 0.1 g/ 100 g, cobalt content 10 g/ 100 g. Sample solution 0.5g /100 ml

Cr concentration required (mg/ ℓ)	Concentration of Cr stock solution (mg/ ℓ)	Volume of Cr stock solution (ml)	*Volume of 1000 mg/ ℓ Co (ml)	Volume of 32% HCl (ml)	Final volume (ml)
0	-	-	-	5	100.00
1	25	4.00	-	5	100.00
5	1000	0.50	-	5	100.00
25	1000	2.50	-	5	100.00
#5	1000	0.50	50.00	5	100.00

* Matrix matched to the cobalt concentration in the sample solutions, in this case 500 mg/ ℓ
# Quality control solution (QC)

Because the calibration solutions had contained no cobalt, the measurement of the 5 mg/ ℓ QC solution gave a reading of 4.9 mg/ ℓ. The sample measurements were multiplied by a correction factor (prepared QC concentration/ measured QC concentration) to calculate the actual chromium concentration in the solutions.

10.4 REFERENCE MATERIALS AND QUALITY CONTROL

Unfortunately, no tungsten carbide certified reference material containing chromium could be obtained. The accuracy of the analysis was checked by adding known concentrations of chromium to sample solutions containing no chromium. One of the samples analysed had also been analysed by two other laboratories by XRF and the results could thus be compared.

Two samples of tungsten carbide-cobalt which contained no chromium were dissolved by the hydrogen peroxide/ aqua regia method. Portions of each solution were spiked with chromium to give a concentration of 1 mg/ ℓ. The ICP-OES was calibrated at 357.869 nm with a series of chromium solutions, as in Table 10.4. The spiked solutions were then measured at this wavelength. The readings obtained were within 5% of the prepared concentration (0.95 to 1.05 mg/ ℓ). When no matrix matching of the calibration solutions was done, the measurements of the spiked solutions were about 7 % lower than expected.

A sample of tungsten carbide was received for analysis which had already been analysed by XRF at two independent laboratories. Triplicate aliquots of this sample were dissolved by the hydrogen peroxide/ aqua regia method to give a dilution factor of 200. The solutions were measured at 357.869 nm after calibration with a series of chromium solutions in hydrochloric acid. A QC solution of 0.5 mg/ ℓ chromium in 250 mg/ ℓ cobalt was measured to obtain a correction factor for the calculation of the actual concentration of chromium in the solution. An average chromium concentration of 0.01 g/ 100 g for this sample was reported. The other laboratories had obtained values of 0.011 and 0.012 g/ 100 g, respectively. According to the calibration data in Section 10.3 the limit of quantification is 0.6 mg/ ℓ. Since the

concentration of chromium in the solution was about 0.5 mg/ ℓ, very accurate results could not be obtained and no confidence limits were reported.

In order to demonstrate the effect of selecting an inappropriate analytical wavelength, one of the samples was analysed at three different chromium emission lines. Two of these wavelengths were shown to be subject to tungsten emission interferences (Section10.2). The results are given in Table 10.5. The sample was known to contain 0.01 g/ 100 g.

Table 10.5: Effect of different analytical wavelengths on the calculated chromium concentration

Analytical wavelength (nm)	Calculated chromium concentration (g/ 100 g)
205.559	<0.04
283.563	0.08
357.869	0.01

When a solution of tungsten carbide which contained no chromium was measured at 283.563 nm, a reading of 3.563 mg/ ℓ was obtained. The same solution measured at 357.869 nm gave a reading of -0.005 mg/ ℓ. This shows that false positive results for chromium and incorrect concentrations may be obtained if care is not taken.

As with the analyses of other elements in a tungsten carbide matrix, at least two aliquots of each sample were dissolved and replicate measurements made on some of the solutions. Quality control solutions of known concentration were measured after at least every three sample solutions. The measurements at the beginning of the analytical run were within 5% of the measurements of the same solutions at the end of the run, indicating good instrumental stability.

10.5 DISCUSSION AND CONCLUSIONS

No chromium could be detected in about half of the commercial samples analysed. A chromium detection limit (LOD) of 0.004 g/ 100 g in the sample was calculated directly from the calibration data in Section 10.3. The dilution factor was 200.

Two of the samples contained chromium in concentrations of about 0.01 g/ 100 g, which at the minimum dilution possible, fell between the LOD and the LOQ.

In the remaining samples, the chromium concentration was found to be between 0.14 and 0.22 g/ 100 g. These concentrations, after sample preparation, fell into the calibration range used. The cobalt concentrations in the reference solutions were adjusted to match those of the different sample solutions.

Table 10.5 illustrates the point made in previous chapters about the advisability of using at least two different analytical wavelengths for each element. In the case of chromium, only one suitable wavelength was available. Therefore, the matrix of the sample solution should be well characterised. The measurement of chromium in samples which contain unusual elements should be re-evaluated, ideally by the method of standard additions.

Since one of the samples had been analysed by two other laboratories by XRF and the ICP-OES results agreed closely with the XRF results, it can be concluded that there is no difficulty in dissolving chromium in tungsten carbide by the hydrogen peroxide/ aqua regia method. The measurement method has also been shown to produce accurate results.

CHAPTER 11

CONCLUSION

The research was undertaken to show whether:

a) an alternative, rapid dissolution method which avoids the use of reagents that have the potential to complicate the analysis could be found

b) the ICP-OES measurement technique is suitable for the measurement of cobalt, tantalum, titanium, vanadium and chromium in a tungsten carbide solution, and

c) accurate and precise results can be obtained with such a technique.

11.1 DISSOLUTION PROCEDURE

The dissolution procedure was proved effective for the dissolution of cobalt, tantalum, titanium, vanadium and chromium in tungsten carbide powders. The material was usually completely dissolved within 10 minutes with the hydrogen peroxide/ aqua regia method, compared to 45 minutes or more for the altemative nitric acid/ hydrofluoric acid method. The hydrogen peroxide/ aqua regia method utilizes less expensive high purity acids and the waste products present fewer problems than with traditional methods. Less expensive equipment is required, since standard laboratory glassware may used instead of PTFE vessels required for use with hydrofluoric acid.

11.2 ICP-OES MEASUREMENT

The measurement experiments proved that the ICP-OES technique is suitable for the measurement of the elements investigated, in a complex tungsten carbide matrix. The main advantage of ICP-OES over atomic absorption spectrometry is the fact that several analytical wavelengths may be evaluated during a single run, thus reducing the time required for analyses and well as the amount of work. The use of more than one analytical wavelength is a convenient

quality control aid, since interferences seldom occur to exactly the same extent at two different wavelengths. Any differences in analytical results at the different wavelengths may be used to indicate a problem.

Another advantage is the multi-element capabilities of ICP-OES. When different target elements are present in the samples in similar concentration ranges, the calibration solutions can be adapted to include them all.

A summary of the analytical wavelengths used for each element, as well as the coefficients of determination (r^2), and the limits of detection (LOD) and quantification (LOQ) achieved are given in Table 11.1.

Table 11.1: Summary of data obtained by ICP-OES measurements

Element	Concentration in sample (%)	Analytical wavelength (nm)	LOD_{soln} (mg/ ℓ)	LOD_{smpl} (g/ 100 g)	LOQ_{soln} mg/ ℓ	LOQ_{smpl} g/ 100 g	r^2
Co	1 - 15	228.616	2	0.4	7	1	0.9998
		238.346	1	0.2	4	0.8	0.9999
Ta	0 – 0.8	240.063	1	0.02	3	0.06	0.9993
		268.517	0.4	0.01	1	0.02	0.9999
Ti	0 - 4	337.280	0.3	0.01	1	0.02	0.9999
		368.520	0.2	0.004	0.7	0.01	0.9999
V	0 - 8	292.402	0.03	0.001	0.1	0.002	1.0000
		311.071	0.1	0.002	0.5	0.01	0.9999
Cr	0 – 0.2	357.869	0.2	0.004	0.6	0.01	1.0000

The ICP-OES technique was found to be rapid and convenient. It also offered more scope for

the investigation and detection of matrix related measurement problems than, for example, atomic absorption spectrometry.

11.3 ACCURACY AND PRECISION

The accuracy of the measurements was evaluated through the use of certified reference materials, secondary reference materials, matrix spiking and the method of standard additions. The ICP-OES results compared well to results obtained in other laboratories using XRF.

11.4 SHORTCOMINGS

The hydrogen peroxide could not be removed from the sample solutions prior to ICP-OES measurement without causing tungsten compounds to precipitate. This caused a slight, but acceptable increase in the RSD values obtained.

Because the cobalt content of the samples was 10 to 50 times higher than the concentrations of the other elements measured, cobalt had to be measured separately after further dilution. This caused an increase in the time taken for the analysis.

11.5 SPECIAL POINTS

The dissolution method described is a new approach to the problems encountered in the sample preparation for the analysis of tungsten carbide compounds.

No information was previously found on the analysis of vanadium in tungsten carbide by ICP-OES. The experimental results obtained show that excellent results can be obtained.

11.6 RECOMMENDATIONS AND FURTHER RESEARCH

The research was done in a commercial laboratory, where turnaround times and the limiting of costs are very important. The data presented was produced from the analysis of more than 100 samples of different compositions.

The exact minimum concentration of hydrogen peroxide required to keep the sample in solution should be studied in order to increase the precision of the results. A further systematic study of the selected wavelengths may show that a single analytical line for each element may produce consistently accurate results, no matter how the composition varies.

It would be helpful if certified reference materials of tungsten carbide, containing tantalum, titanium, vanadium and chromium in concentrations close to those of actual samples, could be obtained and used as quality control aids.

REFERENCES

ANDERSSON, K.M., Bergström, L. 2000. Oxidation and dissolution of tungsten carbide powder in water. International journal of refractory metals & hard materials, 18: 121-129.

BASSET, J., Denney, R.C., Jeffery, G.H., Mendham, J. (Eds). 1978. Vogel's textbook of quantitative inorganic analysis. 4th edition. Essex, UK: Longman Scientific & Technical.

BOSS, C.B., FREDEEN, K.J. 1999.Concepts, instrumentation and techniques in inductively coupled plasma, optical emission spectrometry. 2.nd edition. The Perkin Elmer Corporation, Norwalk, CT, USA.

BOUMANS, P.W.J.M. 1984. Line coincidence tables for inductively coupled plasma atomic emission spectrometry. Vol I & II, 2nd edition. Oxford: Pergamon Press.

BROOKES, K.J.A. 1979. World directory and handbook of hardmetals. 2nd edition. London: An Engineers' Digest Publication.

BROOKES, K.J.A. 2001. Annapolis shows the cutting edge of hardmetals technology. Metal Powder Report, 56(4), 8-14.

CHEN, H., Shao, Z. 1986. X-ray diffraction study of cemented carbides containing titanium carbide. Gen. Res. Inst. Nonferrous Met., **5,** (3), 1999 -202.

FRY, P. R. 1982. Fatigue-crack growth behaviour of tungsten carbide-cobalt hardmetal alloys. Thesis (MSc), University of the Witwatersrand, Witwatersrand.

HARRISON, G.R. (Ed.). 1969. Massachussets Institute of Technology wavelength tables. Cambridge: The M.I.T. Press.

HASWELL, S.J. (Ed.). 1991. Atomic absorption spectrometry, theory, design and applications. Analytical Spectroscopy Library, Vol. 5. Oxford: Elsevier.

Hawley's condensed chemical dictionary. 1987. 11th edition. New York: Van Nostrand Reinhold.

International Organization for Standardization. 1983. ISO 7627-1 Hardmetals - Chemical analysis by flame atomic absorption spectrometry: Part 1: General requirements. Switzerland.

International Organization for Standardization. 1983. ISO 7627-2 Hardmetals - Chemical analysis by flame atomic absorption spectrometry: Part2: Determination of calcium, potassium, magnesium and sodium in contents from 0.001 to 0.02% (m/m). Switzerland.

International Organization for Standardization. 1983. ISO 7627-3 Chemical analysis by flame atomic absorption spectrometry: Part 3: Determination of cobalt, iron, manganese and nickel in contents from 0.01 to 0.5% (m/m). Switzerland.

International Organization for Standardization. 1983. ISO 7627-4 Hardmetals - Chemical analysis by flame atomic absorption spectrometry: Part 4: Determination of molybdenum, titanium and vanadium in contents from 0.01 to 0.5% (m/m). Switzerland.

International Organization for Standardization. 1983. ISO 7627-5 Hardmetals - Chemical analysis by flame atomic absorption spectrometry: Part 5: Determination of cobalt, iron, manganese, nickel, titanium and vanadium in contents from 0.5 to 2% (m/m). Switzerland.

PIIPPANEN, T., Jaatinen, J., Tummavuori, J. 1997a. The analysis of chromium, cobalt, iron, nickel, niobium, tantalum, titanium and zinc in tungsten carbides with cobalt as a binder by inductively coupled plasma atomic emission spectrometry. Fresenius' Journal of Analytical Chemistry, 357 (4), 405-410.

PIIPPANEN, T., Jaatinen, J., Piirjeta, A., Tummavuori, J. 1997b. Determination of cobalt, copper, iron, nickel, and zinc in cemented tungsten carbides with cobalt as a binder by FASAS: Matrix effect control by multivarate technique. Fresenius' Journal of Analytical Chemistry, 358, 771-774.

ROGERS, D.E.C., Matthews, P.M., VAN Maarseveen, I.L., Norval, E., Theodorou C.A., Wardale, I.M., Olsen, S.D., Claase, C., Human, H.G.C., Ferreira, N.P., Adlem, L.H. 1987. A compilation of bulk chemical characterization methods and techniques used in support of materials research. Electronic Materials Division, National Institute for Materials Research, CSIR, South Africa.

STOCH, H. 1986. A manual of analytical methods used at Mintek. Johannesburg: Mintek.

The Merck index, an encyclopedia of chemicals, drugs and biologicals. 1989. 11th edition. Rahway, USA: Merck & Co., Inc.

THOMPSON, M., Walsh, J.N. 1983. A handbook of inductively coupled plasma spectrometry. Glasgow: Blackie & Son.

THOMSEN, V.B.E., Baker, P.J. 1995. Rapid chemical characterisation of tungsten carbides by spark optical emission spectrometry. J. Hard Mater., **6,** (2), 97 - 99.

TISSUE, B.M. 1995-2000. Encyclopedia of analytical instrumentation. Internet: http://www.chem.vt.edu/chem-ed/ac-meths.html.

International Organization for Standardization. 1985. ISO 7627-6 Hardmetals - Chemical analysis by flame atomic absorption spectrometry: Part 6: determination of chromium in contents from 0.01 to 2% (m/m). Switzerland.

KAWAGUCHI, H. 1995. Inductively coupled plasma as atomization, excitation and ionization sources in analytical atomic spectroscopy. Memoirs of the School of Engineering, Nagoya University, Nagoya, Japan, Vol. 47, (2), 145 - 190.

KINSON, K., Knott, A.C., Belcher, C.B. 1976. Analysis of tungsten carbide by x-ray fluorescence spectrometry, Tantala, **23,** (11 – 12), 815 - 818.

KUBSCH, M., Herman, U., Stahlberg, R., Goerner, W. 1975. Nondestructive activation analysis of special materials. Zentralinst. Kernforsch., Rossendorf Dresden, Ber., Zfk-294, 131-2.

LUYCKX, S. (University of the Witwatersrand). 1997. Course literature: The preparation and properties of hardmetals. Sandvik, Benoni.

Microstructure of defects in solid materials. 1999. Internet: http://www.infim.ro/1/190/results.htm

MILLER, J.C., Miller, J.N. 1993. Statistics for analytical chemistry. 3rd edition. UK: Ellis Horwood Ltd.

MILTON, M.J.T., Quinn, T.J. 2001. Primary methods for the measurement of amount of substance.. Paris: Bureau International des Poids et Measures. Metrologia, 38 (4), 289-296

MOORE, G.L. 1989. Introduction to inductively coupled plasma atomic emission spectrometry. Analytical spectroscopy library, Vol 3. Oxford: Elsevier.

NAISH, W.A., Clennel, J.E., Kingswood, V.S. 1953. Select methods of metallurgical analysis, 2nd edition. London: Chapman & Hall Ltd.

TOWNSHEND, A., Worsfold, P., Haswell, S., Werner, H., Wilson, I. (eds.). 1995. Encyclopedia of Analytical Science. Vol. 1 – 10. London: Academic Press.

VASILESCU, E., Abraham, B., Maruntu, A., Toderascu, I. 1980. Rapid and precise determination of chemical composition of metallic carbide homogeneous powders. Inst. Cercetari Metall. Bucharest, Rom., 21.

WILLIAMS, W.J. 1979. Handbook of anion determination. UK: Butterworths

APPENDIX 1

Properties of sintered carbides
Brookes 1979

APPENDIX 1

Properties of sintered carbides
(Brookes, 1979)

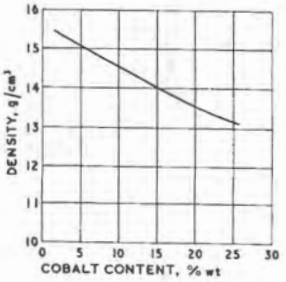

Figure 4.1. (left) Density of typical WC/Co grades; variation with cobalt content.

Figure 4.2. (right) Density of WC/TiC/Co and WC/TiC/Ta(Nb)C/Co grades; variation with TiC content (calculated figures, assuming zero porosity). Practical values are typically 0.1 to 0.2 g/cm³ lower.

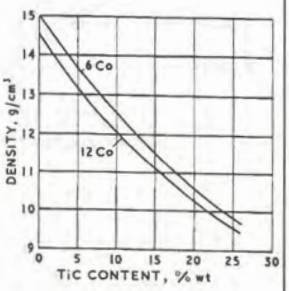

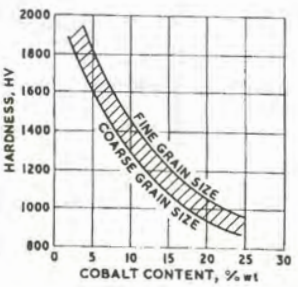

Figure 4.3. (left) Hardness of typical WC/Co grades; variation with cobalt content and grain size. Higher values relate to finer grain size.

Figure 4.4. (right) Relative abrasion resistance (reciprocal wear rate under standard conditions) of typical WC/Co grades. Highest values relate to finest grain size.

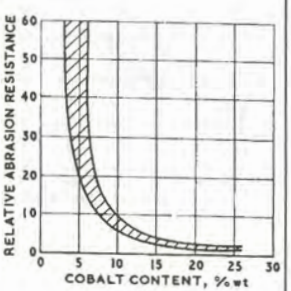

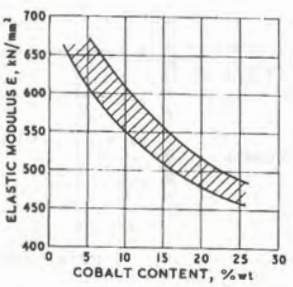

Figure 4.5. (left) Elastic modulus E of typical WC/Co grades; variation with cobalt content.

Figure 4.6. (right) Modulus of rigidity G of typical WC/Co grades; variation with cobalt content.

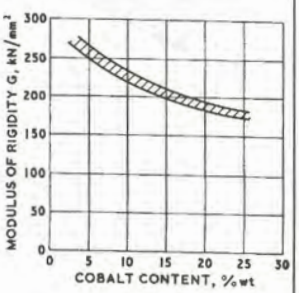

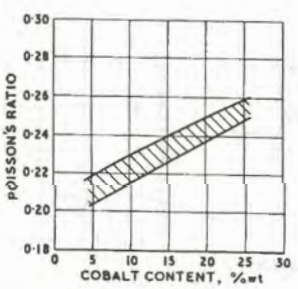

Figure 4.7. (left) Poisson's ratio of typical WC/Co grades; variation with cobalt content.

Figure 4.8. (right) Transverse rupture stress of typical WC/Co grades; variation with cobalt content.

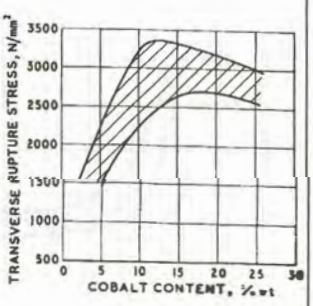

APPENDIX 1

Properties of sintered carbides
(Brookes, 1979)

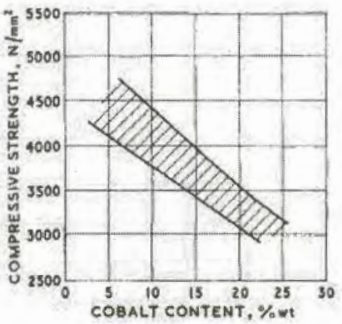

Figure 4.9. (left) Compressive strength of typical WC/Co grades; variation with cobalt content.

Figure 4.10. (right) Tensile strengths of typical WC/Co grades.

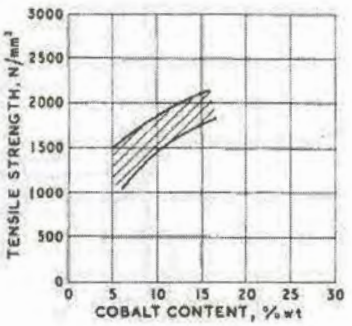

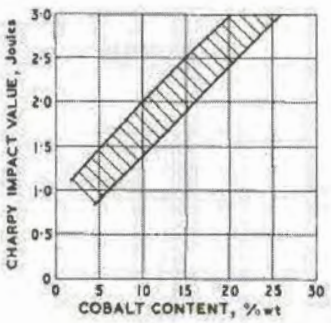

Figure 4.11 (left) Charpy impact values of typical WC/Co grades; variation with cobalt content.

Figure 4.12. (right) Fatigue strength endurance limit (10^8 stress cycles) of typical WC/Co grades.

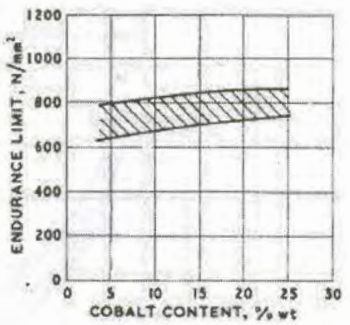

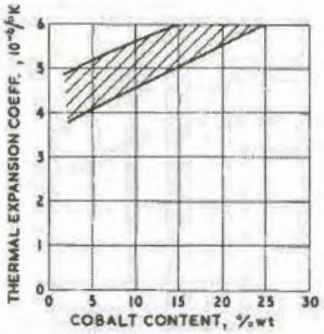

Figure 4.13. (left) Thermal expansion coefficient of typical WC/Co grades.

Figure 4.14. (right) Thermal conductivity of typical WC/Co grades; variation with cobalt content.

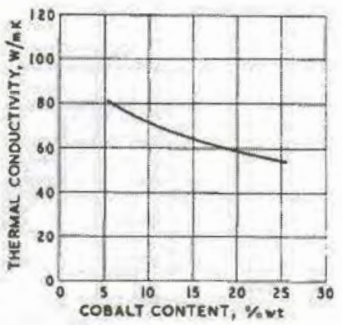

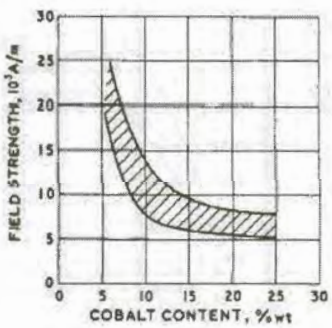

Figure 4.15 (left) Magnetisation coercive field strength (coercive force) of typical WC/Co grades; variation with cobalt content. Lower values tend to be associated with coarser grain sizes.

Figure 4.16. (right) Magnetic permeability of typical WC/Co grades.

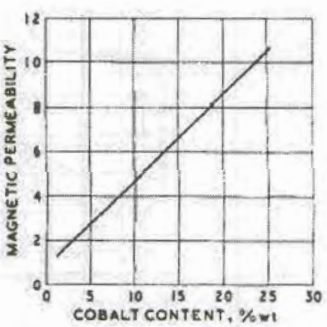

APPENDIX 2

Tables of typical carbide grades for machining and
tables of historical developments of sintered carbides
Brookes 1979

APPENDIX 2

Tables of typical carbide grades for machining and tables of historical development of sintered carbides (Brookes, 1979)

Designations			Compositions						Properties		
ISO Application Code	U.S. Industry Code	BHMA Properties Code	WC	TiC	Ta(Nb)C	Co	Ni	Mo	Density g/cm³	Hardness HV	Transverse Rupture Stress N/mm²
P01	C8	919	-	80	-	-	10	10	5.8	1900	850
P01	C8	919	50	35	7	6			8.5	1900	1100
P05	C7	926	78	16	-	6			11.4	1820	1300
P10	C7	727	69	15	8	8			11.5	1740	1400
P15	C6	635	78	12	3	7			11.7	1660	1500
P20	C6	444	79	8	5	8			12.1	1580	1600
P25	C6	344	82	6	4	8			12.9	1530	1700
P30	C5	353	84	5	2	9			13.3	1490	1850
P40	C5	263	85	5	-	10			13.4	1420	1950
P50	-	182	78	3	3	16			13.1	1250	2300
M10	-	453	85	5	4	6			13.4	1590	1800
M20	-	363	82	5	5	8			13.3	1540	1900
M30	-	263	86	4	-	10			13.6	1440	2000
M40	-	273	84	4	2	10			14.0	1380	2100
K01	C4	930	97	-	-	3			15.2	1850	1450
K05	C4	830	95	-	1	4			15.0	1780	1550
K10	C3	741	92	-	2	6			14.9	1730	1700
K20	C2	560	94	-	-	6			14.8	1650	1950
K30	C1	280	91	-	-	9			14.4	1400	2250
K40	C1	290	89	-	-	11			14.1	1320	2500

* Very considerable variation between manufacturers is possible.

Table 1.2 Historical Development
WC-base sintered carbides

1923-25	WC-Co
1929-31	WC-TiC-Co
1930-31	WC-TaC(VC, NbC)-Co
1932	WC-TiC-TaC(NbC)-Co
1938	WC-Cr_3C_2-Co
1956	WC-TiC-Ta(Nb)C-Cr_3C_2-Co
1959	WC-TiC-HfC-Co
1968-69	WC-TiC-TaC(NbC)-HfC-Co
1968-69	WC-TiC-NbC(TaC)-HfC-Co
1965-78	TiC, TiN, Ti(C,N), HfC, HfN and Al_2O_3 coatings on WC-base alloys
1967-70	Sub-micron WC/Co
1965-75	Hot isostatic pressing
1969-71	Thermochemical surface hardening
1974-77	Polycrystalline diamond layers on WC-base hardmetal
1973-78	Multi-carbide, carbonitride/nitride and multiple carbide/carbonitride/nitride/oxide coatings
1976-79	Complex hardmetals with Ru additions

Table 1.3 Historical Development
WC-free sintered carbides

1929-31	TiC-Mo_2C-Ni, Cr, Mo
1930-31	TaC-Ni
1931	TiC-TaC-Co
1931	TiC-Cr, Mo, W, Ni, Co
1938	TiC-VC-Ni, Fe
1944	TiC-NbC-Ni, Co
1949	TiC-VC-NbC-Mo_2C-Ni
1950	TiC(Mo_2C, TaC)-Ni, Co-Cr
1952-66	TiC - heat-treatable steels and alloys
1957	TiC-TiB_2
1965-70	TiC-Mo_2C(mixtures)-Ni, Mo
1968-70	(Ti, Mo)C(solid solution)-Ni, Mo, Cr
1969-70	TiC-TiN-Ni
1968-73	TiC-Al_2O_3
1972-75	TiC-TaN-Ni

APPENDIX 3

Certificate of analysis for NIST
standard reference material 889: cemented carbide

National Institute of Standards & Technology

Certificate of Analysis

Standard Reference Material 889

Cemented Carbide

(W-75,Co-9,Ta-5,Ti-4)

(In Cooperation with the American Society for Testing and Materials)

This Standard Reference Material (SRM) is a sintered tungsten carbide base material in the form of a fine powder (150 μm) intended for use in checking chemical and instrumental methods of analysis. SRM 889 was developed under the cooperative program for certification with the National Institute of Standards and Technology (NIST) and the American Society for Testing and Materials (ASTM).

	Certified Value[a]	Estimated Uncertainty[b]
	Percent by Weight	
Cobalt	9.50	0.15
Tantalum	4.60	.15
Titanium	4.03	.10

[a] The certified value is the present best estimate of the "true" value based on the NIST/ASTM cooperative program for certification.

b The estimated uncertainty is based on judgment and represents an evaluation of the combined effects of method imprecision, possible systematic errors among methods, and material variability. No attempt was made to derive exact statistical measures of imprecision because several methods were involved in the determination of the certified constituent.

The overall coordination of the technical measurements leading to certification was performed under the direction of J.I. Shultz, Research Associate, ASTM-NIST Research Associate Program.

The technical and support aspects involved in the preparation, certification, and issuance of this Standard Reference Material were coordinated through the Office of Standard Reference Materials by W.P. Reed.

PLANNING, PREPARATION, TESTING, AND ANALYSIS:

The material for this SRM was provided by GTE Products Corp., Towanda, Pennsylvania through the courtesy of R. Dyck.

The preparation of the material was under the direction of M.E. Shaffer of the Hard Materials Section, GTE Products Corp., Towanda, Pennsylvania.

Homogeneity testing was performed at GTE Products Corp. by J.S. Mras and at NIST by G.A. Sleater.

Cooperative analyses for certification were performed in the following laboratories:

- GTE Products Corp., Towanda, Pennsylvania, J. Mras, J.R. Barton, L.J. Kring and M. Fedorchak.
- Ledoux & Company, Teaneck, N.J., S. Kallmann and C.L. Maul.

September 5, 1988
Gaithersburg, MD 20899

Stanley D. Rasberry, Chief
Office of Standard Reference Materials

Metallurgical Industries, Inc., Tinton Falls, N.J., R. Liu.
- National Institute of Standards and Technology, Gas and Particulate Science Division, Gaithersburg, MD, Z. Wang and P.A. Pella.
- Timken Company, Canton, Ohio, N.J. Stecyk.
- Valeron Corporation, Troy, Michigan, R. Fike.

Elements other than those certified may be present in this material as indicated below. These are not certified, but are given as additional information on the composition.

Element	Concentration, % by Weight
Molybdenum	(<.05)
Nickel	(<.05)
Iron	(<.05)
Niobium	(<.05)
Carbon	(6.0)

APPENDIX 4

Calibration data

APPENDIX 4: FIGURE A1

Co **228.616nm**

Std Conc (x_i)	Signal (y_i)	x_i^2	$\ddot{y}_i$	$\|yi - \ddot{y}i\|$	$(yi - \ddot{y}i)^2$	$(x_i - x_m)^2$
0	0.29306	0	19.5251	-19.232	369.8714804	1600
10	766.25	100	783.3215	-17.0715	291.4367455	900
50	3907.7	2500	3838.507	69.19282	4787.646273	100
100	7624.6	10000	7657.489	-32.8893	1081.703285	3600
160	3074.71	12600			6530.657784	6200
40						

a	19.52510306
b	76.37964155

No. of Stds	4
DF	2
sy/x	57.14305638
s_a	40.73079601
s_b	0.725717542
Lowest signal detectable	190.954
Lowest conc. Detectable	**2.244ppm**
Lowest quantitation signal	590.956
Lowest conc.quantifiable	**7.481ppm**

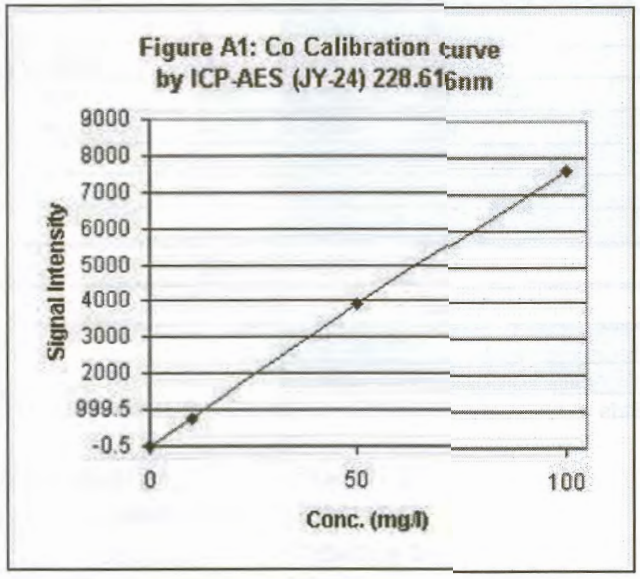

SUMMARY OUTPUT

Regression Statistics	
Multiple R	0.99991
R Square	0.999819
Adjusted R Square	0.999729
Standard Error	57.14306
Observations	4

ANOVA

	df	*SS*	*MS*	*F*	*Significance F*
Regression	1	36169867.79	36169868	11076.9448	9.0265E-05
Residual	2	6530.657784	3265.329		
Total	3	36176398.44			

	Coefficients	*Standard Error*	*t Stat*	*P-value*	*Lower 95%*	*Upper 95%*	*Lower 95.0%*	*Upper 95.0%*
Intercept	19.5251	40.73079601	0.47937	0.67897567	-155.72549	194.7757	-155.725	194.7757
X Variable 1	76.37964	0.725717542	105.2471	9.0265E-05	73.2571288	79.50215	73.25713	79.50215

APPENDIX 4: FIGURE A2

Co **238.346nm**

Std Conc (x_i)	Signal (y_i)	x_i^2	$\ddot{y}_i$	$\lvert yi - \ddot{y}i \rvert$	$(yi - \ddot{y}i)^2$	$(x_i - x_m)^2$
0	0.312	0	-17.0536	17.36558	301.5633911	1600
10	790.1	100	788.0731	2.026935	4.108467456	900
50	3970.2	2500	4008.58	-38.3796	1472.997163	100
100	8053.2	10000	8034.213	18.98713	360.5110689	3600
160	3203.45	12600			2139.18009	6200
40						

a	-17.0535806
b	80.51266452

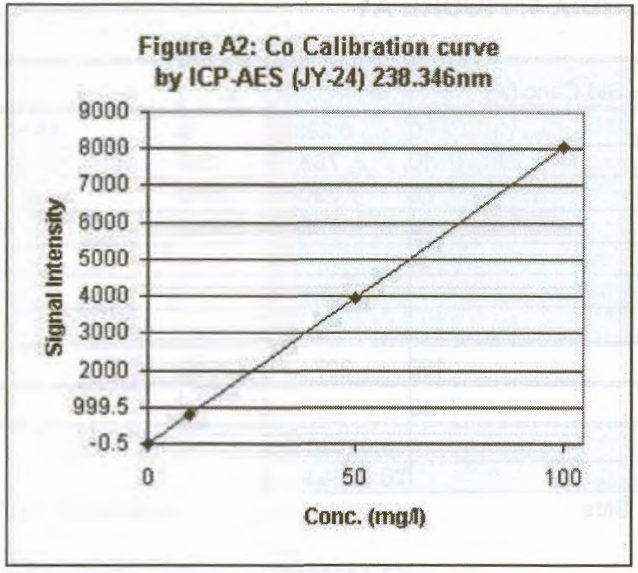

No. of Stds	4
DF	2
sy/x	32.70458752
s_a	23.31138668
s_b	0.415348677
Lowest signal detectable	81.060
Lowest conc. Detectable	**1.219ppm**
Lowest quantitation signal	309.992
Lowest conc.quantifiable	**4.062ppm**

SUMMARY OUTPUT

Regression Statistics	
Multiple R	0.999973
R Square	0.999947
Adjusted R Square	0.99992
Standard Error	32.70459
Observations	4

ANOVA

	df	*SS*	*MS*	*F*	*Significance F*
Regression	1	40190192.71	40190193	37575.3242	2.6612E-05
Residual	2	2139.18009	1069.59		
Total	3	40192331.89			

	Coefficients	*Standard Error*	*t Stat*	*P-value*	*Lower 95%*	*Upper 95%*	*Lower 95.0%*	*Upper 95.0%*
Intercept	-17.0536	23.31138668	-0.73156	0.54054436	-117.354452	83.24729	-117.354	83.24729
X Variable 1	80.51266	0.415348677	193.8436	2.6612E-05	78.7255622	82.29977	78.72556	82.29977

APPENDIX 4: FIGURE A3

Ta **240.063nm**

Std Conc (x_i)	Signal (y_i)	x_i^2	$\ddot{y}_i$	$\|yi - \ddot{y}i\|$	$(yi - \ddot{y}i)^2$	$(x_i - x_m)^2$
0	-3.403	0	-96.832	93.42902	8728.98204	42.25
1	343.68	1	321.9051	21.7749	474.1463886	30.25
5	1844.7	25	1996.854	-152.154	23150.70947	2.25
20	8314.86	400	8277.91	36.94965	1365.276477	182.25
26	2624.96	426			33719.11437	257
6.5						
a	-96.8320214					
b	418.7371187					

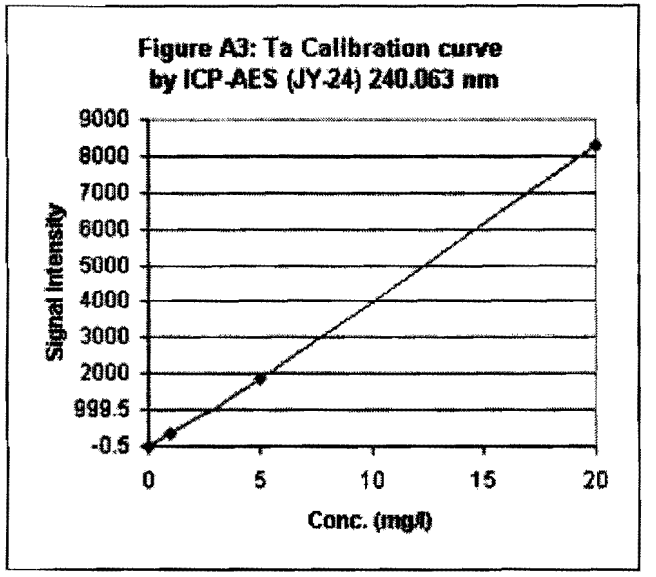

No. of Stds	4
DF	2
sy/x	129.8443575
s_a	83.58557302
s_b	8.099468491
Lowest signal detectable	292.701
Lowest conc. Detectable	**0.930ppm**
Lowest quantitation signal	1201.612
Lowest conc.quantifiable	**3.101ppm**

SUMMARY OUTPUT

Regression Statistics	
Multiple R	0.999626
R Square	0.999252
Adjusted R Square	0.998878
Standard Error	129.8444
Observations	4

ANOVA

	df	*SS*	*MS*	*F*	*Significance F*
Regression	1	45062579.06	45062579	2672.82103	0.00037393
Residual	2	33719.11437	16859.56		
Total	3	45096298.18			

	Coefficients	*Standard Error*	*t Stat*	*P-value*	*Lower 95%*	*Upper 95%*	*Lower 95.0%*	*Upper 95.0%*
Intercept	-96.832	83.58557302	-1.15848	0.3663056	-456.471966	262.8079	-456.472	262.8079
X Variable 1	418.7371	8.099468491	51.69933	0.00037393	383.887894	453.5863	383.8879	453.5863

APPENDIX 4: FIGURE A4

Ta **268.517nm**

Std Conc (x_i)	Signal (y_i)	x_i^2	$\ddot{y}_i$	$\|yi - \ddot{y}i\|$	$(yi - \ddot{y}i)^2$	$(x_i - x_m)^2$
0	9.6677	0	6.06506	3.60264	12.97901414	60.0625
1	42.087	1	43.25682	-1.16982	1.36847152	45.5625
10	373	100	377.9826	-4.98263	24.82657888	5.0625
20	752.45	400	749.9002	2.549805	6.501503998	150.0625
31	294.30	501			45.67556854	260.75
7.75						
a	6.065060115					
b	37.19175676					

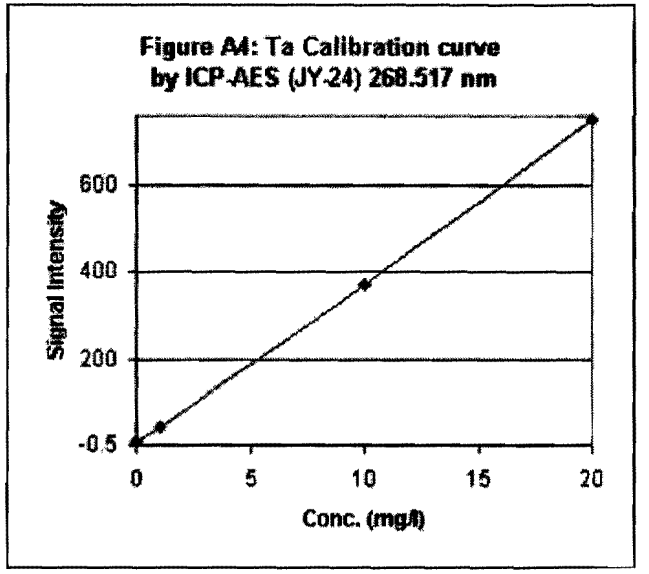

No. of Stds	4
DF	2
sy/x	4.778889439
s_a	3.312101915
s_b	0.295947601
Lowest signal detectable	20.402
Lowest conc. Detectable	**0.385ppm**
Lowest quantitation signal	53.854
Lowest conc.quantifiable	**1.285ppm**

SUMMARY OUTPUT

Regression Statistics	
Multiple R	0.999937
R Square	0.999873
Adjusted R Square	0.99981
Standard Error	4.778889
Observations	4

ANOVA

	df	*SS*	*MS*	*F*	*Significance F*
Regression	1	360676.3805	360676.4	15792.9673	6.3313E-05
Residual	2	45.67556854	22.83778		
Total	3	360722.0561			

	Coefficients	*Standard Error*	*t Stat*	*P-value*	*Lower 95%*	*Upper 95%*	*Lower 95.0%*	*Upper 95.0%*
Intercept	6.06506	3.312101915	1.831182	0.20854974	-8.18577415	20.31589	-8.18577	20.31589
X Variable 1	37.19176	0.295947601	125.6701	6.3313E-05	35.9183961	38.46512	35.9184	38.46512

APPENDIX 4: FIGURE A5

Ti **337.280nm**

Std Conc (x_i)	Signal (y_i)	x_i^2	$\ddot{y}_i$	$\lvert yi - \ddot{y}i \rvert$	$(yi - \ddot{y}i)^2$	$(x_i - x_m)^2$
0	-14.319	0	-126.538	112.2193	12593.18003	232.5625
1	2351.4	1	2237.318	114.082	13014.7114	203.0625
10	23232	100	23512.02	-280.025	78413.81593	27.5625
50	118120	2500	118066.3	53.72329	2886.192241	1207.563
61	35922.27	2601			106907.8996	1670.75
15.25						
a	-126.538339					
b	2363.856301					

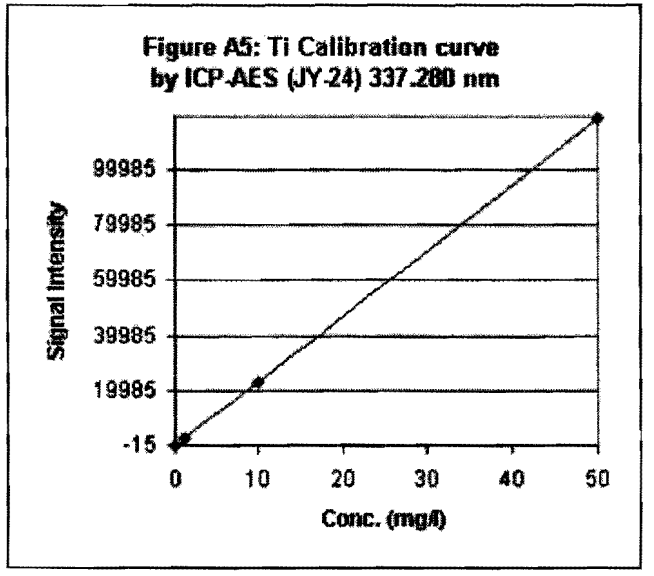

No. of Stds	4
DF	2
sy/x	231.2011025
s_a	144.2362246
s_b	5.656322535
Lowest signal detectable	567.065
Lowest conc. Detectable	**0.293ppm**
Lowest quantitation signal	2185.473
Lowest conc.quantifiable	**0.978ppm**

SUMMARY OUTPUT

Regression Statistics	
Multiple R	0.999994
R Square	0.999989
Adjusted R Square	0.999983
Standard Error	231.2011
Observations	4

ANOVA

	df	*SS*	*MS*	*F*	*Significance F*
Regression	1	9335844603	9.34E+09	174652.1	5.7256E-06
Residual	2	106907.8996	53453.95		
Total	3	9335951511			

	Coefficients	*Standard Error*	*t Stat*	*P-value*	*Lower 95%*	*Upper 95%*	*Lower 95.0%*	*Upper 95.0%*
Intercept	-126.538	144.2362246	-0.8773	0.47284902	-747.137157	494.0605	-747.137	494.0605
X Variable 1	2363.856	5.656322535	417.914	5.7256E-06	2339.51909	2388.194	2339.519	2388.194

APPENDIX 4: FIGURE A6

Ti **368.520nm**

Std Conc (x_i)	Signal (y_i)	x_i^2	$\ddot{y}_i$	$\lvert y_i - \ddot{y}_i \rvert$	$(y_i - \ddot{y}_i)^2$	$(x_i - x_m)^2$
0	-1.9728	0	-84.1301	82.15727	6749.816891	232.5625
1	2796.3	1	2681.425	114.8752	13196.30987	203.0625
10	27328	100	27571.42	-243.419	59252.66228	27.5625
50	138240	2500	138193.6	46.38624	2151.682857	1207.563
61	42090.58	2601			81350.4719	1670.75
15.25						
a	-84.1300693					
b	2765.554877					

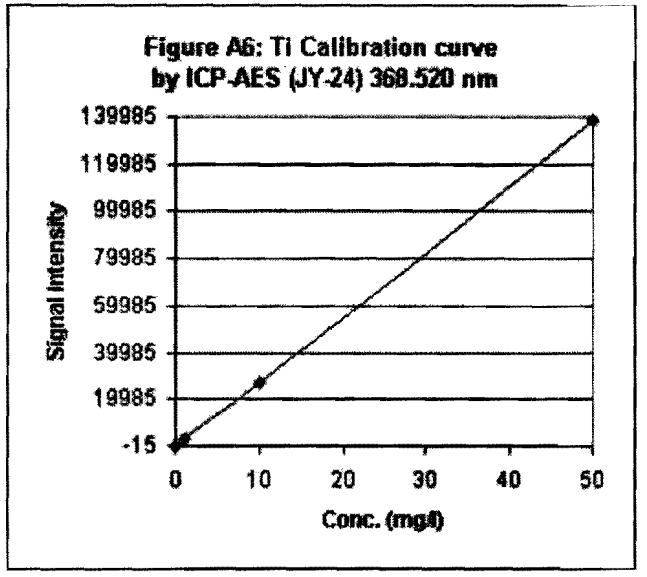

No. of Stds	4
DF	2
sy/x	201.6810253
s_a	125.8199435
s_b	4.934115433
Lowest signal detectable	520.913
Lowest conc. Detectable	**0.219ppm**
Lowest quantitation signal	1932.680
Lowest conc.quantifiable	**0.729ppm**

SUMMARY OUTPUT

Regression Statistics	
Multiple R	0.999997
R Square	0.999994
Adjusted R Square	0.99999
Standard Error	201.681
Observations	4

ANOVA

	df	*SS*	*MS*	*F*	*Significance F*
Regression	1	12778386826	1.28E+10	314156.428	3.1831E-06
Residual	2	81350.4719	40675.24		
Total	3	12778468177			

	Coefficients	*Standard Error*	*t Stat*	*P-value*	*Lower 95%*	*Upper 95%*	*Lower 95.0%*	*Upper 95.0%*
Intercept	-84.1301	125.8199435	-0.66865	0.57255917	-625.48997	457.2298	-625.49	457.2298
X Variable 1	2765.555	4.934115433	560.4966	3.1831E-06	2744.32508	2786.785	2744.325	2786.785

APPENDIX 4: FIGURE A7

V **292.402nm**

Std Conc (x_i)	Signal (y_i)	x_i^2	$\ddot{y}_i$	$\lvert y_i - \ddot{y}_i \rvert$	$(y_i - \ddot{y}_i)^2$	$(x_i - x_m)^2$
0	13.472	0	-28.9639	42.43592	1800.807691	60.0625
1	4384.7	1	4384.166	0.533999	0.2851547	45.5625
5	21983	25	22036.69	-53.6857	2882.154835	7.5625
25	110310	625	110299.3	10.71578	114.8279601	297.5625
31	34172.79	651			4798.075641	410.75
7.75						
a	-28.9639245					
b	4413.129926					

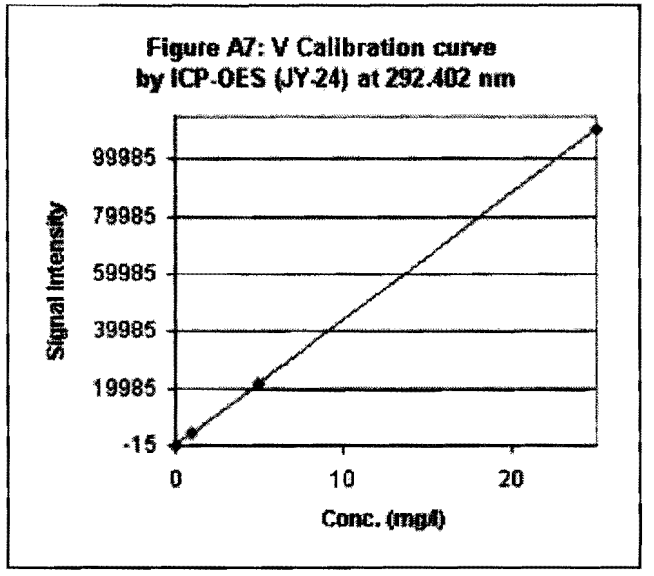

No. of Stds	4
DF	2
sy/x	48.97997367
s_a	30.83118803
s_b	2.41673906
Lowest signal detectable	117.976
Lowest conc. Detectable	**0.033ppm**
Lowest quantitation signal	460.836
Lowest conc.quantifiable	**0.111ppm**

SUMMARY OUTPUT

Regression Statistics	
Multiple R	1
R Square	0.999999
Adjusted R Square	0.999999
Standard Error	48.97997
Observations	4

ANOVA

	df	*SS*	*MS*	*F*	*Significance F*
Regression	1	7999650241	8E+09	3334524.44	2.9989E-07
Residual	2	4798.075641	2399.038		
Total	3	7999655039			

	Coefficients	*Standard Error*	*t Stat*	*P-value*	*Lower 95%*	*Upper 95%*	*Lower 95.0%*	*Upper 95.0%*
Intercept	-28.9639	30.83118803	-0.93944	0.44667602	-161.619912	103.6921	-161.62	103.6921
X Variable 1	4413.13	2.41673906	1826.068	2.9989E-07	4402.73153	4423.528	4402.732	4423.528

APPENDIX 4: FIGURE A8

V **311.071nm**

Std Conc (x_i)	Signal (y_i)	x_i^2	$\ddot{y}_i$	$\lvert yi - \ddot{y}i \rvert$	$(yi - \ddot{y}i)^2$	$(x_i - x_m)^2$
0	19	0	-27.4153	46.41532	2154.38217	16
1	973.58	1	1021.737	-48.1573	2319.121504	9
5	5212.2	25	5218.348	-6.14758	37.79274779	1
10	10472	100	10464.11	7.889516	62.24446475	36
16	4169.195	126			4573.540887	62
4						
a	-27.4153226					
b	1049.152581					

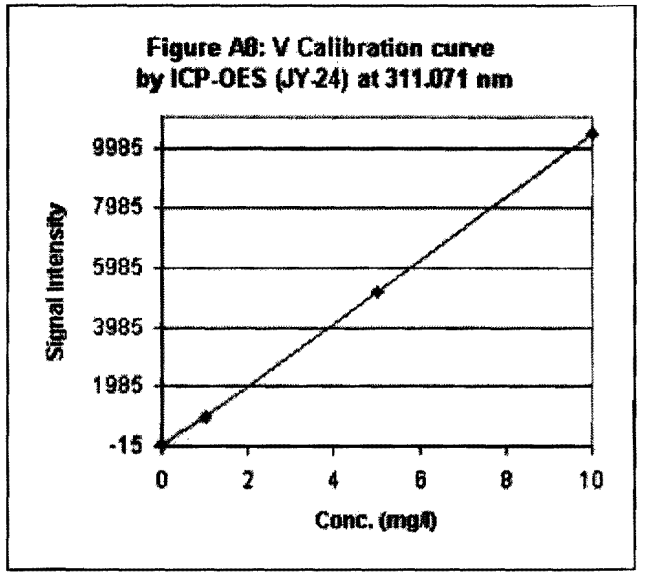

No. of Stds	4
DF	2
sy/x	47.82018866
s_a	34.08558227
s_b	6.073170033
Lowest signal detectable	116.045
Lowest conc. Detectable	**0.137ppm**
Lowest quantitation signal	450.787
Lowest conc.quantifiable	**0.456ppm**

SUMMARY OUTPUT

Regression Statistics	
Multiple R	0.999966
R Square	0.999933
Adjusted R Square	0.999899
Standard Error	47.82019
Observations	4

ANOVA

	df	*SS*	*MS*	*F*	*Significance F*
Regression	1	68244710.52	68244711	29843.2712	3.3507E-05
Residual	2	4573.540887	2286.77		
Total	3	68249284.06			

	Coefficients	*Standard Error*	*t Stat*	*P-value*	*Lower 95%*	*Upper 95%*	*Lower 95.0%*	*Upper 95.0%*
Intercept	-27.4153	34.08558227	-0.80431	0.50562912	-174.073848	119.2432	-174.074	119.2432
X Variable 1	1049.153	6.073170033	172.7521	3.3507E-05	1023.02182	1075.283	1023.022	1075.283

APPENDIX 4: FIGURE A9

Cr **357.869nm**

Std Conc (x_i)	Signal (y_i)	x_i^2	$\ddot{y}_i$	$\lvert yi - \ddot{y}i \rvert$	$(yi - \ddot{y}i)^2$	$(x_i - x_m)^2$
0	8.5556	0	-256.874	265.4298	70452.97672	60.0625
1	4285.9	1	4308.124	-22.2243	493.9180794	45.5625
5	22263	25	22568.12	-305.118	93097.06954	7.5625
25	113930	625	113868.1	61.9126	3833.169481	297.5625
31	35121.8639	651			167877.1338	410.75
7.75						
a	-256.874196					
b	4564.998464					

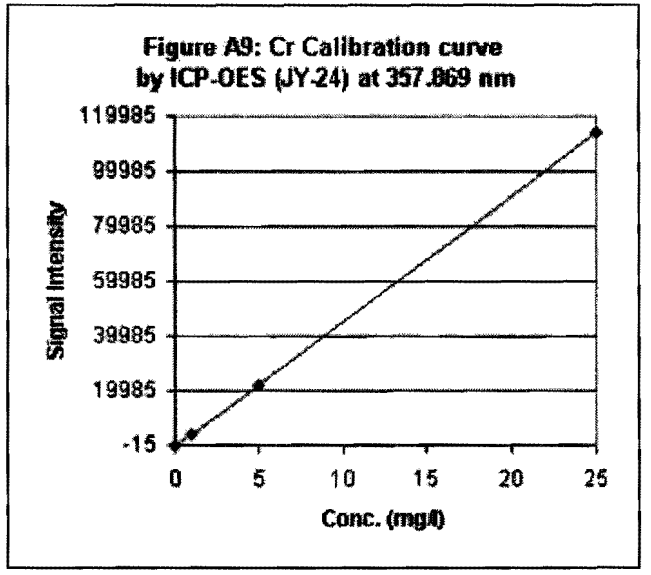

No. of Stds	4
DF	2
sy/x	289.7215334
s_a	182.3696177
s_b	14.29525771
Lowest signal detectable	612.290
Lowest conc. Detectable	**0.190ppm**
Lowest quantitation signal	2640.341
Lowest conc.quantifiable	**0.635ppm**

SUMMARY OUTPUT

Regression Statistics	
Multiple R	0.99999
R Square	0.99998
Adjusted R Square	0.999971
Standard Error	289.7215
Observations	4

ANOVA

	df	*SS*	*MS*	*F*	*Significance F*
Regression	1	8559705909	8.56E+09	101975.84	9.8061E-06
Residual	2	167877.1338	83938.57		
Total	3	8559873786			

	Coefficients	*Standard Error*	*t Stat*	*P-value*	*Lower 95%*	*Upper 95%*	*Lower 95.0%*	*Upper 95.0%*
Intercept	-256.874	182.3696177	-1.40854	0.29431686	-1041.54788	527.7995	-1041.55	527.7995
X Variable 1	4564.998	14.29525771	319.3366	9.8061E-06	4503.49089	4626.506	4503.491	4626.506